FATE AND BEHAVIOUR OF ENGINEERED NANOPARTICLES IN SIMULATED WASTEWATER AND THEIR EFFECT ON MICROORGANISMS

Report to the
Water Research Commission

by

EFC Chaúque[1], JN Zvimba[2], JC Ngila[1], N Musee[2], A Mboyi[3], MNB Momba[3]

[1]Department of Applied Chemistry, University of Johannesburg
[2]Nanotechnology Sustainability Research Group, Natural Resources and the Environment, CSIR
[3] Department of Environmental, Water & Earth Sciences, Tshwane University of Technology

Edited by EFC Chaúque, AA Adelodun[1] and JC Ngila[1]

WRC Report No. KV 350/16
ISBN 978-1-4312-0762-6

April 2016

Obtainable from:
Water Research Commission
Private Bag X03
Gezina, 0031
South Africa

EXECUTIVE SUMMARY

Despite the numerous advantages of nanotechnology and nanomaterials (NMs) applied in a variety of study fields ranging from catalysis and water treatment materials, to environmental remediation and biomedicine, concerns have been raised for the human health and the environment. Nanomaterials, especially zinc oxide and silver, are increasingly being applied in consumer products such as sunscreen, clothing, electronic appliances, and a variety of medical equipment have been produced over the past years. It is expected that such products will be on the increase. As such, substances from these NMs might increasingly be released into wastewater processes, where the knowledge of their fate and ecotoxicological effects on the microbial population of wastewater systems is still lacking. Studies have reported that these ecotoxicological effects can ultimately inhibit the performance of the WWTPs.

Activated sludge usually consists of various microbial strains of bacteria including their extracellular products, and about 9% protozoan population. Regrettably, the presence of NMs in the system can inhibit the functions of these essential microbial communities resulting in detrimental effects on the performance of WWTPs. NMs are reported to (i) exert antimicrobial properties through different mechanisms, e.g. adsorption on the cell wall, degradation of the lipopolysaccharide molecules, as well as the accumulation of NMs inside cells; (ii) generate reactive oxygen species that cause oxidation; (iii) cause damage to deoxyribonucleic acid (DNA) thereby dismantling cell replication abilities. Despite these reports, information in relation to the impact of NMs on the biological processes during wastewater treatment is insufficient. It has been suggested that the fate and behaviour of NMs changes with the presence of natural organic matter; contaminants and extracellular polymeric substances (EPS), lead to the precipitation of these NMs in the sludge. These nano-wastes may represent an environmental risk if disposed at landfills. The focus of this project was on the investigation of the potential impact of ENMs on wastewater treatment plants, using laboratory scale activated sludge based wastewater treatment systems (OECD 303A). The present study therefore aimed to investigate the physicochemical behaviour, chemical effect, fate and potential impacts on microbial population (particularly the bacteria and protozoa), and to examine the resistance limits of these organisms after their exposure to engineered nanoparticles (ENMs).

The methodology involved the use of commercial nanopowders of zinc oxide and silver as the source of nanoparticles. Before the application of the nanoparticles in the WWTP process, they were characterized in terms of shape and size using high resolution transmission electron microscope (HRTEM, JEOL-JEM 2100) and scanning electron microscopy (SEM, Jeol JSM-6480 LV). The actual surface areas were also determined using Brauner, Emmett, and Teller (BET). The X-ray diffraction (XRD) powder peaks patterns were recorded by PANalytical X'Pert PRO diffractometer system using Cu-Kα (λ=1.5438Å) radiation operating in voltage 40 kV and 50 mA. The FTIR spectra of nZnO and nAg were obtained using 150 mg of KBr. Analysis of the wastewater samples for the metal ions was done using inductively coupled plasma optical emission spectrometer (ICP-OES). Wastewater samples were collected from Northern Johannesburg Water and Daspoort wastewater treatment plants (WWTPs). The physicochemical properties such as pH, dissolved oxygen (DO), chemical oxygen demand (COD) and metal contents were determined. The main reagents used for the experiments were D-glucose anhydrate (2.5 g/L) and $MgSO_4.H_2O$ (0.5 g/L) and KNO_3 (0.18 g/L) as sources of carbon and nutrients respectively. The stock suspension at concentrations of 40 g *n*ZnO/L and 2 g *n*Ag/L were used to prepare the culture media at varying concentrations.

The results obtained suggest that the removal of ZnO ENPs from the influent wastewater occurred as the sludge settled out. The removal efficiency was directly proportional to ionic strength and pH. The ZnO ENPs suspension in the wastewater was used to monitor the particle size distribution using the dynamic light scattering analysis (DLS). The formation of agglomerates was observed from the TEM and EDS analyses and the results confirmed the presence of ZnO aggregates. It was observed that the commercial NMs were in nanosize at a range between 1-100 nm with different shapes. The total surface area recorded from BET was found to be 15.88 m^3g^{-1} and 5.37 m^3g^{-1} for *n*ZnO and *n*Ag respectively. The zincite phase and faced centred cubic phases were obtained from XRD diffractograms. The vibration band peaks of the FTIR revealed the bonds attributed to C=O and C=N and C=C groups for Amides.

The antimicrobial activities of the target NMs towards protozoan consortium and bacterial consortium were observed. The toxic effects of NMs were found to be highly dependent on pH variations (pH 2, 7, 10), with an overall inhibition obtained at 20 g-*n*ZnO/L and at 0.65 g-*n*Ag/L, for both bacteria and protozoa. At pH 7, MIC values were observed at 0.65 g-*n*Ag/L and 0.105 g-*n*Ag/L for protozoan isolates and bacterial isolates, respectively. At pH 10 protozoan and bacterial growth was impaired by their exposure to 0.65 g-*n*Ag/L. A decrease in COD removal was observed after an increase in *n*ZnO and *n*Ag concentrations, which resulted in an increase of COD release into the system. Similar observations were noted with DO uptake because the increase in NMs concentrations was directly proportional

to the decrease in DO uptake. The HRTEM images revealed some interactions between *n*ZnO and *n*Ag with microbial cell membranes.

Overall, the results obtained indicated the suitability of the OECD 303A method used to assess the fate and behaviour of ZnO ENPs in WWTPs and their effect on microbes. In light of the low concentrations of ZnO ENPs found in the treated effluent attained as a result of their removal with the waste activated sludge (WAS), it is predicted that there will be low likelihood of ZnO ENPs' release and dispersion into the aquatic systems from WWTPs as point sources. The elevated concentration of ZnO ENPs in the sludge necessitates additional treatment steps to ensure the mitigation of possible dispersion of ENPs from various disposal mechanisms such as landfilling, incineration and agricultural applications. The fate and behaviour of ZnO ENPs in wastewater were also found to be affected by the presence of electrolytes, ionic strength, organic matter and pH during the activated sludge wastewater treatment. Thus, the release of zinc from ZnO ENPs suspension in wastewater was found to be more significant under acidic conditions and low ionic strength. Further, it was observed that the release of zinc from ZnO ENPs in wastewater was relatively lower compared to the release of Zn from de-ionized water. This observation may imply that the release of significant levels of nanomaterials into water from sediments and sludge is not likely to occur if the pH conditions are around neural pH. Under alkaline conditions, a large fraction of the metal-oxide ENPs showed strong tendency to settle out in the sewage sludge bio-solid rather than being dissolved or dispersed in the filtrate. The depositions of ENPs on sludge suggest their removal by abiotic, bio-sorption and bio-solid settling mechanisms. Furthermore, the size of ZnO ENPs was found to significantly increase upon exposure to wastewater matrix, an observation that may possibly suggest a significant sorption and stabilization capacity of synthetic organic matter from domestic waste and natural organic matter (NOM) such as humic substances.

Under the conditions of this study, which simulated the real WWTPs, the consortium of bacteria collected from a well operated WWTP and employed in the aeration chamber, were able to remove the organic matter in the wastewater spiked with ZnO ENPs. Both the COD and DOC were not significantly affected by changes in ENPs' concentration, a phenomenon suggesting adaptation ability of microorganisms responsible for organic matter degradation during activated sludge wastewater treatment upon long term exposure to ENPs. The toxicity of ENPs demonstrated a pH-dependence towards selected single bacterial isolates and the consortium of protozoan and bacterial isolates. Exposure of target bacterial and protozoan isolated to ENPs results in cell growth reduction, which progressively lead to cell inhibition. The toxicity effects of the target ENPs towards wastewater bacterial and protozoan population may diminish the performance of biological treatment processes and affect the efficiency of wastewater treatment plants, in producing effluent of high quality in the long term.

Recommendations for further studies: based on the results obtained in this study, some gaps were identified for future work and these include:

i. Investigation on the bacterial species highly sensitive to the presence of ZnO ENPs, in order to understand which stages of the activated sludge wastewater treatment processes are more affected by the presence of nanoparticles. This will help to develop methodologies for overcoming the potential adverse effects of ENP.;

ii. Investigations on the impacts of ENP sludge accumulation on sludge treatment processes, such as anaerobic digestion.

iii. Elucidation of the mechanism governing ENPs accumulation on sludge and biofilms, which may help assess the possible mitigation of their long-term impacts.

ACKNOWLEDGEMENTS

The project team wishes to thank the following people for their contributions to the project:

Name	**Affiliation**
Dr V Naidoo	Water Research Commission (**Chairperson**)
Dr S Kumari	Durban University of Technology (DUT)
Prof J Limson	Rhodes University (RU)
Prof TAM Msagati	University of South Africa (UNISA)
Dr H Tutu	University of the Witwatersrand (WITS)
Prof L Tichagwa	University of Fort Hare (UFH)
Prof N Torto	Rhodes University (RU)
Prof MS Onyango	Tshwane University of Technology (TUT)
Prof LF Petrik	University of the Western Cape (UWC)
Mr J Nathoo	Nuwater

This page was left blank intentionally

CONTENTS

LIST OF FIGURES

LIST OF TABLES

ACRONYMS AND ABBREVIATIONS

APHA	American Public Health Association
AS	activated sludge
BET	Braunner, Emmett, and Teller (surface area)
CCDs	charge-coupled devices
CFU	colony forming unit
CNTs	carbon nanotubes
COD	chemical oxygen demand
CSIR	Council for Scientific and Industrial Research
DLS	dynamic light scattering
DNA	deoxyribonucleic acid
DO	dissolved oxygen
DOC	dissolved organic carbon
DRS	diffuse reflectance spectroscopy
EDL	electrical double layer
EDS	energy dispersive X-ray spectrometry
ENPs	engineered nanoparticles
EPS	extracellular polymer substance
ETAAS	electrothermal atomic absorption spectrometry
F/M	food per microorganism ratio
FAAS	flame atomic absorption spectrometry
FTIR	Fourier Transform infrared spectroscopy
GFAAS	graphite furnace atomic absorption spectrometry
HDPE	high density polyethylene
HFL	human fetal lung fibroblasts
HRT	hydraulic retention time
HRTEM	high resolution transmission electron microscopy
ICP-MS	inductively coupled plasma mass spectrometry
ICP-OES	inductively coupled plasma optical emission spectrometry
MHA	Muller Hinton agar
MIC	minimum inhibition concentration
NA	nutrient agar
NB	nutrient broth
NIR	near infrared
NMs	nanomaterials
NOM	natural organic matter
NPs	nanoparticles
OECD	Organization for Economic Co-operation and Development
OUR	oxygen uptake rate
PTFE	polytetrafluoroethylene
QD	quantum dots

RAS	return activated sludge
ROS	reactive oxygen species
SRFA	Suwannee River fulvic acid
TEM	transmission electron microscopy
TOC	total organic carbon
TSS	total suspended solids
VOCs	volatile organic carbon
WAS	waste activated sludge
WRC	Water Research Commission
WWTP	wastewater treatment plant
XRD	X-ray diffraction spectroscopy

CHAPTER 1

INTRODUCTION

Preamble

This chapter presents the problem statement, background to the study, key research questions, aims and objectives of the study. The focus of the study was to investigate the fate and behaviour of ZnO ENPs after they were introduced into a simulated wastewater treatment system. This was achieved by investigating the physicochemical parameters and stability of ZnO ENPs in wastewater as well as monitoring of the impact of the ENPs on the bacterial degradation of the organic matter, in a simulated wastewater treatment plant.

1.1 Problem Statement

Wastewater treatment plants (WWTPs) have been utilized for the removal and/or degradation of contaminants from wastewater for generations, and they still play a pivotal role on the sustainable wastewater recycling (Sonune and Ghate, 2004). The treated wastewater effluent is discharged into the natural water reservoirs that include rivers and lakes. The sludge generated during wastewater treatment has several applications that include its use as fertilizer in agriculture (Sykes, 2003). However, under certain circumstances the sludge is disposed of for incineration where the residue ashes are landfilled or the sludge is landfilled without any further treatment (Metcalf and Eddy, 2004). The methodology employed for pollutant removal or degradation in WWTPs depends upon the nature of the wastewater. Among the methodologies employed in treating municipal wastewater, the biological processes constitute the oldest, cheapest and most used methodology worldwide up to date (Sonune and Ghate, 2004).

The biological wastewater treatment processes employ activated sludge (AS) consisting of a consortium of bacteria essentially to degrade organic matter present in wastewater (Strom and Jenkins, 1984). The AS typically treats biodegradable organic material present in domestic sewage as well as effluents from other forms of diverse sources such as pulp and paper mills, food industries, abattoirs, textile mills, edible oils, coal gasification wastes, petrochemical wastes, and oil refinery wastes (Metcalf and Eddy, 2004). The AS can also adsorb toxic substances thereby removing them from wastewater (Kiser et al., 2010; Sheng et al., 2008).

However, the presence of toxic substances in WWTPs may inhibit the bacterial activity and thus adversely impact on the wastewater biological treatment processes.

Nanotechnology is currently among the most promising emerging technologies aimed to address both societal- and industrial-related challenges in an endeavour to improve the quality of life. The potential market value for nanoproducts from 2011 to 2015 has been predicted to go up to US$1 trillion per annum (Navarro et al., 2008) while the production is predicted to increase to about 58 000 tons by 2020 (Royal Society and Engineering Council Report, 2004). The ENMs constitutes the basic building blocks of nanotechnology; and are widely applied in electronic, biomedical, personal care and automotive products (Rupasinghe, 2011). Due to the increasing widespread use of ENMs, their disposal to the sewage as their final sinks is inevitable and metal-oxides such as ZnO ENPs will certainly be released into the environment during manufacturing, transportation, use, and disposal phases of their lifecycle because they are produced in large quantities as well as applied in diverse commercial products (Brar et al., 2010).

Therefore, WWTPs are a significant point source for ENMs entering into the environment (e.g. aquatic systems, soils and air) through treated effluent, bio-solids, and plant-generated aerosols (Westerhoff et al., 2011; Musee et al., 2011; Brar et al., 2010; Gottschalk et al., 2010; Kiser et al., 2010; Kiser et al., 2009; Limbach et al., 2008; Stone et al., 2010; Nowack & Bucheli, 2007). Considering the ZnO ENPs application in a broad range of products including sunscreens, paints, cosmetics, dye-synthesised cells, plastic additives, catalysts and electronics, due to the distinctive physicochemical (e.g. thermal, electronic and optical) properties (Keller et al., 2010; Musee, 2011; Zhou et al., 2010) their production will increase, thus increasing their likelihood release into the wastewater systems. However, little is known about the removal efficiency and adverse effects of ENMs in WWTPs (Westerhoff et al., 2011; Kaegi et al., 2010; Musee, 2011).

Currently, the disposal of nanoproducts to the sewage system is already occurring (Brar et al., 2010; Kiser et al., 2009) though inadequate, the available data suggest that ENMs may present unknown and likely unpredictable health and environmental risks (Auffan et al., 2009; Baun et al., 2008; Biswas and Wu, 2005; Boxall et al., 2007; Bystrzejewska-Piotrowska et al., 2009; Maynard et al., 2006; Moore, 2006). Moreover, only recently studies have been initiated in determining the possible removal mechanisms of ENMs during wastewater treatment as well as their fate and behaviour in terms of uptake and bioaccumulation (Limbach et al., 2008; Kiser et al., 2009; Choi et al., 2009; Brar et al., 2010; Chauque et al., 2013). Notably, these studies are too few to provide solid scientific basis to draw firm conclusions on the potential effects of ENMs in the wastewater systems. As a result, concerns have been raised over the environmental fate, behaviour and toxicity of ENMs. In this regard, understanding the stability of ENMs in aquatic systems in terms of forming aggregates and/or agglomerates that sediment or dissolve, are among the important factors related to the fate of nanoscale materials in the aquatic environment (Bian et al., 2011). Therefore, given that the WWTPs are among the most significant point sources of ENMs releases into the aquatic systems, it becomes imperative that these nanoscale materials' fate and behaviour are studied in the environmental system such as water systems including WWTPs.

The extensive production, manufacturing and application of metal and metal oxides commercial nanomaterials (NMs) has remarkably increased over the past years. This is due to their unique surface -to- volume ratio, size/quantum effect and increased atoms at the grains boundaries, making them different from the bulk material counterparts (Heinlaan et al., 2008; Akbari et al., 2011; Premanathan et al., 2011). Of all the commercial NMs, zinc oxide (*n*ZnO) and silver (*n*Ag) are among the most produced NMs, due to their physicochemical properties indicating different spectra of activities and morphologies. It has been reported that *n*ZnO have unique ceramic texture, photocatalytic capacity, piezoelectric properties used as additives (to functionalize as semiconductor), and photo-oxidizing ability against chemical and biological species (Adams et al., 2006; Ju-Nam and Lead 2008; Padmavathy and Vijayaghavan, 2008; Aruoja et al., 2009; Premanathan et al,. 2011). On the other hand, silver nanomaterials have found usage in medical devices for over 2 000 years, leading to a widespread attraction, exploitation and application in the medical field as a bactericidal and as a therapeutic agent and food preservation (Prabhu and Poulose 2012). This is owing to their high optical, thermal conductivity and electric properties, which lead to major applications as catalysts, optical sensors of zeptomole (10−21) concentration in textile engineering, electronics and optics (Choi et al., 2008a; Ju-Nam and Lead 2008; Bystrzejewska-Piotrowska et al., 2009; Rai et al., 2009; Thwala et al., 2013).

The emergence of nanoproducts has introduced engineered nanomaterials (ENMs) among the increasing emerging contaminants into WWTPs (Musee et al., 2011; Gottschalk et al., 2010; Nowack & Bucheli, 2007). However, the adverse impacts of these contaminants to the treatment efficiency of WWTPs are largely non-quantified (Brar et al., 2010). In addition, the fate and behaviour of ENPs from influent point to the effluent discharge point of WWTPs is currently not well understood. This is presently of concern given there are no known techniques nor adequate scientific knowledge to inform our collective understanding on how ENMs should be managed to mitigate against both short- and long-term effects to the human health and other biological life forms in the environment. Therefore there are key questions that ought to be raised with regards to ENMs, as stated below.

1.2 Key questions

The following key questions were generated to meet the objectives of this research;

i. Can engineered metal-oxides based nanomaterials such as ENPs be transformed and removed from wastewater through processes like: adsorption, aggregation, sedimentation, flocculation, and precipitation, during activated sludge wastewater treatment process or will they persist in the treated wastewater effluent?
ii. Do engineered metal-oxides based nanomaterials such as ENPs affect the efficiency of WWTPs on the organic matter removal?
iii. Do ENPs significantly affect the microorganisms with respect to their livelihood and population?

1.3 Aim and objectives of the study

The aim of the study was to investigate the fate and behaviour of ZnO ENPs after they are introduced into a simulated wastewater treatment system. This was achieved by investigating the stability of ZnO ENPs in wastewater as well as monitoring of the physicochemical characteristics of ZnO ENPs in a simulated wastewater treatment plant. This was achieved through the following objectives:

i. Investigate the stability of ENPs in wastewater to assess how they are influenced by the presence of natural organic matter as well as variations in pH and ionic strength variables;
ii. Characterize the physicochemical parameters of ENPs before and after they are introduced into a simulated wastewater treatment plant;

iii. Monitor the wastewater quality parameters COD, DO, DOC, and TSS to ascertain the plausible impact of ENPs on the WWTP efficiency; and
iv. Analyse the suitability of the OECD sewage treatment plants model for assessing the fate, behaviour, and potential impact on the organic matter removal efficiency.
v. Determine the microbial concentrations of the test isolates at different concentrations of ENPs and investigate the effects of the selected environmental factors on interactions of microbial populations and the NMs.

CHAPTER 2
LITERATURE REVIEW

Preamble

This chapter reviews the methodologies used for the treatment of wastewater, their role as water recycling facilities and the ability to remove pollutants from wastewater. The chapter also outlines the nanotechnology and the impacts associated with the use of nano-products to the environment and the human health, as well as a review of the risks arising from the disposal of nano-products into the sewerage systems. The analytical techniques used for the characterization and quantification of the ZnO engineered nanoparticles throughout the study have also been reviewed. The methodologies on bacterial assays involved assessment of pure bacterial culture growth; determination of minimum inhibition concentration (MIC); bacteria activities in the killing kinetics for *n*Ag and *n*ZnO in broth; bacterial susceptibility of *n*Ag and *n*ZnO; extraction and analysis of extracellular polymer substance (EPS); determination of the effect of pH on survival limit of single bacterial isolates exposed to nanomaterials; comparing survival limit of consortium isolates (bacteria/protozoa) exposed to nanomaterials with change of pH.

2.1 Introduction

Through their lifecycles, *n*ZnO and *n*Ag are likely to enter natural water bodies channelled via wastewater treatment plants (WWTPs) (Aruoja et al., 2009). Thereafter, leading to environmental risks associated to possible detrimental implication on microbial driven processes and public health concern (Neal 2008; Tso et al,. 2010; Baalousha et al,. 2013; Li et al., 2013; Beddow et al., 2014; Musee et al., 2014). It has been reported that municipal wastewater treatment plants (WWTPs) are the main sources of pollutants as they transport contaminated effluent into water surface, landfills and soils (Kiser et al., 2010). Biological treatment of wastewater involves confining naturally occurring bacteria at very much higher concentrations in tanks. These bacteria, together with some protozoa and other microbes, are collectively referred to as activated sludge. During water treatment, the bacteria remove small organic carbon molecules by degrading them and as a result the bacteria grow as they feed on the waste, while at the same time the wastewater is cleansed. It has been reported that the control of the treatment process can be affected by the changes in the composition of the bacterial flora of the treatment tanks, and the changes in the sewage passing into the plant (Davies 2005). High concentrations of toxic chemicals can produce a toxic shock that kills the bacteria. This can result in inefficient performance of the wastewater treatment systems to produce effluents of the required standards.

Currently, majority of investigations have been focused on human health implications of NMs; very few efforts consider the environmental implications of NMs, including the fate, transport, and toxicity, to promote sustainable use of these novel materials (Ju-Nam and Lead, 2008). Furthermore, there is still a knowledge gap on the actual uptake mechanism, induce effect, transport in biological compartments and toxicity modes of action in particle specific (Ju-Nam and Lead 2008; Baker et al., 2013). Even if the exact antibacterial mode of action is yet to be discovered for *n*ZnO, the catalytic oxidation in silver promoted by metallic silver reacting with monovalent silver ions are likely to contribute to toxicity (Ju-Nam and Lead 2008). To date, antimicrobial research studies of *n*ZnO and *n*Ag have vastly increased towards microbial species and freshwater organism, including duckweed, nematodes (*Caenorhabditis elegans*), waterflea (*Daphnia magna*), zebra fish, and pond snails (*Lymnaea stagnalis*) (Adams et al., 2006; Heinlaan et al., 2008; Aruoja et al., 2009; Azam et al., 2012; Baker et al., 2013). It has been pointed out that it is the rate of exposure and effect of nanomaterials on bacterial strains that varies due to different cell physiological characteristics and metabolism (Adams et al., 2006). In addition, the bioavailability and toxicity of NMs towards bacteria may alter the normal ecological process, functions and productivities (Neal 2008). Thus, bacterial cells actively produce extracellular polymeric substances (EPS), which are polysaccharides rich in organic matter. These polymeric substances are known as a protective barrier for cell wall during exchange processes and in contact with environment (Kiser et al., 2010) and may stabilise NMs, due to their ability to produce soluble biomass associated products (Laspidou and Rittmann 2002).

A number of studies have depicted that NMs are able to (i) adhere to a cell, block essential pores and membrane functions; (ii) enter the cell by endocytosis via pores, degrades the lipopolysaccharide molecules and accumulate inside cells (Li et al., 2008; Liang et al., 2010; Musee et al., 2011; Baker et al., 2013), facilitate reactive oxygen species (ROS) production by redox reaction with oxygen, damage deoxyribonucleic acid (DNA), resulting in the loss of cell replication ability (Neal 2008; Padmavathy and Vijayaraghavan, 2008; Liang et al., 2010;

Musee et al., 2011; Baker et al., 2013). Regardless of the belief that *n*ZnO are non-toxic, biosafe and biocompatible, toxicological activities reports have shown *n*ZnO to cause damages on the cell membrane due to oxidative stress (Huang et al., 2008). In addition, experimental studies showed near complete inhibition of *B. Subtilis* due to *n*ZnO and that in the presence of both light and in darkness, while *E. coli* has been found less susceptible to *n*ZnO in dark conditions (Adams et al., 2006; Dasiri et al., 2013). This is owing to novel physicochemical properties of NMs; among such is the size scale that is relative to that of bacteria and recalcitrant environmental pollutants (Choi and Hu 2008; Choi et al., 2008b).

2.2 Organization for Economic Co-operation and Development (OECD) guidelines for the testing of chemicals

The transition from the use of soap-based detergents to the newly developed synthetic detergents in the mid-20th century caused excessive foaming in wastewater treatment plants and in water systems including rivers and lakes (Scott and Jones, 2000). The removal of these detergents was limited and even compromised the degradation of the organic matter in the wastewater treatment plants. However, to conduct biodegradation studies of the emerged surfactants in the large scale wastewater treatment plants was impractical and costly. Therefore, the Organization for Economic Co-operation and Development (OECD) adopted model units in representation to the two main types of aerobic biological wastewater treatment (activated sludge and percolating or trickling filtration) to conduct biodegradation studies. This protocol provided guidance for the construction of the simulated wastewater treatment plant and is known as the OECD guideline for the testing of chemicals, revised in OECD 303 in 2001. Nowadays, OECD accounts for 40 countries members worldwide and represent 80% of the world trade and investment, giving it a pivotal role in the world economy.

2.3 Wastewater treatment processes

Wastewater is a combination of liquids and solids discharged to the sewer systems originating from sanitary housing, commercial, industrial and institutional facilities as a result of human activity in addition to the storm water, groundwater and surface water that might have infiltrated to the sewerage. In general, wastewater is comprised of suspended solids, sediments, minerals, toxic compounds, inorganic chemicals, dissolved and suspended organic matter (volatile or biodegradable), nutrients, pathogens and parasites (Sonune and Ghate, 2004). The process of reducing the load of solids, transforming the organic matter from highly complex form to relatively stable organic solids, and removal or inactivation of pathogens and parasites in wastewater, is known as the *wastewater treatment* (Sonune and Ghate, 2004).

Wastewater treatment processes were first introduced to the human civilization in the early 20th century in Britain and readily widespread to the entire world due to the pivotal role they play as water recycling facilities. Currently, South Africa has over 50 wastewater treatment plants distributed in eight provinces. The methodology employed in wastewater treatment processes depends upon the application required to the treated wastewater effluents. The effluents can be used to supplement the public water supply, irrigation in agriculture or for disposal in the environment (e.g. water systems including rivers and lakes) to replenish the anthropogenic water usage. Though the composition of wastewater depends on the lifestyle and dietary of each society, Table 2.1 indicates the general characteristics of raw wastewater (Metcalf and Eddy, 2004).

Table 2.1: Typical characteristics of untreated domestic wastewater.

Contaminant	Unit	Concentration		
		Low strength	**Medium strength**	**High Strength**
Solids, total (TS)	mg/L	390	720	1230
Dissolved, total (TDS)	mg/L	270	500	860
Fixed	mg/L	160	300	520
Volatile	mg/L	110	200	340
Suspended solids, total (TSS)	mg/L	120	210	400
Fixed	mg/L	25	50	85
Volatile	mg/L	95	160	315
Settleable solids	mg/L	5	10	20
Biochemical oxygen demand, 5-d, 20ºC (BOD_5, 20ºC)	mg/L	110	190	350
Total organic carbon (TOC)	mg/L	80	140	260
Chemical oxygen demand (COD)	mg/L	250	430	800
Nitrogen (total as N)	mg/L	20	40	70
Organic	mg/L	8	15	25
Free ammonia	mg/L	12	25	45
Nitrites	mg/L	0	0	0
Nitrates	mg/L	0	0	0
Phosphorus (total as P)	mg/L	4	7	12
Organic	mg/L	1	2	4
Inorganic	mg/L	3	5	10
Chlorides	mg/L	30	50	90
Sulfate	mg/L	20	30	50
Oil and grease	mg/L	50	90	100
Volatile organic carbon (VOCs)	mg/L	< 100	100-400	> 400
Total coliform	No./100 mL	10^6-10^8	10^7-10^9	10^7-10^{10}
Fecal coliform	No./100 mL	10^3-10^5	10^4-10^6	10^5-10^8
Cryptosporidium oocysts	No./100 mL	10^{-1}-10^0	10^{-1}-10^1	110^{-1}-10^2
Giardia lamblia cysts	No./100 mL	10^{-1}-10^2	10^{-1}-10^2	110^{-1}-10^3
Alkalinity (as $CaCO_3$)	mg/L	50	100	200

Wastewater treatment usually involves physical, mechanical, biological and chemical processes. Biological processes can be divided into two categories namely suspended growth (e.g. activated sludge and aerated lagoons) and attached growth or biofilm (e.g. trickling filters and rotating biological contactors) (Sykes, 2003). In the process operations, different stages can be distinguished into: (i) *preliminary treatment*, involving screening, grinding and grit removal to prevent damages of the equipment; (ii) *primary treatment*, involving sedimentation processes for the removal of floating and settleable materials; (iii) *advanced primary treatment*, involving the addition of chemicals for the removal of suspended and dissolved solids; (iv) *secondary treatment* (with or without nutrient removal), involving biological and/or chemical processes for the removal of organic matter and (v) *advanced (tertiary) treatment*, involving a combination of biological, chemical and physical processes to enhance efficient removal of residual suspended solids, organic matter, nutrients (phosphorus and nitrogen) and toxic substances that are not significantly eliminated during the conventional secondary treatment following the removal or inactivation of pathogens and parasites (Metcalf and Eddy, 2004). The diagram below (Figure 2.1) is an illustration of a typical activated sludge process for municipal wastewater treatment as adapted from Metcalf and Eddy, 2004.

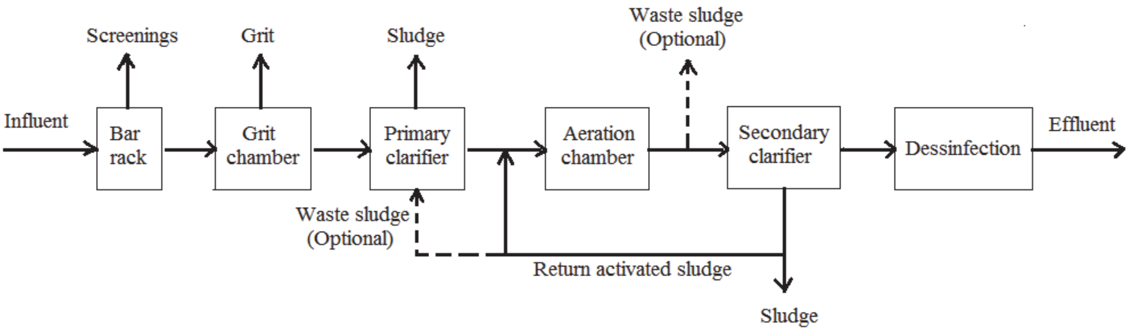

Figure 2.1: Typical (simplified) flow diagram of an activated sludge process for wastewater treatment.

Historically, wastewater treatment processes were comprised of bioreactors employing microorganisms (activated sludge) for the degradation of organic matter and removal of contaminants and were denoted as *conventional wastewater treatment* processes. Over the last decades, the water quality regulations became stringent due to the increased attention given to trace contaminants in water favouring therefore, the emergency of alternative technologies in order to upgrade or improve the conventional wastewater treatment processes (Abdulgader et al., 2013). Currently, membrane systems including microfiltration, ultrafiltration, nanofiltration and reverse osmosis became competitive with conventional biological treatment in terms of price and cost while producing far better treated water effluents (Baker, 2012). Membrane technologies in wastewater treatment plants are usually combined with other process units either for pre-treatment or post-treatment of wastewater. Membranes can also be combined with bioreactors as one unit process or applied as bioreactors effluent receptors. In addition, membrane processes are coupled with processes including coagulation, flocculation, sedimentation, adsorption and ozonation to enhance high quality effluents and such processes are known as *advanced wastewater treatment* processes (Metcalf and Eddy, 2004; Sonune and Ghate, 2004).

2.3.1 Activated sludge wastewater treatment processes

Activated sludge (AS) is a consortium of microorganisms employed essentially to degrade the organic matter present in wastewater. The AS consists of aerobic and anaerobic microorganisms of autotrophic or heterotrophic nature that are comprised of bacteria, fungi, protozoa, and rotifers including human and animal viruses through fecal excretion though the former tends to reduce during the wastewater treatment (Sykes, 2003). The predominance of these species of microorganisms depends upon the environmental conditions, process design and mode of operation, and the characteristics of the influent wastewater. During the AS wastewater treatment processes, the AS is mixed together with the influent wastewater and the compressed air or oxygen is forced into the wastewater liquor by mechanical means to develop a biological floc that transforms the dissolved organic matter into a flocculent microbial suspension that can gravitationally settle out in the clarifier. The AS process can treat any biodegradable organic material present in domestic wastewater as well as effluents from pulp and paper mills, food industries, abattoirs, textile mills, edible oils, coal gasification wastes, petrochemical wastes and oil refinery wastes.

2.3.1.1 Activated sludge performance characteristics

2.3.1.1.1 Food per microorganism ratio (F/M)

The chemical oxygen demand (COD) and biochemical oxygen demand (BOD) are used as the surrogate parameters to measure the organic matter available for the microorganisms while the volatile suspended solids is used as an indication of the amount of microorganisms in the AS (Sykes, 2003). The ratio of organic matter available to the amount of microorganisms is known as food to microorganism's ratio (F/M) (Sykes, 2003). This parameter is of utmost importance and provides an indication of microorganism's growth rate. When the F/M ratio is high is an indication that microorganisms are developing rapidly and the opposite behaviour is found for lower F/M ratio.

2.3.1.1.2 Formation of flocs

With time the microorganisms lose their motility, accumulate slime and agglomerate forming flocs that can grow in size, compact and settles out. However, the mixing process prevents the settlement of the flocs, keeping them small and thus improving the contact between the cells, food and oxygen. The optimal conditions for the formation of flocs depend on the availability of nutrients, oxygen, appropriate pH and temperature (Spellman, 2003; Sykes, 2003).

i. *Mixing:* The mixing process in the AS process is of utmost importance. In one hand it allows well distribution of oxygen and nutrients, favouring their appropriate contact to the microorganisms. On the other hand, inappropriate mixing results in the scission of flocs and lead to poor settlement of the sludge (Spellman, 2003).

ii. *Temperature:* The biochemical reactions are temperature dependent and an increase in the temperate favours the process to occur more efficiently. Generally, in winter more bacteria are required for the organic matter removal compared to the summer season (Sykes, 2003).

iii. *Dissolved oxygen (DO):* The DO should be kept around 2 mgL^{-1} or above to provide the microorganisms with enough oxygen for the oxidation of the organic matter from wastewater and lead to the formation of flocculent microbial suspension (Sykes, 2003). If the DO is less than the aforementioned value, the microorganisms on the surface of the floc exhaust the DO before it gets into the centre of the floc and this phenomenon leads to cell death and consequently the scission of the floc.

iv. *pH:* Most of the enzymes used for the biochemical reaction require neutral conditions. Therefore, the pH should be kept within 7.0-7.5 range for the optimal microorganisms development (Sykes, 2003).

v. *Nutrients:* The microorganisms' nutrients are comprised of carbon, nitrogen, phosphorus including trace amounts of metals such as sodium, potassium, magnesium, and iron, among others (Sykes, 2003). The municipal wastewater is rich in organic matter. Therefore, enough nutrients are provided to the microorganisms. However, wastewater treatment plants that receive lots of industrial wastewater have deficiencies in nutrients and lead to poor microorganisms´ activity, resulting in poor organic matter removal. In general, the nutrients presents the carbon, nitrogen and phosphorus (C:N:P) in the ratio of 100:10:1 (Sykes, 2003).

2.3.1.1.3 Oxygen uptake rate

The oxygen uptake rate (OUR) measures the respiration rate of microorganisms. High oxygen uptake rate is an indication of high F/M ratio and young sludge while the opposite indicates lower F/M ratio and mature sludge (Sykes, 2003).

2.3.1.1.4 Filamentous bacteria

The development of filamentous bacteria in the wastewater treatment plant results in the bulking and foaming, whose formation directly affects the efficiency of the activated sludge wastewater treatment process (Strom and Jenkins, 1984).

Appropriate amounts of filamentous bacteria are beneficial to the activated sludge processes because the filaments allow the formation of larger and stronger flocs, removal of small particulates and consequently reducing the turbidity of the effluents (Strom and Jenkins, 1984). Absence of filamentous bacteria can lead to turbid effluents. However, excessive growth of filamentous bacteria causes filamentous bulking that result in poor compaction and settlement of the sludge and may compromise the disinfection of the effluents due to high turbidity. Filamentous bulking is nowadays one of the effluent noncompliance main cause and in some circumstances leads to excessive sludge recycle rates (Strom and Jenkins, 1984). On the other hand, foaming is caused by the production of bio surfactants, hydrophobicity of the cell walls, and the particle bridging that prevents the liquid drainage and film thinning during the activated sludge processes. Foaming compromises the quality of the effluents due to high turbidity.

2.3.2 Biological removal of contaminants

The flocculent nature of the activated sludge enables it with high active surface area for the sorption and removal of toxic substances from wastewater including metals, synthetic organic chemicals and suspended solids (Kiser et al., 2010; Sheng et al., 2008; Dobbs et al., 1989). The biomass ability to sequester and thus remove contaminants from wastewater has been reported elsewhere (Metcalf and Eddy, 2004). The removal mechanisms of metal and metal-based nanomaterials in municipal wastewater treatment plants can be predicted based on the established mechanisms for the removal of heavy metals in the same facilities. The metal ions removal in these engineered systems is governed by adsorption and complexation with microorganisms. The metallic ions are complexed by carbonyl groups in microbial polysaccharides and polymers, and adsorption occurs in the negatively charged microbial surfaces or they are absorbed by protein materials in the biological cells (Metcalf and Eddy, 2004). In addition, chemical precipitation, carbon adsorption, ion exchange, and reverse osmosis processes are usually employed in these facilities for the removal of heavy metals with predominance of precipitation processes employing hydroxide (OH^-) and sulfide (S^{2-}) and in special occasions also carbonate (CO_3^{2-}). Furthermore, co-precipitation of metal ions with phosphorus enhances their removal from the wastewater (Metcalf and Eddy, 2004). The metal ions removal mechanisms aforementioned may apply for the removal of Zn^{2+} released from ZnO nanoparticles in similar engineered systems and may attenuate their bioavailability while the nanoparticles are expected to settle out with the bio-solids.

2.3.3 Applications of bio-solids and treated wastewater effluents

Wastewater treatment plants (WWTPs) play important role on the water recycling and protection of the human health and the environment. The process operations of municipal WWTPs are designed to provide effluents and the bio-solids with pre-determined characteristics in accordance with their final application (e.g. reuse or disposal). In most cases, the effluents are released back to water streams including rivers and lakes for replenishment (Metcalf and Eddy, 2004; Spellman, 2003). In semi-arid regions, because of water shortages, the wastewater effluents are recharged to the groundwater for replenishment or to control the saltwater intrusion. Other applications of wastewater effluents include non-potable uses (e.g. fire protection and toilet flushing), and potable reuse (e.g. blending in water supply reservoirs) (Metcalf and Eddy, 2004).

On the other hand, any application of biosolids result in their extended treatment in the environment. When biosolids are applied in agricultural or forest land, the plants aid in the removal of nutrients. However, this application has raised concerns because the disposal of nanomaterials in wastewater treatment plants is already occurring and their likelihood to be included in the bio-solids has been reported elsewhere (Brar et al., 2010; Gottschalk et al., 2009; Kiser et al., 2009), while the adverse effects to the plants is not yet well understood. In the disposal of bio-solids to the landfills, the soil microorganisms and sunlight aid in the destruction of pathogens and toxic substances. During this process, certain nanomaterials may be washed out of the matrix of biosolids through rainfall and released to the groundwater due the nanomaterial dissolution.

2.4 Nanotechnology and Engineered Nanomaterial Waste

Materials with dimensions at the nanoscale (10^{-9} m of magnitude) with at least one dimension less than 100 nm are usually denominated nanomaterials (NMs). They include nanostructured components with one dimension at the nanoscale (e.g. nanolayers), or two dimensions on the nanoscale (e.g. nanowires and nanotubes), and nanoparticles (e.g. quantum dots) (Farré et al., 2011; Peralta-Videa et al., 2011). These materials occur in nature as a result of anthropogenic sources including industrial and combustion processes, as well as a result of the emerging technologies (Farré et al., 2011; Peralta-Videa et al., 2011). The designing and manufacturing of nanoscale materials, products and devices with specific chemical and physical properties is the nanotechnology denomination (Kaegi et al., 2011; Maynard et al., 2006). Nanotechnology has emerged and expanded in the late 21st century and currently is one of the most promising technologies with an estimated market value from 2011 to 2015 to go up to US$1 trillion per annum (Navarro et al., 2008). Nanotechnology is widely applied in electronic, biomedical, personal care and automotive industry.

Engineered nanomaterials (ENMs) encompass those nanoparticles synthesized and modified in order to enhance their performance in several technological and industrialized processes (Peralta-Videa et al., 2011). Nanomaterial composition differs according to their formulation. Fullerenes and carbon nanotubes (CNTs) are NMs classified as carbon-based materials, quantum dots (QD) as semiconductors, metal and metal-oxides as inorganic nanoparticles (Musee, 2010; Peralta-Videa et al., 2011; Farré et al., 2011).

Nanomaterials can be more toxic than larger particles (bulk materials) of the same composition because of their large specific surface area and unique catalytic properties (Liu et al., 2011). They also differ from their bulk counterparts mainly because of the high surface/volume ratio. For example, it has been estimated that 10 nm nanoparticles have 35-40% of the atoms localized at the surface compared with less than 20% for particles larger than 30 nm. Therefore, the physicochemical, optical, reactivity, and electrical properties change compared to their respective bulk counterparts. In addition, the media where nanomaterials are present determine their behaviour, reactivity, and potential toxicity (Auffan et al., 2008; Peralta-Videa et al., 2011).

Due to the anticipated high-volume production and widespread use, nanomaterials will inevitably be released into the environment during their lifecycle and will potentially be released in the sewerage as their final sinks. Therefore, environmental risk assessment of nanomaterials merits profound understanding.

2.4.1 ZnO engineered nanoparticles (ENPs)

Zinc oxide is an inorganic compound, naturally occurring as a white powder known as "Zincite". In nature three crystal forms of ZnO can be found, namely wurtzite, zincblend and rock salt with the former being the most stable at room temperature (Rupasinghe, 2011). Due to the distinct physicochemical properties such as high band gap, high thermal conductivity, heat capacity and melting point, ZnO is widely used in electronics and ceramics (Degen and Kosec, 2000). However, as the particle size of a material decreases to the nanoscale, the surface area and the number of atoms in the surface increase and thus, differences in physicochemical properties from nanoscale materials to the bulk counterparts are observed. Therefore, the thermal, electronic and optical properties of ZnO nanoparticles become more prominent compared to the bulk counterpart. As a result, ZnO nanoparticles are widely applied in various products including dye sensitized cells, cosmetics, sunscreens, paints, plastic additives, and electronics.

Nowadays, ZnO is manufactured in different morphologies such as nanorods, nanowires, nanoparticles and tetrapods to enhance distinct properties and applications. As nanoparticle, ZnO is applied in sunscreens and cosmetics due to the photo-catalytic property; as nanorod arrays are used in photoelectric systems including nanolasers, schottky diodes, biosensors and solar cells; as thin films are used in drug delivery and medicine; and as nanotubes are used in dye sensitized solar cells (Rupasinghe, 2011). Therefore, due to the broad spectrum of ZnO nanomaterials´ application, their likelihood to be released to the sewerage during the lifecycle is predictable.

2.4.2 Ecotoxicity of ZnO engineered nanoparticles (ENPs)

The unique and distinct physicochemical characteristics of nanomaterials have made nanotechnology a multifaceted and multidisciplinary area. As a result, the introduction of a variety of nano-products to the society was predictable (Maynard et al., 2006). Currently, it is impossible to ignore the advances of nanotechnology in providing the society with a better quality of life. However, it is also undeniable that nanotechnology may adversely impact the environment including human beings. However, the available published data, though inadequate suggests the likelihood of highly unpredictable health and environmental risks to the society (Auffan et al., 2009; Baun et al., 2008; Boxall et al., 2007; Bystrzejewska-Piotrowska et al., 2009; Maynard et al., 2006; Moore, 2006). Therefore, their manipulation has raised concerns over the environmental fate, behaviour and toxicity.

From the available published data on ZnO nanoparticles ecotoxicity, the majority of the studies are dedicated to the bacteria compared to other species (Ma et al., 2013). The toxicological mechanisms of ZnO nanoparticles toward different bacteria lies on particle dissolution with dependence to particle size, generation of reactive oxygen species (ROS) and photo-induced toxicity under environmentally relevant UV radiation (Ma et al., 2013; Larner et al., 2012; Li et al., 2011; Nair et al., 2009). However, the ZnO ability to generate ROS was found to depend upon the surface functionalization. Findings on cytotoxicity and genotoxicity of ZnO nanoparticles suggested diminished ROS viability due to surface coating with oleic acid and poly(methacrylic acid) (Yin and Casey, 2010).

Adverse impact to human cells due to exposure to ZnO NPs has been reviewed and caution on its manipulation advised. Qiang and co-workers (2011) reported cellular mitochondrial dysfunction, morphological modifications and apoptosis to the human fetal lung fibroblasts (HFL1) induced by ZnO, TiO_2, SiO_2, and Al_2O_3 nanoparticles with ZnO presenting the most prominent toxicity. In addition, ZnO nanoparticles selectivity to kill cancerous cells compared to normal cells was observed and dependence on the surface coating played a pivotal role on the nanoparticle´s toxicity (Premanathan et al., 2010; Nair et al., 2009).

The occurrence of nanomaterials in WWTPs resulted in environmental impact studies for aquatic life due to their likelihood to be released to water systems. Therefore, the toxicity toward crustaceans (e.g. Daphnia magna and Thamnocephalus platyurus) through exposure to CuO and ZnO nanoparticles was investigated and found to be due to the particle dissolution rather than the nanoparticle bioaccumulation (Wiench et al., 2009; Heinlaan et al., 2008). The water chemistry also played a role on the toxicity to crustaceans. The presence of tannic acid decreases the toxicity of ZnO nanoparticles more efficiently compared to humic, fulvic, and alginic acid, because it complexes the most free Zn^{2+} ions and thus reducing their bioavailability (Li et al., 2011). The natural waters remarkably decreased the toxicity of nanoCuO (but not that of nanoZnO) compared to artificial waters toward crustaceans and depended mainly on the concentration of dissolved organic carbon (DOC) (Blinova et al., 2010). Comparable toxicity for nanoparticulate ZnO, bulk ZnO, and $ZnCl_2$ to the freshwater alga Pseudokirchneriella subcapitata was observed and attributed solely to the dissolved zinc (Franklin et al., 2007).

The working force in the activated sludge wastewater treatment processes are the bacteria. Their ability to overcome or tolerate the presence of pollutants in wastewater including nanomaterials is of utmost importance because it may directly affect the performance of the current conventional wastewater treatment processes. Therefore, antibacterial activity of SiO_2, TiO_2 and ZnO nanoparticles toward Gram-positive bacteria (e.g. Bacillus subtilis, Streptococcus agalactiae) and Gram-negative bacteria (e.g. Escherichia coli and Pseudomonas aeruginosa) were investigated (Premanathan et al., 2010; Nair et al., 2009; Huang et al., 2008; Jones et al., 2007; Adams et al., 2006). The findings suggested that ZnO nanoparticles present the highest toxicological effects and the Gram-positive bacteria were the most susceptible. Cellular bioaccumulation of ZnO nanoparticles and bacterial cell damage was observed to E. coli and S. aureus (Applerot et al., 2009; Huang et al., 2008). However, dosages of ZnO nanoparticles up to 20 mgL^{-1} were found to be fatal to E. coli (Jiang et al., 2009). In addition, the isotonic and rich nutrient media improved the tolerance of E. coli to ZnO nanoparticles (Li et al., 2011). Particle size dependence of ZnO nanoparticles antibacterial toxicity toward Gram negative E. coli and Gram positive S. aureus was observed (Nair et al., 2009). The toxicity increased with reduction in particle size.

The disposal or reuse of the bio-solids raised concerns over the environmental impacts through their likelihood of adsorbing nanomaterials during the wastewater treatment (Brar et al., 2010). The toxicity studies of nanoparticles to the plants and terrestrial organisms have been initiated though scarce. Toxicity of TiO_2 and ZnO nanoparticles toward earthworm was investigated and ZnO nanoparticles were found to exert the most prominent toxicological effect to Eisenia fetida (Hu et al., 2010). Biotransformation of ZnO and CeO_2 nanoparticles by terrestrial plants was also investigated. The findings suggested no adverse effect to the soybean germination though they produced a differential effect on plant growth and element uptake (López-Moreno et al., 2010). In addition, only CeO_2 nanoparticles presented genotoxicity to the soybean plants.

The findings bring to light the importance of care during the manipulation and disposal of nanomaterials in order to prevent unintended environmental impacts, as well as the need for studies on mechanisms and factors that increase the toxicity to enhance risk management (Musee, 2010; Adams et al., 2006).

2.4.3 Stability of ZnO nanomaterials in the aquatic environment

Understanding the stability of ENMs in aquatic systems in terms of forming agglomerates or aggregates that settles out and sediment or the propensity to dissolve are among the important factors related to the fate of nanoscale materials in the aquatic environment (Bian et al., 2011). Studies on the stability of ZnO nanoparticles with respect to aggregation or dissolution in aqueous environments have been initiated and it was shown to directly affect their fate and behaviour. The water properties including pH, ionic strength, natural organic matter, and type of electrolyte coupled to the presence of complexing agents and UV radiation have an impact on the stability of ZnO nanoparticles (Bian et al., 2011; Han et al., 2010). In addition, the storage conditions may also affect the particle dispersity, size, phase, and surface functionality (Bian et al., 2011) owing to nanoparticles aging (Labille et al., 2010).

Natural organic matter (NOM), the main constituent of municipal wastewater, contains various compounds with diverse functional groups that can interact and impact the stability of nanomaterials. Nanomaterials coated with NOM can enhance stability in aqueous environment even at high ionic strength (Keller and Zhou, 2010). Some of the NOM constituents' effects on the stability of ZnO nanoparticles have been investigated and found to determine their uptake and distribution in the aqueous environment. The humic acid, one of the most prominent constituents of NOM, presents functional groups such as carboxylic ($–COO^-$) and phenolic ($-ArO^-$) in the molecule with high complexation capacity for metal ions (Zhang et al., 2009). The interaction with nanomaterials results in particle aggregation or disaggregation in accordance to the pH of the media. At low pH to pH_{PZC}, the humic acid adsorbs to the positively charged ZnO nanoparticles´ surface and lead to particle aggregation. At neutral conditions lead to partial disaggregation and enhanced stability of nanoparticle´s suspension. At pH greater than pH_{PZC} the humic acid coats the surface of ZnO nanoparticles and enhances nanoparticle´s stability via electrostatic and steric interactions (Omar et al., 2014). Further increase to high pH values, the molecule become opened and linear in shape, and thus disposing the functional groups for effective interaction with ZnO nanoparticles (Zhang et al., 2009) resulting in their dissolution (Bian et al., 2011). These findings may support in part the aggregation of ZnO nanoparticles in the freshwater systems that are usually rich in humic acid (Franklin et al., 2007). In addition, the presence of humic acid above its critical concentration (e.g. > 3 mgL^{-1}) can enhance the stability of ZnO nanoparticles at a given ionic strength (Bian et al., 2011). Coupled to these findings, a decrease in the released zinc from ZnO nanoparticles´ suspensions in wastewater and deionized water with changes in the pH and ionic strength was observed and the abiotic, bio-sorption, and biosolid settling were pointed out as the possible removal mechanisms (Chauque et al., 2013). The naturally occurring amino acids enhanced the stability of aqueous suspensions of ZnO nanoparticles (Molina et al., 2011) while the presence of citric acid led to the dissolution of ZnO nanoparticles with effect being exacerbated as the nanoparticle´s size became smaller (Mudunkotuwa et al., 2012).

The stability of particles in water can be assessed using Derjaguin – Landau – Verwey – Overbeek (DLVO) theory. This theory accounts for two forces between the particles: van der Waals (vdW) attraction and electrical double layer (EDL) repulsion. The sum of these two forces determines whether the net interaction between particles is repulsive or attractive (Zhang et al., 2008; Bian et al., 2011). The aggregation occur when the net interaction between particles is attractive and disaggregation or stability of particles occurs when the net interaction is repulsive. Bian and co-workers (2011) investigating the stability of ZnO NPs in natural water and Zhang and co-workers in the tap water, both found the increase in ionic strength to result in the compression of the EDL repulsive energy such that the net repulsive energy barriers between ZnO NPs became negligible leading to nanoparticle´s aggregation.

Predicting the reactivity of ZnO nanoparticles in aqueous media with hydroxide or hydrogen ions due to its amphoteric nature based in the bulk counterpart, the following chemical reactions can be expected (Degen and Kosec, 2000):

$$ZnO_{(s)} + 2H^{+}_{(aq)} \rightarrow Zn^{2+}_{(aq)} + H_2O_{(l)} \tag{2.1}$$

$$ZnO_{(s)} + H^{+}_{(aq)} \rightarrow Zn(OH)^{+}_{(aq)} \tag{2.2}$$

$$ZnO_{(s)} + OH^{-}_{(aq)} + H_2O_{(l)} \rightarrow Zn(OH)^{-}_{3\ (aq)} \tag{2.3}$$

$$ZnO_{(s)} + 2OH^{-}_{(aq)} + H_2O_{(l)} \rightarrow Zn(OH)^{2-}_{4\ (aq)} \tag{2.4}$$

$$Zn(OH)_{2\ (s)} \rightarrow Zn(OH)_{2\ (aq)} \tag{2.5}$$

$$Zn(OH)_{2\ (aq)} \rightarrow Zn^{2+}_{(aq)} + 2OH^{-}{}_{(aq)} \tag{2.6}$$

$$Zn(OH)_{2\ (aq)} \rightarrow Zn(OH)^{+}_{(aq)} + OH^{-}{}_{(aq)} \tag{2.7}$$

$$Zn(OH)_{2\ (aq)} + OH^{-}_{(aq)} \rightarrow Zn(OH)^{-}_{3\ (aq)} \tag{2.8}$$

$$Zn(OH)_{2\ (aq)} + 2OH^{-}_{(aq)} \rightarrow Zn(OH)^{2-}_{4\ (aq)} \tag{2.9}$$

$$Zn^{2+}_{(aq)} + OH^{-}_{(aq)} \rightarrow Zn(OH)^{+}_{(aq)} \tag{2.10}$$

$$Zn(OH)^{+}_{(aq)} + OH^{-}_{(aq)} \rightarrow Zn(OH)_{2(s)} \tag{2.11}$$

$$Zn(OH)_{2\ (s)} \rightarrow ZnO_{(s)} + H_2O_{(l)} \tag{2.12}$$

The predominance of one or more of the above chemical reactions is dependent on the pH of the media. Therefore, the reactions aforementioned coupled with the presence of multi-dentated complexing agents in the wastewater will definitely determine the fate and behaviour and speciation of ZnO nanoparticles in the wastewater treatment plant. In highly acidic solutions, the dissolution of ZnO is more likely to result from direct proton attack of the ZnO surface. At pH 6, soluble ionic forms will include Zn^{2+} and $Zn(OH)^{+}$. In aqueous solutions of pH greater than 9, the dissolution of ZnO is related to its hydroxide which produces soluble species in the form of hydroxyl complexes such as $Zn(OH)^{-}_{3\ (aq)}$, $Zn(OH)^{2-}_{4\ (aq)}$. Between pH 6 and pH 9 solid $Zn(OH)_2$ precipitate out of solution (Bian et al., 2011). Therefore, ZnO nanoparticles in wastewater might encounter change in charge dispersion due to the interaction with polyelectrolytes and thus contribute to a completely changed behaviour (Brar et al., 2010).

In aqueous environment, natural organic matter (NOM) can adsorb onto the surface of nanoparticles (Zhang et al., 2009) and suspensions of nanoparticles coated with NOM can enhance the stability over high ionic strength (Keller and Zhou, 2010). It was observed that at high TOC and low ionic strength, the three metal oxide (ZnO, CeO_2 and TiO_2) nanoparticles suspension underwent aggregation and remained stable above 300 nm (Keller et al., 2009).

2.4.4 Behavior of ZnO nanoparticles in wastewater treatment plants

Wastewater treatment plants constitute a barrier for pollutant removal before the wastewater is replenished to the aquatic systems. On the other hand, they also represent an important source for nanomaterial entering the water systems, soils and air through treated effluent, bio-solids, and plant-generated aerosols (Westerhoff et al., 2011; Kiser et al., 2010; Musee, 2010; Limbach et al., 2008). However, little is known about the removal efficiency and adverse effects of nanomaterials in these engineered systems (e.g. WWTPs) (Westerhoff et al., 2011; Kaega et al., 2010). Nevertheless, the disposal of ENMs to the sewage systems as their final sinks is already occurring (Brar et al., 2010; Gottschalk et al., 2009; Kiser et al., 2009). Westerhoff and co-workers (2011) through the determination of titanium (Ti) in the raw sewage and treated effluents of WWTPs reported the occurrence of nanomaterials in 10 large scale WWTPs in the United States of America (USA).

Currently, studies have been initiated in determining the potential removal mechanisms of ENMs during wastewater treatment as well as their fate and behaviour in terms of uptake and bioaccumulation (Limbach et al., 2008; Kiser et al., 2009; Choi et al., 2009; Brar et al., 2010). The published data suggest chemical transformation and pollutant adsorption to the wastewater biomass as the main removal mechanisms. Kaegi et al. (2010) have investigated the behaviour of metallic silver nanoparticles in a pilot wastewater treatment plant fed with municipal wastewater whereas Limbach et al. (2008) have used a model wastewater treatment to investigate the removal of CeO_2 nanoparticles from synthetic wastewater. Kaegi and co-workers (2011) suggested wastewater biomass adsorption and chemical transformation of Ag nanoparticles to Ag_2S to be responsible for the removal of 95% of the influent Ag nanoparticles. Li and co-workers (2011) carrying out similar studies reported the total removal of Ag nanoparticles. Furthermore, the colloidal and chemical behaviour of Ag nanoparticles was found to largely depend on the nature of the surface coating. They suggested that chemically inert types of surface-coatings affect the flocculation and chemical transformation of nanoparticles in a WWTP which can lead to different nanoparticles´ release pathways.

Despite the widespread use of ZnO nanoparticles is on rise due to their incorporation in cosmetics, sunscreens, pigments, paints, plastics, among other applications, these materials are being directly discharged to the sewerage systems, where their fate and behaviour is not yet well understood. However, the antibacterial activity of ZnO nanoparticles to a wide spectrum of bacteria including Gram-negative and Gram-positive usually found in the activated sludge wastewater treatment has been suggested (Premanathan et al., 2010; Nair et al., 2009; Huang et al., 2008; Jones et al., 2007; Adams et al., 2006). Therefore, the behaviour of ZnO nanoparticles in simulated activated sludge processes could bring to light the adverse impacts of these nanoparticles to the bacteria that could be reflected in the diminished efficiency on the microbial removal of organic matter.

2.4.5 Impact of ZnO nanoparticles to the WWTPs and byproducts

The activated sludge activity is sometimes inhibited by the presence of toxic substances in wastewater. However, the emergency of nanotechnology has resulted in the nanoproducts being released to the sewerage. The presence of nanomaterials in the wastewater may lead to unpredictable and likely unknown impacts to the bacteria. Therefore, considering that the bacteria constitutes the driving force of the biological wastewater treatment and play a pivotal role for the removal of organic matter, any impact to the bacteria would directly affect the efficiency of these engineered systems. However, the published data suggest the likelihood of nanomaterials to possess unpredictable environmental risks (Musee et. al., 2011; Auffan et al., 2009; Baun et al., 2008; Bystrzejewska-Piotrowska et al., 2009; Boxall et al., 2007; Maynard et al., 2006; Moore, 2006; Biswas and Wu, 2005; Brumfiel, 2003;).

Liu et al., 2011 investigated the impact of nano and bulk ZnO in addition to the Zn^{2+} on the endogenous respiration, BOD biodegradation, and nitrification in a pilot scale wastewater treatment plant in order to assess the toxicity of ZnO nanoparticles to the activated sludge. Their findings suggested adverse effects on the activated sludge activity of all forms of zinc with prominence to Zn^{2+} and the particle dissolution was pointed as the main mechanism of toxicity. In addition, the long-term exposure of ZnO nanoparticles to the anaerobic digestion of waste activated sludge resulted in the reduction of the production of methane though in a dose dependent fashion (Mu and Chen, 2011). Dosages up to 150 mg/g-TSS of ZnO nanoparticles were found to induce 75.1% of methane production inhibition (Mu and Chen, 2011).

The likelihood of the activated sludge to possess nanomaterials due to the release of nanoproducts to the sewerage is predictable and this may compromise its utilization in areas such as agriculture. The presence of ZnO in the sludge has been reported to reduce the wheat biomass and induce significant changes in the soil enzyme activity due to exposure to TiO_2 and ZnO nanoparticles (Du et al., 2010). The soil enzyme activity constitutes a bio-indicator of the soil quality and health. In addition, TiO_2 nanoparticles were retained in the soil matrix while the ZnO nanoparticles dissolved and thus enhanced the plant uptake of Zn^{2+}. Investigations on the toxicity of nanomaterials to the soil microorganisms are important considering that they provide alternative route for further degradation of the activated sludge in the environment (Metcalf and Eddy, 2004). Therefore, environmentally relevant concentrations of ZnO and TiO_2 nanoparticles were used to investigate impacts to the soil microbial biomass. The nanoparticles were found to reduce both microbial biomass and the diversity with ZnO nanoparticles presenting the most prominent toxicological effect (Ge et al., 2011).

On the basis of these studies, it is evident that the findings are too limited to provide a complete understanding on the fate and behaviour of ZnO nanoparticles in WWTPs given the wide diversity of surface-coating that enhance different toxicological activities underpinned by its distinctive physicochemical properties that lead to its widespread use.

2.5 Nanomaterials characterization techniques

Various techniques have been used for characterization of nanomaterials. These include; TEM, SEM/EDX, DLS, BET, CRD and diffuse reflectance spectroscopic techniques. Description of each techniques is given in the sections that follow.

2.5.1 Transmission electron microscopy (TEM)

Transmission electron microscope is an analytical technique used for the determination of particle size and shape. When a radiation of electron beam of uniform current density is focused into a plane of a thin specimen with the aid of magnetic lenses, some electrons penetrate and appear on the other side of the specimen (Tomlinson, 2011; Reimer and Kohl, 2008). The transmitted electrons can therefore be detected directly or sorted according to predetermined criteria and selectively detected. Usually a set of deflector coils or electrodes are used to scan the focused probe in an X-Y raster while the detected electrons are collected and their intensity plotted as a function of the probe position to form an image (e.g. a fluorescent screen) (Crewe, 2008). The image can be obtained by direct exposure of a photographic emulsion or an image plate inside a vacuum, or digitally via a fluorescent screen coupled by a fiber-optic plate to a charge-coupled devices (CCDs) camera (Reimer and Kohl, 2008). Since its invention in the primordial 1930s up to date, TEM has evolved into a sophisticated characterization technique capable of atomic-resolution imaging that is widely applied in areas such as materials science, physics, and chemistry (Spence, 1999).

2.5.2 Energy dispersive X-ray spectrometry (EDS)

Energy dispersive X-ray spectrometry (EDS) is an analytical technique that uses the X-ray spectrum emitted by a thin specimen irradiated with a focused beam of electrons to obtain a localized chemical analysis (Brydson, 2008). The basic principle of EDS is based on the excitation of electrons from inner-shell to higher-energy state, causing the higher levels electrons to release energy in order to fill the resulting vacant holes in the inner shell. As the electrons refill the vacated lower energy levels, the excess energy is released in characteristic frequencies corresponding to the energetic difference of the transition involved (ΔE), that is used for qualitative and quantitative analysis (Brydson, 2008). The qualitative analysis involves the identification of the lines in the spectrum whereas the quantitative analysis is given by the measurement of the line intensities comparing with standard reference materials. EDS is usually coupled to the transmission electron microscopy (TEM) and scanning electron microscopy (SEM) and covers elements with atomic number ranging from 4-90 though many instruments are unable to determine light elements ($Z < 10$).

2.5.3 Dynamic light scattering analysis (DLS)

Dynamic light scattering analysis (DLS) is an analytical technique that determines the size of particulates suspended in a liquid under the Brownian motion with light scattering (Mayinger and Feldman, 2002). The Brownian motion occurs when particles in a suspension undergo thermal induced collisions with the molecules of the solvent. When diffusing particles in a fluid are irradiated with monochromatic light such as laser, the intensity of the scattered light at a fixed angle oscillates with size dependence of the diffusing particle. Generally, the aleatory mobility of particulates in a suspension increases with the reduction of the particle size and therefore, resulting in differences in the scattered light spectrum that is accounted to determine the size of particles (Clark et al., 1970). The particle size determined by DLS is usually given in terms of the hydrodynamic radius due to the fact that the measured particle size is that of a sphere presenting the same translational diffusion coefficient as the particle being measured. Hydrodynamic radius therefore depends on the particle size and surface properties, as well as the type and concentration of ions in the suspension. The hydrodynamic radius is calculated using the Stokes-Einstein equation (Clark et al., 1970).

$$\mathrm{D} = \frac{\mathrm{k_B T}}{3\pi\eta \mathrm{D_t}} \tag{2.13}$$

Where, D is the hydrodynamic diameter, D_t is the translational diffusion coefficient, k_B is the Boltzmann's constant, T is the temperature and η the dynamic viscosity. The DLS is applied for size determination of particles and macromolecules, zeta potential and quantification of the molecular weight of organic materials.

2.5.4 Surface area analysis with BET technique

The knowledge of surface area of powdered materials is of utmost importance in many applications because it determines both reactivity (e.g. catalysis) and adsorptive ability (e.g. activated carbon) of materials. Generally, as the particle size of a material reduces, the amount of atoms in the surface of the material increases resulting in the increased interaction of the material with the medium. Therefore, the BET surface area of ZnO nanoparticles will provide an indication of the effective surface area of the nanopowder interacting with the bacteria in the bioreactors in the current study. In addition, it will provide also an indication of the degree of pulverization of the nanopowder.

The Braunner, Emmett and Teller (BET) theory is an approach universally known for multilayer adsorption (Hammond and Conner Jr., 2013). This theory allows the determination a specific surface area expressed in units of area per mass of the sample (m^2g^{-1}) or volume specific surface area that is the surface area in a fixed volume of particles (m^2cm^{-3}). The BET adsorption isotherm is used to obtain the number of molecules in one monolayer, which is directly proportional to the surface area of the adsorbate and is given by BET equation (Hammond and Conner Jr., 2013):

$$\frac{P/P^0}{V(1-P/P^0)} = \frac{1}{CV_m} + \frac{C-1}{CV_m} P/P^0 \qquad (2.14)$$

Where, P/P_0 is the relative pressure at which a gas volume V (m^3 at S.T.P.) is adsorbed, P is the pressure of the gas, and P^0 is the saturated vapour pressure at the temperature of the vessel holding the adsorbent. V_m is the volume of the gas required to form a monolayer on the adsorbent at the system temperature and C is a constant. Therefore, the plot of the left-hand term, $[P/n(P-P^0)]$, versus P/P^0 yields a straight line with slope $[(C-1)/n_mC]$ and intercept $(1/n_mC)$. The surface area, SA_{BET}, and the value of C are therefore given in terms of the slope, S_{BET}, and the intercept, I_{BET}, by the following (Hammond and Conner Jr., 2013):

$$SA_{BET} = \frac{A_m}{S_{BET} + I_{BET}} \quad (2.15), \qquad \text{and} \qquad C = 1 + \frac{S_{BET}}{I_{BET}} \qquad (2.16)$$

where, A_m is the area one molecule occupies on the surface. As a rule of thumb, the C should be greater than 50 for the BET theory to give rise to a reasonable calculation of the monolayer volume and, thus, the surface area.

2.5.5 X-ray diffraction spectroscopy (XRD)

X-ray diffraction is an analytical technique applied in the analysis of crystalline solids including geological and electronic materials, ceramics, metals, organics, and polymers. The materials can be powders, single crystals, multilayer thin films, sheets and fibers. X-ray diffractometers can be classified in two groups: (i) single crystal, usually applied for the determination of molecular structures mainly of new compounds and (ii) the powder diffractometers, usually applied for routine phase identification and quantification. The powder diffractometers can also be configured to enhance many applications including variable-temperature studies, texture and stress analysis, grazing incidence diffraction, and reflectometry (Formica, 1997). The basic principle of X-ray diffractometry is governed by the Bragg´s equation:

$$n\lambda = 2d\sin\theta \tag{2.17}$$

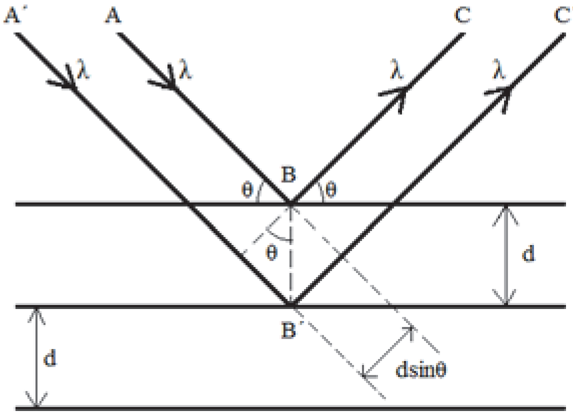

Fig. 2.2: Illustration of Bragg's law. Where *n* is the order of reflection (*n* =1,2,3,…..), λ the wavelength, *d* the distance between the parallel lattice planes, and θ the angle between the incident beam and the lattice plane, known as the Bragg angle (Formica, 1997).

In general, d-spacing is a function of the lattice parameters (A, B, C) and angles (α, β, γ) defining the unit cell, and the Miller indices (h, k, l) denoting a particular reflection (Fig. 2.2). Therefore, the geometry of the crystal lattice determines the position of the peaks in an X-ray diffraction pattern and the more symmetrical the material, the fewer peaks. In addition, the radiation of typical diffractometers contain several wavelengths, denoted $K_{\alpha1}$, $K_{\alpha2}$ and K_{β}, that are characteristic of the material producing the X-rays and as a rule, the smaller the wavelength the more energetic and penetrating radiation (Formica, 1997).

2.5.6 Diffuse reflectance spectroscopy in the UV-Vis-NIR region (DRS)

When the matter is irradiated with light in the ultraviolet (UV), visible (Vis) and near infrared (NIR) region of the electromagnetic spectrum, the electrons are promoted from the ground state to high-energy atomic or molecular orbitals. The electronic transitions usually include transition metal ions (d-d transitions and ligand-to-metal or metal-to-ligand charge transfer transitions), and inorganic and organic molecules (mainly $n - \pi^*$ and $\pi - \pi^*$ transitions) (Weckhuysen, 2004). Liquid and gaseous phase solutions are suitable for analysis but the determination of solids would require the powders to be transparent. This is necessary in order to reduce losses of the incident radiation through reflection and disappearance of the transmittance that would make the analysis impractical. However, the reflected diffuse light can be collected and measured, giving rise to the technique known as diffuse reflectance spectroscopy (DRS). This technique (DRS) is based on the reflection of light by a powdered material with individual particle size in the range 0.2-3 μm (Weckhuysen, 2004). The DRS spectrum is basically the ratio of the light scattered from a powdered sample material and the scattered light from a reference material measured as a function of the wavelength. An ideal reference material should not absorb the radiation and usually MgO, $BaSO_4$, and polytetrafluoroethylene (PTFE) are employed. DRS is largely applied in the analysis of building materials, metallurgy, optical materials, textiles, paper, ceramics, and mainly in the catalysis studies of dye, printing inks, paints and pigments (Zanjanchi et al., 2006).

2.6 Wastewater characterization techniques

The characterization of wastewater is based on parameters such as Total and dissolved organic carbon (TOC and DOC); chemical oxygen demand (COD); total suspended solids (TSS). Each of these is discussed in the sections that follow.

2.6.1 Chemical oxygen demand (COD)

In the activated sludge processes the bacteria is responsible for the degradation of the organic matter. The chemical oxygen demand (COD) is usually one of the parameters largely employed to quantify the extent of organic matter removal in wastewater. Generally, the greater the difference between the amounts of COD of influent and effluent wastewater, the greater the removal organic matter and consequently the better the wastewater treatment efficiency. COD is defined as the amount of a substance expressed in terms of equivalent oxygen, necessary to oxidize the sample under controlled conditions (Eaton et al., 2005). The dichromate ion ($Cr_2O_7^{2-}$) is usually the oxidant of choice owned by its unique chemical properties. Any oxidizeable compound can react with dichromate ion, however in wastewater the organic material predominates and is of the most interest.

2.6.2 Total and dissolved organic carbon (TOC and DOC)

The bacteria usually transform the dissolved organic matter into settleable flocculent material that can be removed from the wastewater during activated sludge processes. The difference between influent and effluent DOC is correlated to the bacterial activity in these engineered systems. The removal of DOC is of utmost importance because they can deplete oxygen of receiving water streams leading to the proliferation of undesirable microorganisms. The total carbon materials in water or wastewater are classified in two categories: inorganic carbon (e.g. carbonate, bicarbonate and dissolved CO_2) and total organic carbon (TOC) comprising of all carbon atoms covalently bonded in the organic molecules. The portion of TOC that passes through a 0.45 μm filter is designated dissolved organic carbon (DOC) and suspended organic carbon to the carbon-based particulates retained in the filter (Eaton et al., 2005). Generally, the determination of TOC and DOC consists in the transformation of the organic material of the samples into CO_2 molecules that are detected and quantified. The generated CO_2 can be titrated chemically, or measured directly using a nondispersive infrared analyser, or can be reduced to methane and measured with a flame ionization detector. The organic matter decomposition methodologies may involve (i) high temperature, catalysts, and oxygen, or (ii) low temperatures (< 100ºC) with ultraviolet radiation and chemical oxidants (Eaton et al., 2005). However, high temperature combustion methodologies are suitable for samples rich in suspended organic materials and refractory organic matter that would not be efficiently decomposed by oxidants and UV radiation at lower temperatures. Conformed to this, in the present study we monitored the DOC of wastewater samples instead of TOC due to the utilization of low temperatures UV radiation-based instrumentation.

2.6.3 Total suspended solids (TSS)

The efficiency in the organic matter degradation and contaminants´ removal in the activated sludge processes depends upon the amount of the biomass in the aeration chamber. The total suspended solids (TSS) is a parameter usually employed to characterize the amount of biomass in the activated sludge and municipal WWTPs usually operate with biomass ranging from 1000-5000 mgL^{-1} of TSS (Metcalf and Eddy, 2002). Total solids is the material residue left in the vessel after evaporation followed by drying in the oven at a defined temperature. Therefore, TSS represents the fraction of total solids retained by filter of 2.0 μm (or smaller) nominal pore size after drying in the oven at 103-105ºC (Eaton et al., 2005). The amount of solids in the effluent also affects the efficiency of the disinfection process.

2.7 Metal determination techniques

Various methods that are currently used for the analysis of metals in complex matrices include flame atomic absorption spectrometry (FAAS), graphite furnace (or electrothermal) atomic absorption spectrometry (GFAAS or ETAAS), inductively coupled plasma optical emission spectrometry (ICP-OES), and inductively coupled plasma mass spectrometry (ICP-MS), among others. These analytical techniques differ in the sample size requirement, sensitivity and the capability for simultaneous multi-element analysis. Therefore, the most suitable technique for a particular application depend upon the nature and quantity of the samples, the expected analyte concentration range and the number of elements to be determined including the cost of the analysis. Therefore, the ICP-OES was the analytical technique employed for the metal analysis throughout the study and a brief description of the technique is discussed below.

2.7.1 Inductively coupled plasma optical emission spectroscopy (ICP-OES)

The low cost, simultaneous multi-element determination ability, high dynamic linear range, relatively low matrix interference and sensitivity make the ICP-OES the analytical technique of choice for the analysis of trace elements in myriad types of samples including biological fluids, water, wastewater, soil and sludge (Martin et al., 1994). In the ICP-OES, the sample is introduced in the liquid form, converted into aerosols and directed to the central channel of argon gas plasma. The high temperature of the plasma (approximately 10 000 K) readily vaporizes the aerosols, and promote the atoms and ions to excited states. As they return to the ground state, spontaneously emit the excess energy in the form of light at a characteristic wavelength that is used for elemental identification and quantification by means of optical spectrometry (Hou and Jones, 2000). The amount of photons emitted is directly related to the concentration of the sample.

CHAPTER 3

METHODOLOGY/EXPERIMENTAL WORK

3. Preamble

This chapter outlines the experimental procedures followed in achieving the objectives prescribed for this report. The lab-scale wastewater treatment plant construction and performance is also described in details in this chapter.

3.1 Materials and reagents

The non-functionalized ZnO nanopowder (CAS#: 544906) was purchased from Sigma (Gauteng, South Africa). The nitric acid (65%, Merck, South Africa), hydrochloric acid (fuming, ≥ 37%, Sigma-Aldrich, South Africa), hydrochloric acid solution (1 molL^{-1} (1 N) titrisol / Amp, MERCK, South Africa), sodium hydroxide solution (1 molL^{-1} (1 N) titrisol / Amp, MERCK, South Africa), and sodium chloride (MERCK, South Africa) were of analytical grade. The COD digest vials (HR 20-1500 mgL^{-1}) were sourced from Aqualytic (Aqualytic Laboratories and Environmental, Gauteng, South Africa). The 0.45 filter membrane (PALL, Pall Corporation) and 0.45 µm PVDF (polyvinylidene difluoride) syringe filters were sourced from Separations (Gauteng, South Africa) and Microfiltration (Gauteng, South Africa), respectively. The 100 mL and 10 L polyethylene bottles, the 25 L high density polyethylene (HDPE) holding containers, the 210 L HDPE drums, and the HDPE (260 mm diameter and 4000 ml capacity) funnels were sourced from PLASTPRO SCIENTIFIC (PTY) LTD (Gauteng, South Africa). The 425 µm stainless steel mesh was obtained from ERIEZ MAGNETICS (PTY) LTD (Gauteng, South Africa). The Watson – Marlow (Falmouth, Cornwall, UK) 120S/DV and 313S pumps were used to pump wastewater and recycle the sludge, respectively. The stirring of the holding containers and aeration chambers was enabled using IKA RW 20 digital and IKA RW 16 basic stirrers, respectively. The temperature of the aeration chambers was kept within 20-25ºC using GP200 Immersion thermostat (Fisher Scientific, England).

3.2 Experimental approach

This study was carried out using published standard methods prescribed for sampling, preservation, testing and analysis of chemicals (Boeije et al., 1999; Martin et al., 1994; OECD 303A, 2001).

3.2.1 Wastewater collection, preservation and preliminary analysis

Raw wastewater was withdrawn from wastewater treatment plant in Johannesburg (Johannesburg Water, Northern Wastewater Treatment Works; Gauteng, South Africa) that collects and treats mainly domestic sewage on a weekly basis and stored in the fridge at 4ºC before use. The wastewater collection and storage followed the procedure previously used by Akan and co-workers (2008). The following parameters were determined; pH, conductivity, salinity, total dissolved solids (TDS), dissolved oxygen (DO), chemical oxygen demand (COD), dissolved organic carbon (DOC), and total suspended solids (TSS) before the ZnO ENPs were introduced into the wastewater.

Generally, unless specified, no preservatives were added to the samples prior to storage either for the sake of keeping the bacteria alive and viable or to avoid any interference on the biological treatment process. All the wastewater parameters were characterized following the Standard Methods for the Examination of Water and Wastewater (Eaton et al., 2005). Parameters such as pH, conductivity, dissolved oxygen (DO), chemical oxygen demand (COD) and dissolved organic carbon (DOC) were analysed using pH and conductivity probe, DO probe (Model: PHC101 and LDO, HACH), photometer (HACH, DR 3900, USA) and fusion UV/Persulfate TOC Analyser (TELEDYNE TEKMAR, USA), respectively. The wastewater physicochemical characteristics were continuously monitored in the influent, aeration chamber and effluent before and after the nZnO were introduced into the simulated wastewater treatment plant. The concentration of zinc was determined in the influent, effluent and waste activated sludge using inductive coupled plasma-optical emission spectrometer (ICP-OES). The filtered wastewater sample was supplemented with carbon source: D-glucose anhydrate (2.5 g/L) and nutrients: $MgSO_4.H_2O$ (0.5 g/L) and KNO_3 (0.18 g/L) as described by Kamika & Momba (2011; 2013) and the pH was adjusted at 7 using 1.0 M HCl and 1.0 M NaOH (Merck, South Africa). The culture media was sterilized by autoclaving at 121ºC and approximately 1 ml was plated on the sterile nutrient agar at 37ºC for 24 h to confirm the sterility of the media prior adding the test organisms for the experimental study.

3.2.2 Procedure for preparation of nZnO suspensions

The stock suspensions of nZnO of three concentrations 5, 10 and 20 mgL^{-1}, were prepared by adding 0.1250, 0.2500 and 0.5000 g, respectively, of ZnO nano-powder to 1 L deionized water. Using a sonicator (Model 2000U, Ultrasonic Power Corp.), the stock suspensions were sonicated at 20 KHz for 30 minutes to break the aggregates before each set concentration (5, 10 or 20 mgL^{-1}) was introduced into the 25 L wastewater holding container. Ice was added into the sonicator to minimize possible nZnO dissolution due to heat generated during the sonication process. ZnO ENPs suspension of concentration 100 mg L^{-1} was prepared by adding 0.100 g of nano-powder to one litre of raw domestic wastewater, and sonicated at 20 KHz for 30 minutes. Ice was introduced into the sonicator to control the temperature and prevent the generation of heat so as to reduce particle dissolution. The ZnO ENPs suspension was then introduced into reagent bottles of 100 mL capacity, and adjusted to appropriate pH in the range 3-11 using sodium hydroxide or hydrochloric acid with thorough mixing and allowed to stabilize for one week prior to analysis. The ionic strength of the wastewater-ZnO ENPs suspension was adjusted using sodium chloride covering the range 0.01-1.0 M. Triplicate samples were prepared to examine the effects of pH and ionic strength. After one week of stabilization, the wastewater – ZnO suspension was filtered using 0.45 μm filter membrane (PALL, Pall Corporation) to separate the solution from the sludge. The supernatant was analysed for zinc using ICP-OES while the sludge in the filter paper was analysed using XRD for the morphological nature of ZnO ENPs. EDS and TEM were used for elemental analysis and determination of ENPs size respectively. The stability of ZnO ENPs in de-ionized water treated in a similar manner was also investigated as a control. The dynamic light scattering investigation was done to determine the ZnO ENPs size changes over a period of 2-hr. This was done by filtering a suspension of ZnO ENPs (100 mg L^{-1}) prepared in both de-ionized water and in a raw domestic wastewater filtered through a 0.45 μm filter membrane.

3.2.3 Nanoparticles characterization

The non-functionalized *n*ZnO and *n*Ag sourced from Sigma (Gauteng, South Africa) were characterized for purity, BET surface area, particle distribution and particle size using BET, XRD and TEM before use.

3.2.4 Simulated activated sludge wastewater treatment plant set up

The simulated wastewater treatment plant was constructed following the Organization for Economic Co-operation and Development (OECD 303A, 2001) specifications. The tests were conducted in aerobic digesters each designed to hold 3 L of activated sludge. Each model unit comprised of: influent holding container (25 L), a stirred and aerated tank reactor (aeration chamber), and a clarifier (settling vessel) simulating biological treatment using an activated sludge system. The aeration chambers (3 L) were individually continuously stirred using an IKA RW 16 basic stirrer to ensure thorough mixing of the substrate essentially to mimic actual WWTP operational conditions. The aeration chamber was aerated at a flow rate of 290 Lmin^{-1} to maintain the dissolved oxygen above 2 mgL^{-1} by using compressed air through a glass frit. In this study, two model units were used as test and control units. Both units were fed with wastewater and deionised water spiked nZnO for the test and control units, respectively, using Watson – Marlow (Falmouth, Cornwall, UK) 120S/DV pumps at 29 rpm.

For the test unit, the influent wastewater was spiked with nZnO (at varied concentrations: 5, 10, 20 mgL^{-1}) in 25 L containers and continuously stirred using IKA RW 20 digital stirrer at 1800 rpm to keep the ENPs well dispersed in suspension. Settling vessels of 1.5 L were used to separate treated effluent from the waste activated sludge. As per standard practice, a portion of the sludge from the settling vessel was re-introduced as return activated sludge (RAS) into the aeration chamber to replenish the biomass – and maintain the total suspended solids (TSS) in the range of 2 to 3 gL^{-1} of dry sludge. In this study, as previously done by Musee and co-workers (2014) the aeration chamber was designed to have a hydraulic retention time (HRT) of 6 hours, and with feed flow rate of 0.50 Lh^{-1} using peristaltic pumps. The experiment was operated for 77 days to establish the long-term effects of nZnO on the removal of organic matter from WWTPs where COD and DOC were monitored continuously as surrogate parameters as previously reported by Musee et al. (2014).

Initially, raw wastewater was filtered using 425 μm stainless steel mesh to remove big particulates to avoid clogging of the tubing before it was pumped into the operating units. This operation mimics the screening process of raw wastewater employed in large scale WWTPs. The simulated WWTP was stabilized and optimized for 14 days before introducing nZnO over 21 days for each nanoparticle concentration (5, 10 and 20 mgL^{-1}). The continuous sampling process took place at the influent holding container, aeration chamber, settling vessel and waste activated sludge for the monitoring of various physicochemical parameters. The influent and effluent samples from the aeration chamber and settling vessel, respectively, were filtered using 0.45 μm PVDF (polyvinylidene difluoride) syringe filter prior to DOC analysis. However, only effluent samples were similarly filtered prior to COD analysis. The fate and behaviour of nZnO in deionized water was treated in a similar manner, and served as the control unit.

3.2.5 Design of simulated wastewater treatment plant

The abovementioned lab-scale WWTP is a well-established approach for the test of chemicals (Boeije et al., 1999). Figure 3.1 shows a schematic representation of the lab-scale simulated WWTP developed and used in this study. The detailed technical information regarding the dimensions of the components used (aeration chambers and settling vessels) are given in the appendix. Figure 3.2 is a photograph of the fabricated simulated WWTP set up, illustrating all the components that constitute the lab-scale WWTP.

The simulated WWTP system consists of two units, a test and control units. Each unit included an influent container, aeration chamber (bioreactor), clarifier (settling vessel) and outlet. The test unit was fed with wastewater while the control unit was fed with deionized water. The influent was spiked with nZnO in 25 L containers and continuously stirred at 1800 rpm using IKA RW 20 digital stirrer to keep the ENPs in suspension. The bioreactors (3 L) were continuously stirred using IKA RW 16 basic stirrers and aerated at 290 $mLmin^{-1}$ using compressed air through a glass frit to keep the dissolved oxygen above 2 mgL^{-1}. Optimization of the bioreactor stirring speed was necessary in order to allow appropriate oxygen distribution as well as keeping the activated sludge flocs in suspension. Recirculating water baths equipped with thermostats were connected to the aeration chamber to maintain the temperature of the activated sludge around 25ºC. Settling vessels (1.5 L) were employed to separate the treated effluent from the activated sludge with part of the sludge intermittently recycled back to the bioreactor as return activated sludge (RAS) in order to keep the total suspended solids (TSS) in the range of 2.0-3.0 gL^{-1} of dry sludge and prevent washout. The sludge retention time (SRT) was determined by dividing the sludge mass in the bioreactor by the sludge mass wasted per day. An average of approximately 6 days SRT value was observed. The feed flow rate was adjusted to 0.50 Lh^{-1} using peristaltic pumps in order to achieve a hydraulic retention time of 6 hours. The lab-scale WWTP developed in this study was operated continuously for 77 days generating 12 L of treated effluent per day.

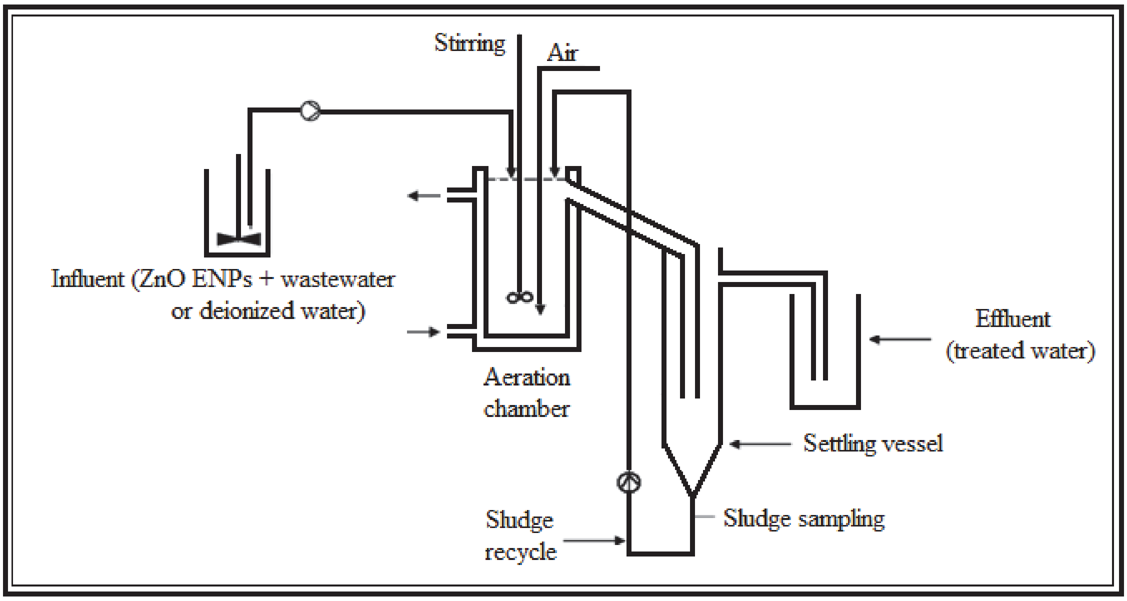

Figure 3.1 Schematic representation of the simulated activated sludge wastewater treatment plant (AS WWTP).

Figure 3.2: Image of the simulated activated sludge wastewater treatment plant

3.2.6 Determination of ZnO ENPs dissolution

To determine the dissolution of ZnO ENPs in wastewater, first, the influent and effluent wastewater were continuously sampled from the set up and acidified with nitric acid to $pH < 2$ and stored in the fridge at 4ºC before analysis. Likewise, the sludge was also continuously sampled, filtered (Whatman 41 filter paper) under a vacuum, dried in the oven at 103-105ºC, grinded with mortar and pestle and stored as a dry powder prior the analysis. The digestion methodology employed followed the procedure suggested by Martin et al., 1994.

The extent of zinc dissolution was determined using inductively coupled plasma optical emission spectrometry (ICP-OES; SPECTRO ARCOS, Analytical Instruments GmbH, Germany) by measuring the concentration of zinc in the raw wastewater at a detection limit of 0.2 μgL^{-1} to determine the background zinc concentration and then after adding ZnO ENPs. The ICP-OES operating conditions were as follows: forward power 1400 W, plasma argon flow rate of 13 L min^{-1}, auxiliary argon flow rate 2.00 L min^{-1}, and nebulizer argon flow rate 0.95 L min^{-1}. Sample introduction was achieved using a pneumatic cross-flow nebulizer mounted onto a Scott double-pass spray chamber. Sample solutions were pumped to the nebulizer using a built in four channel peristaltic pump. The atomic and ionic analytical spectral line selected for investigation was Zn 206.200 nm.

The X-Ray diffraction (XRD) (Philips, X'Pert PRO MPD, mineral powder diffraction) analysis of the sludge was carried out and the Cuα radiation beam with excitation wavelength of 0.15406 nm used as the X-Ray source. The UV-Vis spectrophotometer (UV-2450 UV-Vis spectrophotometer, Shimadzu, Japan) coupled with UV-Probe was used for the solid state analysis of the sludge. Both XRD and UV-Vis patterns were used for qualitative analysis of the sludge.

Aliquots from the test and control units were collected periodically to examine the effect of time on the dissolution. Conversely, the concentration dependent effects of the ZnO ENPs on the treatment of wastewater (determined as a function of DOC and COD removal) was evaluated over time.

3.2.7 Assessment of pure bacterial culture growth

Three wastewater bacterial species, which included *Bacillus licheniformis*-ATCC12759, *Brevibacillus laterosporus* -ATCC64 and *Pseudomonas putida*-ATCC31483, dominate in soil and surface water were purchased from Quantum Biotechnologies (Strydompark Randburg, South Africa). Prior to use, these bacterial isolates were confirmed by culture based-methods using selective agar media according to the Standard Methods (APHA 2001). Briefly, one loop-full of each bacterial culture was inoculated in 100 ml sterile nutrient broth medium and incubated aerobically in a shaking incubator (Scientific Model 353, Lasec South Africa) at 37°C *Brevibacillus* and *Pseudomonas* and at 50°C for *Bacillus* (Kamika & Momba, 2011) at 120 rpm for 24 h. Thereafter, the growth of bacterial species was determined using the nutrient agar and the spread plate method after dilution. Three to five colonies of the isolates were diluted into 100 m1 of nutrient broth and incubated for 24 h at 37°C. For each test isolate, 100 µL aliquot was aseptically inoculated into 100 ml sterile nutrient broth (NB), separately. The inoculated isolates were incubated and shaken (100 rpm) overnight according to Kamika & Momba, 2011. All treatments were set in triplicates, with bacterial growth performance measured using optical density (OD) at a wavelength of 600 nm (spectrophotometer). The obtained OD values were converted to CFU/ml and Cells/ml using a factor previously determined from a calibration curve relating to the biomass of the isolates at 37 ^{0}C. The initial OD values of the *n*ZnO and *n*Ag in each flask were determined and the values were subtracted to assess the biomass growth. All the treatments were set in duplicates and the results obtained were averaged.

3.2.8 Determination of Minimum Inhibition Concentration (MIC)

Prior to evaluate whether these commercial NMs contribute to environmental risk hazard assessment, minimum inhibitory concentration (MIC) of test materials required to exhibits antimicrobial activity, stock solutions of *n*ZnO (20 g/L) and *n*Ag (1 g/L) were prepared in sterile deionized water and stirred vigorously. From this stock solution, aliquots of specific volume corresponding to the final concentration ranging (0.015-20 g/L) for *n*ZnO and (0.015-1 g/L) for *n*Ag were mixed with nutrient agar (NA) in order to make the working culture media. The inoculum used for all the experiments were taken at $OD_{600\ nm} = 1$. A negative control (culture media with test nanomaterials) and positive control (culture media without NMs inoculated with bacterial isolates) were also included. The agar plates were incubated at 37°C and colonies were observed after 24 h of incubation. All treatments were set in triplicates and results were averaged.

3.2.9 Killing kinetics of *n*Ag and *n*ZnO in broth

To assess the killing kinetics, approximately 100 µL of each test isolates were aseptically inoculated in a sterile 100 ml nutrient broth (NB, pH 7.4) containing *n*ZnO (0.015 to 20 g/L) and *n*Ag (0.015 to 1 g/L), separately. The inoculated flasks were incubated overnight at 37°C except for *Bacillus. licheniformis* at 50°C) in a shaking incubator at 100 rpm. These series of the experiment had one positive control and one negative control. The positive control flask contained the NB without NMs but inoculated with the specific microorganism, while the negative control contained only the NB with NMs. Concurrently, the growth and antibacterial rates were determined by measuring the optical density at a wavelength 600_{nm} (spectrophotometer) after 24 h. The OD of positive control was subtracted from the experimental OD values of those of flasks containing NB, NMs and bacteria (Bandyopadhyay et al*.,* 2012). To distinguish the difference between bacteristatic and bactericidal effects, approximately 100 µl of sample from the exposed test isolates that exhibit little or no growth were transferred to NA plates and were incubated at 37°C overnight. The number of colonies were counted after incubation and all treatments were set in triplicates.

3.2.10 Bacterial susceptibility of *n*Ag and *n*ZnO

To examine the susceptibility of *Bacillus, Brevibacillus* and *Pseudomonas* in the presence of *n*ZnO and *n*Ag, blank disks (6mm Ø) were soaked in *n*ZnO and *n*Ag suspensions solution with various concentration ranging from 0.015 to 20 g/L and from 0.015 to 1 g/L, respectively. Bacterial suspensions ($OD_{600\ nm}$ = 1.0) were uniformly applied on the sterile Muller Hinton agar (MHA) plates, and thereafter the soaked disks were carefully placed on the bacterial lawn and incubated overnight at 37°C. All treatments were set in triplicates. The diameters to determine the zone of inhibition were measured after 24 h of incubation using a ruler. To facilitate discussion, the measured zones of inhibition were interpreted in terms of sensitive, moderate or tolerant. A negative control (NMs without test isolates) and positive control (test isolates without NMs) were also included.

3.2.11 Extraction and analysis of extracellular polymer substance (EPS)

These series of the experimental study aimed to assess the bactericidal and bacteriostatic effects of NMs on cell membrane. The exopolysaccharide substances were extracted and examined to check the attachment of NMs on bacterial cell membrane, which could result in the change or disruption of their functional group. The extraction of EPS was performed according to (Bandyopadhyay et al., 2012) with slight modifications. Briefly, all three bacterial cells previously exposed to various concentrations of target NMs were cultivated aerobically at 37ºC agitating at 100 rpm overnight. Supernatants were collected by centrifugation at 8000 rpm for 10 min at 4°C. Three volumes of 95% ethanol (Sigma-Aldrich) were added to pellet to precipitate out the EPS and placed at -20°C overnight. To recover EPS, samples were centrifuged at 10000 rpm for 10 min at 4°C. The supernatant were discarded and pellet was then washed with 95% ethanol and air-dried the pellets at room temperature for 72 h. The extracted EPS was determined after air-drying and analysed using FTIR. All extractions and measurements, including positive control (bacterium without NMs), were performed in triplicates. The FTIR spectra of dry EPS samples were collected and encapsulated in 150 mg of KBr, then analysed at frequency range of 4000-500 cm^{-1} using Smart iTR connected to a component accessary with Nicolet 380 FTIR Spectrometer (Thermo Scientific, USA).

3.2.12 Effect of pH on survival limit of single bacterial isolates exposed to nanomaterials

To check the effect of pH on the survival of bacterial isolates during their exposure to NMs, batch experimental studies were separately conducted in 100 mL Erlenmeyer flasks containing 80 mL of sterile modified wastewater mixed liquor media and known concentrations of NMs. Extreme pH values (pH 2, 7, 10) were then used to evaluate the ability of the bacterial isolates to grow in harsh environment. These series of the experiment also included one positive control and one negative control. The positive control flask contained the mixed liquor without NMs but inoculated with the specific microorganism, while the negative control contained only the mixed liquor with NMs. The flasks were inoculated with known concentration of cells (which were equal to 1.0 OD_{600nm}). All the inoculated flasks as well as the controls were incubated at 37 ±2°C for 5 days and daily aliquots were taken and biomass growth perfomance were measured using OD_{600nm}. The obtained OD values were converted to CFU/ml using a factor previously determined from a calibration curve relating to the biomass of the isolates at 37 ^{0}C. The initial OD values of the *n*ZnO and *n*Ag in each flask were determined and the values were subtracted to assess the biomass growth in all pH values. All the treatments were sets in duplicates and the results obtained were averaged. During the experimental study, the COD removal efficiency of the test organisms was also determined when they were exposed to *n*ZnO and *n*Ag and a formula used by previous investigators (Kamika and Momba, 2011) was applied:

$$\mathrm{mg-COD/L} = \frac{\text{mgin final volume x 1000}}{\text{Sample volume}} \tag{3.1}$$

3.2.13 Comparing survival limit of consortium isolates (bacteria/protozoa) exposed to nanomaterials with change of pH

Batch experimental series were conducted in 100 ml Erlenmeyer flasks containing 80 ml of modified sterile wastewater. With the exception of the controls (no NMs, no biomass), the flasks were separately inoculated with known concentration of bacterial isolates and protozoan isolates ($\mathrm{OD}_{600\mathrm{nm}}$ =1.0). All the flasks inoculated with bacterial and protozoan isolates in the presence of known concentrations of NMs as well as the controls were incubated at 37°C and daily aliquots were taken for 5 days. The biomass growth perfomance was determined by subtracting the initial OD values of the *n*ZnO and *n*Ag in each flask from the OD obtained from the average biomass growth in the flasks over 5 incubation days. All the treatments were sets in duplicates and the results obtained were averaged.

CHAPTER 4

STABILITY STUDIES OF COMMERCIAL ZnO ENGINEERED NANOPARTICLES IN DOMESTIC WASTEWATER

Preamble

The first in the series of experimental work carried out in the fulfilment of this research project was reported here. This constitutes a laboratory study on various physicochemical properties (such as DO, BOD, COD, TSS, etc.) of the wastewater sample and most significantly, the assessment of chemical stability (under the influence of pH, ionic strength) of the commercially available ZnO nanoparticles, engineered and used for the laboratory scale treatment of domestics wastewater. Detailed instrumental analyses were carried out in reaching objective conclusions.

4.1 Results and Discussion

Organic matter in wastewater is highly heterogeneous and varies significantly due to difference in living traits (Huang et al., 2010). Therefore, in this study, several wastewater parameters were determined before the ENPs were introduced, and this is summarized in Table 4.1.

Table 4.1: Characteristics of raw domestic wastewater used in the stability study.

Parameter	Units	Value
pH	-	7.24
Conductivity	µS/cm	775
Salinity	Psu	0.38
Total dissolved solids (TDS)	mgL^{-1}	387
Dissolved oxygen (DO)	mgL^{-1}	3.93
Chemical oxygen demand (COD)	mgL^{-1}	723
Dissolved organic carbon (DOC)	mgL^{-1} C	31
Total suspended solids (TSS)	mgL^{-1}	620

4.1.1 Stability of ZnO ENPs in wastewater- effect of pH and ionic strength

It has been reported that the amount of dissolved zinc (Zn^{2+}) from ZnO ENPs suspensions in nanopure water both in the presence and absence of citric acid reaches a steady state within 6 h (Mudunkotuwa et al., 2012). In this regard, ZnO ENPs suspended in raw domestic wastewater were allowed to stabilize for one week to allow possible reactions and/or interaction with the biomass naturally present in wastewater to occur and reach a steady state prior to analysis for zinc.

The stability of ZnO ENPs in wastewater is critical as it aids to advance our collective understanding on their dissolution, persistence, fate, and eventually their potential toxicity to biological life forms. Han et al. (2010) has reported that the dissolution of bulk ZnO in an aqueous solution decreases with increasing pH – and followed a direct interaction between bulk ZnO, hydrogen, and hydroxyl ions in solution. In our study, the dissolution behaviour of ZnO ENPs in wastewater appears to follow similar solution chemistry as described by Han et al. (2010). Furthermore, our results suggest that significant ZnO dissolution occurs under acidic regime as compared to alkaline conditions in both wastewater and deionized water (Figure 4.1). From our findings, zinc concentrations of 45.6 mg/L and 56.2 mg/L, respectively, were observed in wastewater and de-ionized water (no biomass) under acidic pH conditions (Figure 4.1). The measured zinc under acidic conditions were likely to have resulted from sparingly soluble ZnO ENPs.

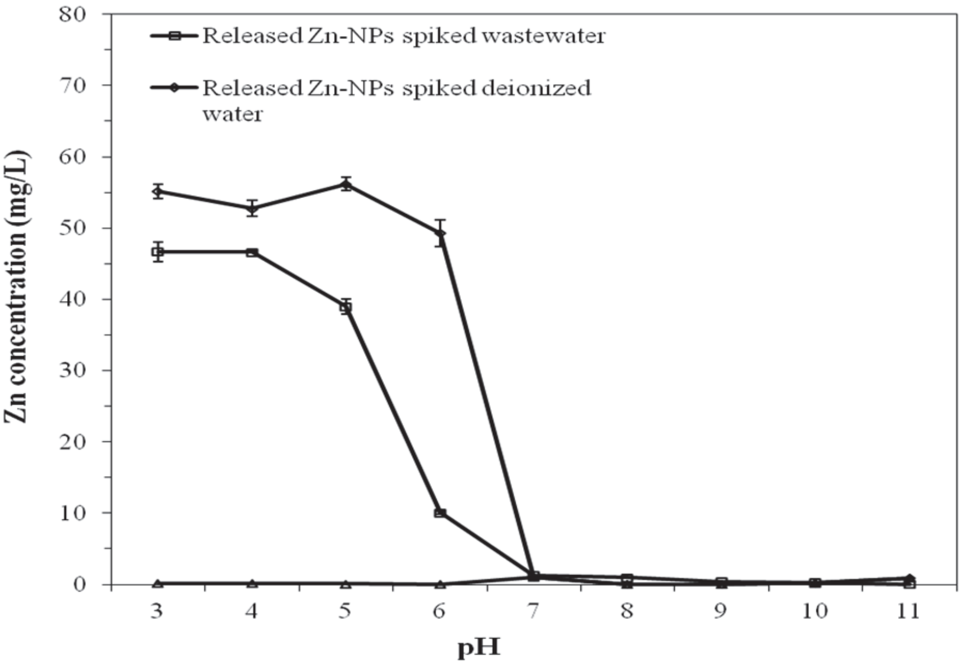

Figure 4.1: pH dependence of zinc release from ZnO ENPs (100 mg L^{-1} suspension) in raw domestic wastewater and de-ionized water.

Generally, as the pH of the wastewater increased, a rapid decrease in the total amount of measured zinc in the pH range 5.0-7.0 was observed, and a plateau was formed at pH value above 7.0 for both wastewater and de-ionised water. The rapid decrease in the measured zinc as pH increases is ascribed to the removal of soluble forms; (Zn^{2+} and $Zn(OH)^{+}$) from deionised water.

On the other hand, removal of soluble forms; (Zn^{2+} and $Zn(OH)^{+}$) both abiotic and bio-sorption/bio-solid settling mechanisms is expected to occur at wastewater pH. The difference in zinc removal between wastewater and deionised water (no biomass) is ascribed to zinc removal via bio-sorption and bio-solid settling mechanisms. Similar removal mechanisms have recently been reported for TiO_2 in wastewater (Wang et al., 2012).

It is likely that under alkaline conditions, released zinc in wastewater is stabilized by both insoluble hydroxide formation and natural organic matter (NOM) as an insoluble complex while the un-dissolved ZnO ENPs sorbs onto the biomass and settles. Humic acid is commonly found in wastewater, and characterized by functional groups such as carboxylic ($–COO^{-}$) and phenolate ($–ArO^{-}$) with high complexation capacity for metal ions (Zhang et al., 2009). In this regard, humic acid molecules are opened and linear in shape because of decrease in intra- and inter-molecular hydrogen bonds that results into increased repulsive forces between the dissociated functional groups as they complex more effectively with the surface atoms at higher pH (Zhang et al., 2009). Thus, over the pH range 7-10, zinc was completely removed from wastewater either by complexation, precipitation of zinc or sorption of un-dissolved ZnO ENPs. Moreover these findings were avertedly confirmed in that, the lowest solubility of ZnO ENPs in wastewater suspensions were observed in the pH range 7-10, which in part justified the removal of zinc in the form of a mixture of zinc-NOM complex, zinc hydroxide and ZnO ENPs in wastewater under alkaline conditions.

Conversely, the zinc ions in the control (deionised water) were likely to have precipitated as $Zn(OH)_2$ thus resulting to the formation of an appropriate surface for the dispersed ZnO ENPs to sorb onto, and finally precipitated and settled. Similar precipitation of $Zn(OH)_2$ was reported by Bian et al. (2011) in the pH range of 6 and 9 in water. Based on these results, the dissolution of ZnO ENPs in wastewater under acidic conditions was observed as slightly lower as compared to that of de-ionised water where no biomass is present. In this regard, the sorption of a mixture of zinc-NOM complex, zinc hydroxide and un-dissolved ZnO ENPs on biomass where useful bacteria colonies are located during wastewater treatment are key aspects regarding the potential of ZnO ENPs exposure and effects.

The stability of particles in water can also be analysed using Derjaguin – Landau – Verwey – Overbeek (DLVO) theory. The DLVO theory accounts for two forces between the particles: van der Waals (vdW) attraction and electrical double layer (EDL) repulsion. The sum of these two forces determines whether the net interaction between particles is repulsive or attractive (Zhang et al., 2008; Bian et al., 2011). Bian and co-workers (2011) investigating the stability of ZnO ENPs in aqueous media and Zhang and co-workers (2008) investigating the stability of ZnO ENPs in the tap water, both groups found that an increase in ionic strength resulted into the compression of the EDL repulsive energy such that the ENPs experienced rapid aggregation. Similar phenomenon was observed in this study where increasing ionic strength of ZnO ENPs suspension using NaCl in wastewater resulted in a decreased release of zinc in the wastewater as aggregation of ZnO ENPs becomes dominant (Fig. 4.2).

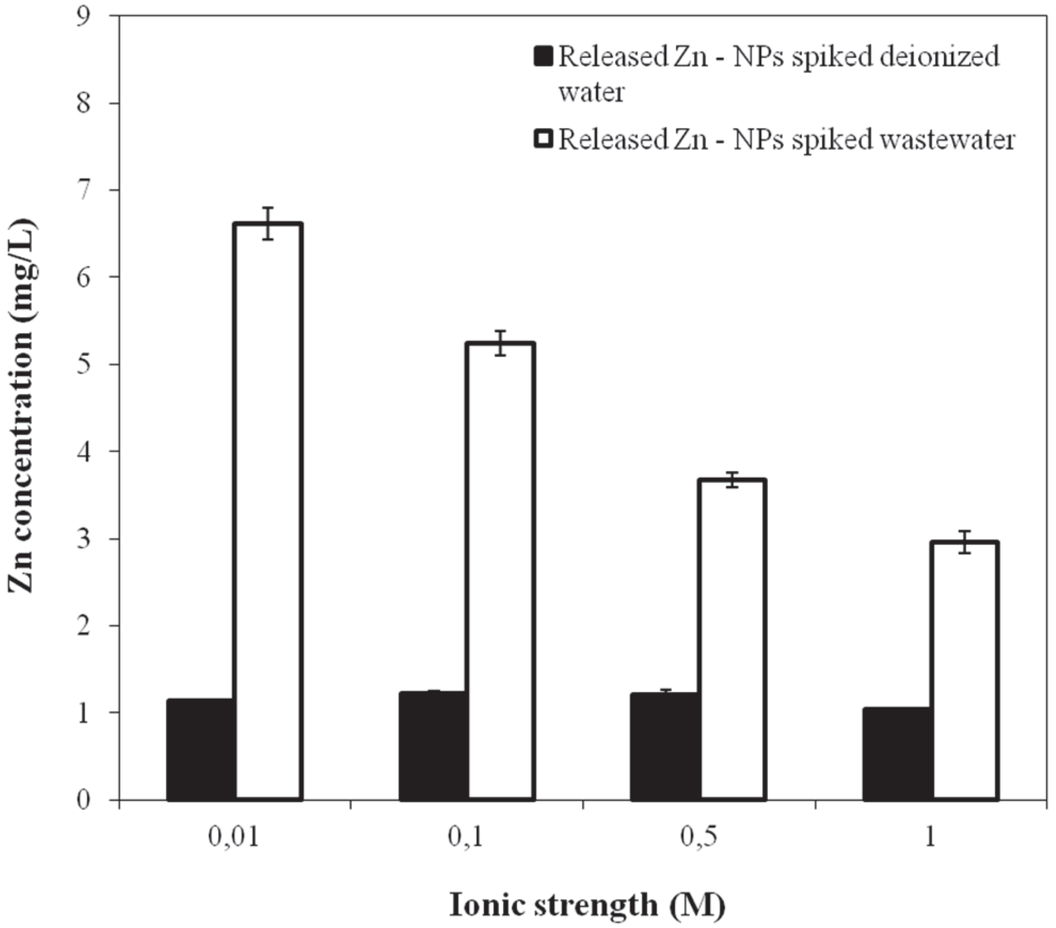

Figure 4.2: Release of zinc from ZnO ENPs suspension in domestic wastewater and de-ionized water as a function of ionic strength

In an aqueous environment, NOM can adsorb onto the surface of ENPs (Zhang et al*.,* 2009) and enhance the stability of ENPs suspensions even at high ionic strength (Keller and Zhou, 2010). In this regard, it has been observed that at absolute zero ionic strength, the release of zinc from ZnO ENPs was more significant compared with releases observed at high ionic strength. As the ionic strength increases the net repulsive energy becomes weaker resulting in some aggregation and decrease in release of zinc as shown in Fig. 4.2.

It has been reported by Zhang and co-workers (2008) that the ENP reported manufacturer's sizes are the sizes of the primary NPs, although in water they usually exist as aggregates. In this study, ZnO ENPs of size less than 100 nm were determined using dynamic light scattering (DLS) in both domestic wastewater and de-ionized water (control). It was observed that ZnO ENPs in de-ionised water over a period of 2 hrs increased their average particle size to 300 nm, almost three times the primary NP size. However, in wastewater, it was difficult to perform a similar study because ENPs easily sorbs on biomass and this motivated for modifications to be made. In this regard, the wastewater was first filtered prior to spiking with ZnO ENPs to aid size determination using DLS.

The results summarized in Fig. 4.3 indicates the formation of dispersed ZnO agglomerates and/or aggregates of significantly larger size (>5000 nm) in wastewater compared to the ZnO ENPs size in de-ionised water (< 500 nm) in less than 1-hr before decreasing to about 1500 nm after 2-hr. This indicates the role of NOM in the stabilizing of ENPs in wastewater and suggests that although ZnO ENPs may form agglomerates rapidly after being introduced into the wastewater, perhaps due to the presence of electrolytes, the agglomeration effect may be reversed over time due to high concentration of NOM in the wastewater. The NOM may therefore cause de-agglomeration which could lead to the formation of smaller aggregates.

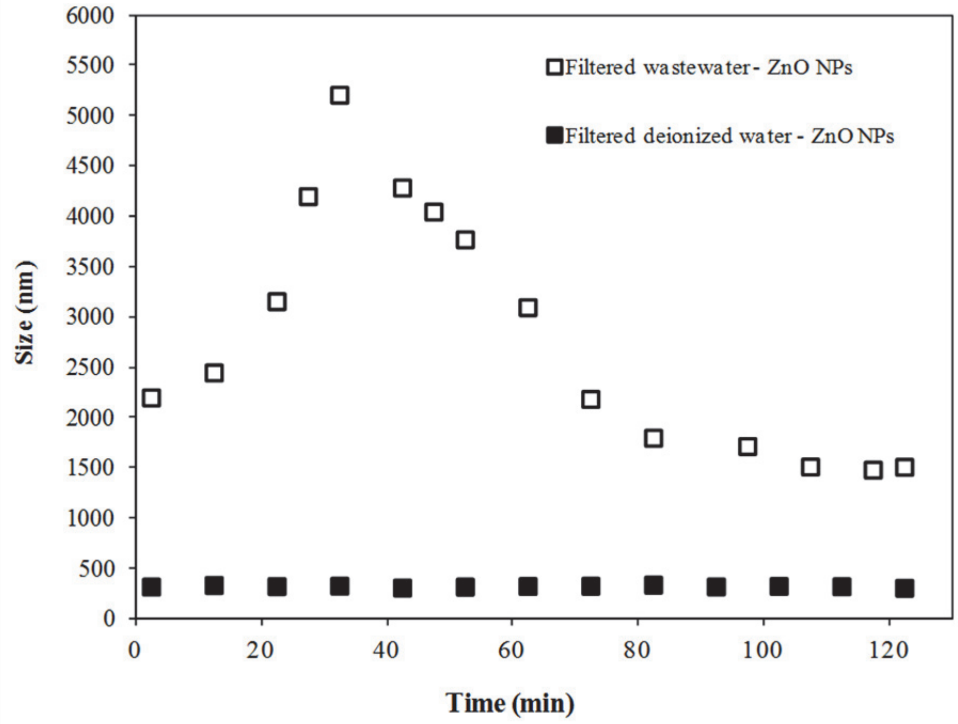

Figure 4.3: Dynamic light scattering (Malvern Zetasizer NanoZS) determination of ZnO ENPs size changes in domestic wastewater.

Although the material that passes through 0.45 µm filter membrane is considered to be soluble, the TEM images of domestic wastewater filtered using 0.45 µm filter membrane (Fig. 4.4a) show the presence of small and dispersed particulates defined by different shapes with average particle size of about 50 nm. The filtered wastewater spiked with ZnO ENPs at a concentration of 100 mg L^{-1} was subjected to TEM after 24-hr, and the results are summarized in Fig. 4.4b. The TEM results therefore further confirms aggregation of ZnO ENPs as observed in the DLS study, and the aggregates were stable for more than 24-hr. Although in lower extent, aggregation phenomenon was also observed with ZnO ENPs in de-ionized water (Fig. 4.4c). However, the average ENPs size difference between DLS (1500 nm) and TEM (200 nm) is expected considering the sensitivity differences between the two techniques and similar differences have been noted elsewhere. The EDS analysis results are given in Fig. 4.5, which suggest the presence of zinc in the dispersed filtrate, and the zinc existed as ZnO as confirmed by XRD given in Fig. 4.6.

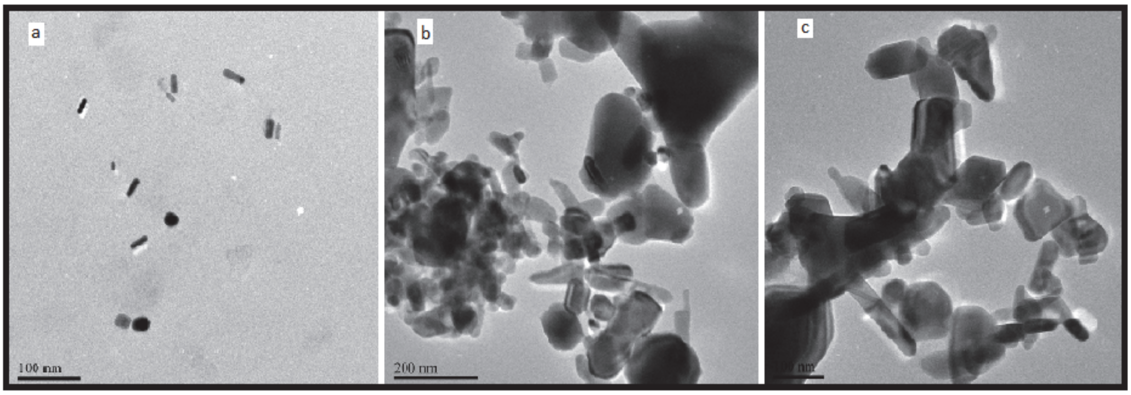

Figure 4.4: TEM images of (a) raw domestic wastewater filtered using 0.45 µm filter membrane and then (b) spiked with ZnO ENPs (100 mg L^{-1}) after 24-hr of stabilization; (c) ZnO ENPs (100 mg L^{-1}) in de-ionized water

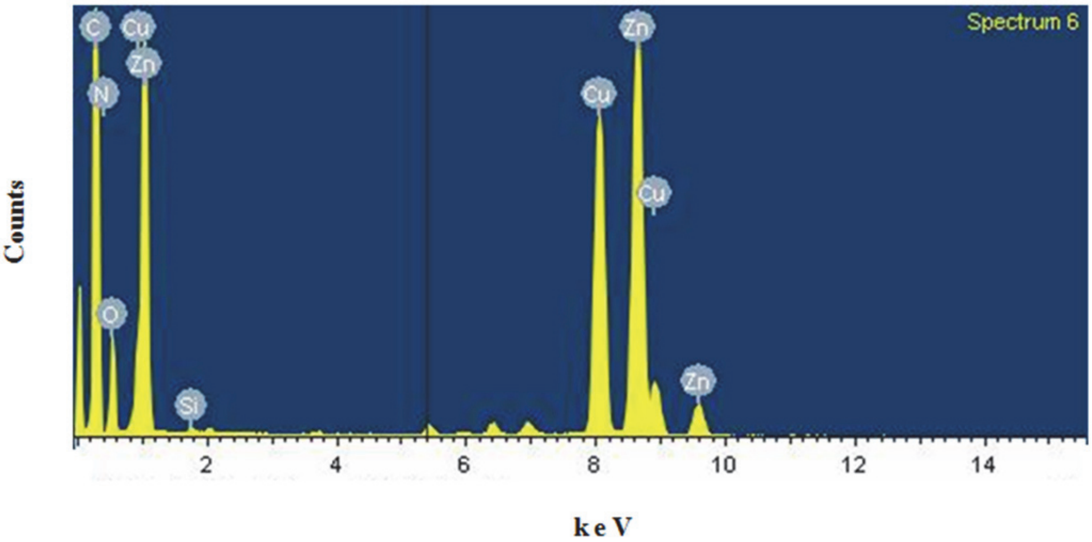

Figure 4.5: EDX image for Zn in the ZnO spiked domestic wastewater filtrate

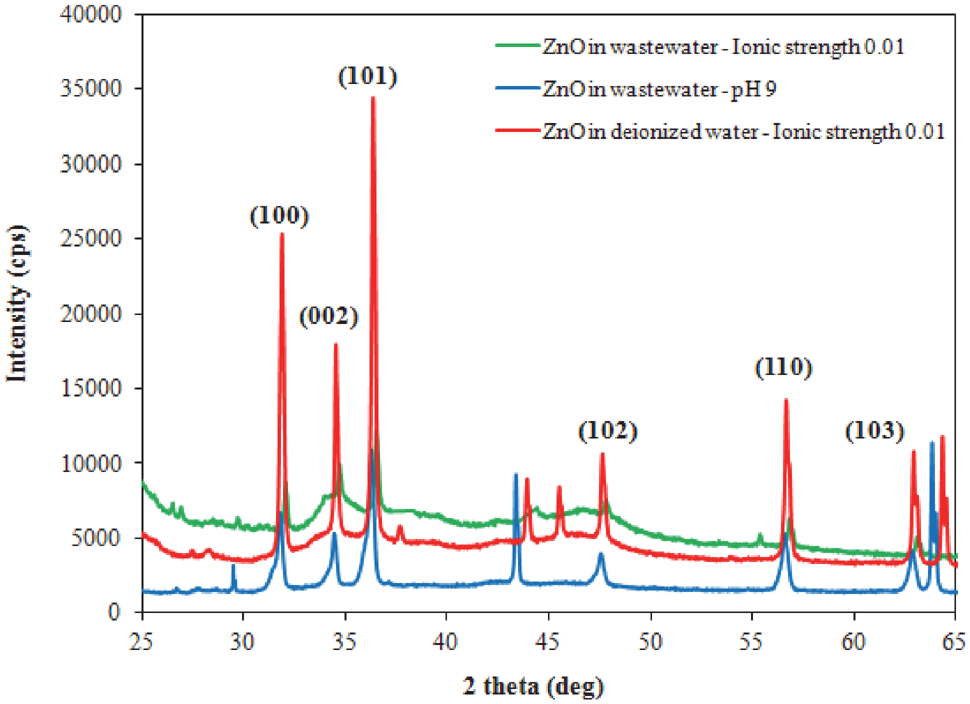

Figure 4.6: X-Ray diffraction (XRD) analysis for sludge exposed to ZnO ENPs.

4.2 Conclusions

The stability of ZnO ENPs in wastewater as pH and ionic strength change were investigated in this study. This was achieved through evaluation of release of zinc in wastewater as pH and ionic strength change and monitoring changes in ZnO ENPs size in wastewater using DLS and their interaction with sludge. The following conclusions were made: (i) the release of zinc from ZnO ENPs in wastewater is more significant under acidic conditions and low ionic strength. However, the release of zinc from ZnO ENPs in wastewater is lower compared to deionised water indicating the role of biomass present in wastewater. Under alkaline conditions, a large percentage of the metal-oxide ENP showed strong affinity for the sewage sludge rather than dissolved or dispersed in the filtrate. The depositions of ENPs on sludge suggest their removal by abiotic, bio-sorption and bio solid settling mechanisms. Therefore, in typical wastewater treatment systems, they are therefore likely to be introduced into the environment through the use of sludge for agricultural purposes as well as possible release as flyash during sludge incineration. (ii) The size of ZnO ENPs was found to significantly increase upon exposure to wastewater, an observation that suggests the sorption and stabilization ability of NOM such as humic acid present in wastewater.

CHAPTER 5

FATE, BEHAVIOR, AND REMOVAL OF ZnO NANOPARTICLES IN A SIMULATED WASTEWATER TREATMENT PLANT: IMPLICATIONS OF ENPs CONCENTRATION

Preamble

The behaviour and fate of ZnO nanoparticles in the treatment of wastewater was investigated and reported in this chapter. After the administration of the engineered nanoparticles in the simulated activated sludge wastewater treatment, the removal efficiency was obtained, reported and is explained. This enabled the determination of the potential implications of ZnO ENPs used in this simulated wastewater treatment set-up by varying the concentration used.

5.1 Results and Discussion

5.1.1 Simulated activated sludge wastewater treatment plant (AS WWTP) performance

The results of characterization of the raw domestic wastewater used in the simulated treatment plant (as described in section 3.2.1) are provided in Table 5.1.

Table 5.1: Characteristics of raw domestic wastewater used in the simulated wastewater treatment plant study

Parameter	Units	Value
pH	-	6.98 ± 0.34
Conductivity	µS/cm	715 ± 52
Salinity	Psu	0.34 ± 0.09
Total dissolved solids (TDS)	mgL^{-1}	344 ± 43
Dissolved oxygen (DO)	mgL^{-1}	3.55 ± 0.38
Chemical oxygen demand (COD)	mgL^{-1}	543 ± 158
Dissolved organic carbon (DOC)	mgL^{-1} C	19 ± 6
Total suspended solids (TSS)	mgL^{-1}	588± 39

Also, according to the analytical description provided in section 3.2.6, the XRD analysis (Fig. 5.1) of the ZnO ENPs confirmed the purity of the nanoparticles while TEM images showed the size distribution of 10 to 130 nm (Fig. 5.2) consisting of heterogeneous mixture of rods, cubes, regular and irregular spheres.

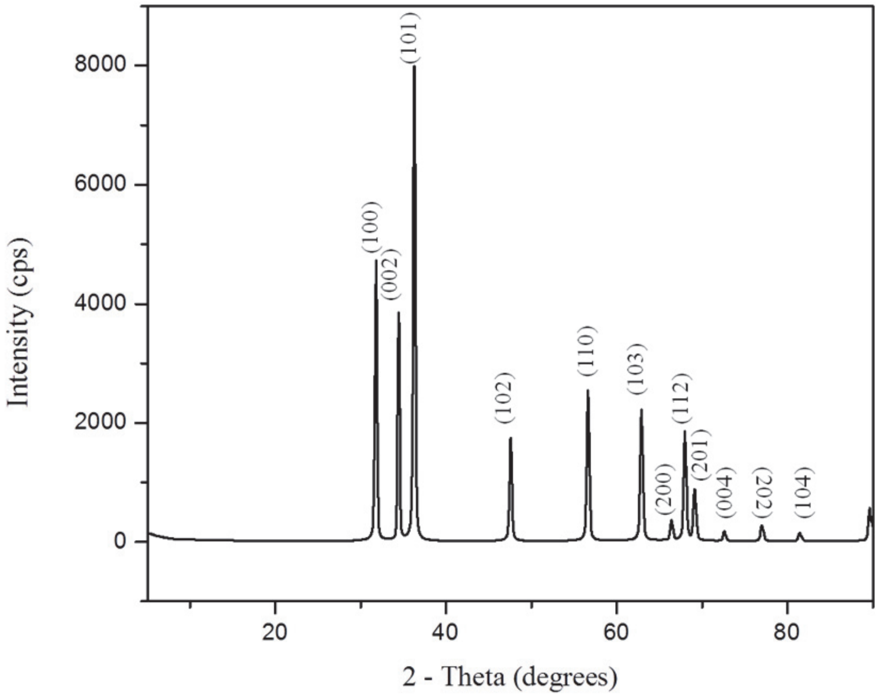

Figure 5.1: XRD pattern of ZnO ENPs

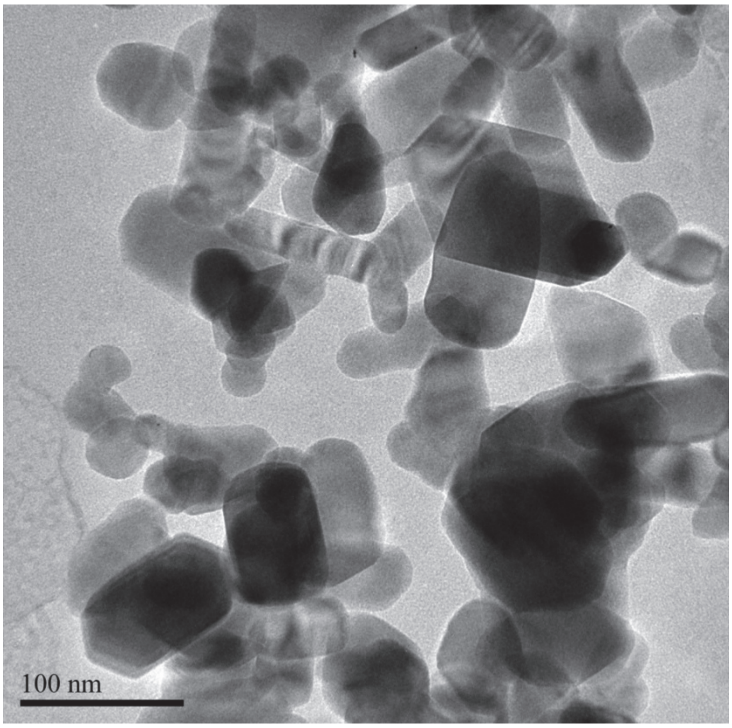

Figure 5.2: Transmission electron microscope (TEM) image of ZnO ENPs

The organic matter removal ability of the simulated AS WWTP was assessed by monitoring both chemical oxygen demand (COD) and dissolved organic carbon (DOC) upon exposure of ZnO ENPs to wastewater. The dissolved oxygen (DO) levels in the aeration chamber were kept above 2 mgL^{-1} during the experiment by continuously bubbling compressed air through a glass frit to provide bacteria with enough oxygen. The ZnO ENPs were added to the influent deionised water and wastewater for the control and test units, respectively, and the nanoparticle concentration increased continuously along the experiment. The ZnO ENPs concentration employed were as follows: 0, 5, 10 and 20 mgL^{-1}. The Figs. 5.3 and 5.4 show the organic matter removal has reached a steady state at around 10 and 50 mgL^{-1} of DOC and COD, respectively, in the effluent regardless of the amount of organic matter in the wastewater influent. The COD data (Fig. 5.4) revealed efficient organic matter removal as the treated wastewater presented an average COD values within 60-100 mgL^{-1} range that correspond to the average of well operated secondary treatment in WWTPs (Sonune and Ghate, 2004). Coupled to this, an average of 43 and 91% for DOC and COD removal efficiencies from the influent wastewater, respectively, were observed throughout the study. However, the values obtained for COD were in compliance to those described in the validity criteria for OECD 303 A, unlike the DOC values. However, in similar studies adding TiO_2 nanoparticles to the synthetic wastewater showed DOC removal efficiencies of above 97% (Gartiser et al., 2013) employing synthetic organic wastewater in a simulated treatment plant. In addition, non-significant impact of ZnO ENPs to the organic matter removal was observed under the conditions of the study. Similar findings were reported by Bolyard and co-workers (2013) when exposed ZnO, TiO_2 and Ag nanoparticles to the landfill leachate and Gartiser et al. (2013) when exposing TiO_2 nanoparticles to the synthetic wastewater. They observed no impact to the biological processes due to the presence of coated nanoparticles. This showed the dependence of the fate and behaviour of nanoparticles to the form in which are disposed to the environment.

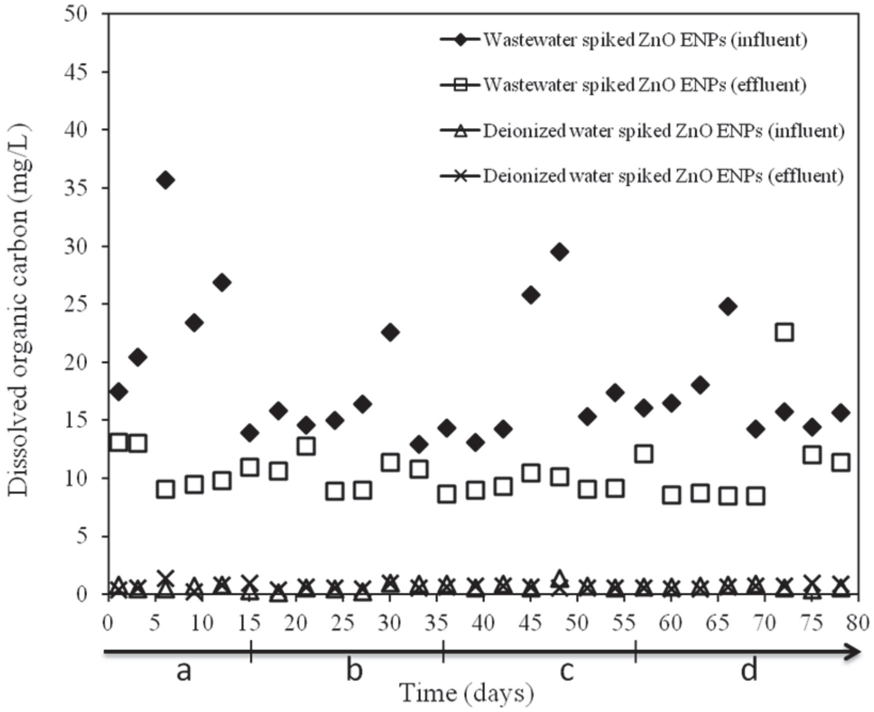

Figure 5.3: Dissolved organic carbon (DOC) analysis for influent and effluent in the simulated wastewater treatment plant (test and control units) upon continuous exposure to (a) 0 mgL^{-1}, (b) 5 mgL^{-1}, (c) 10 mgL^{-1} and (d) 20 mgL^{-1} of ZnO ENPs.

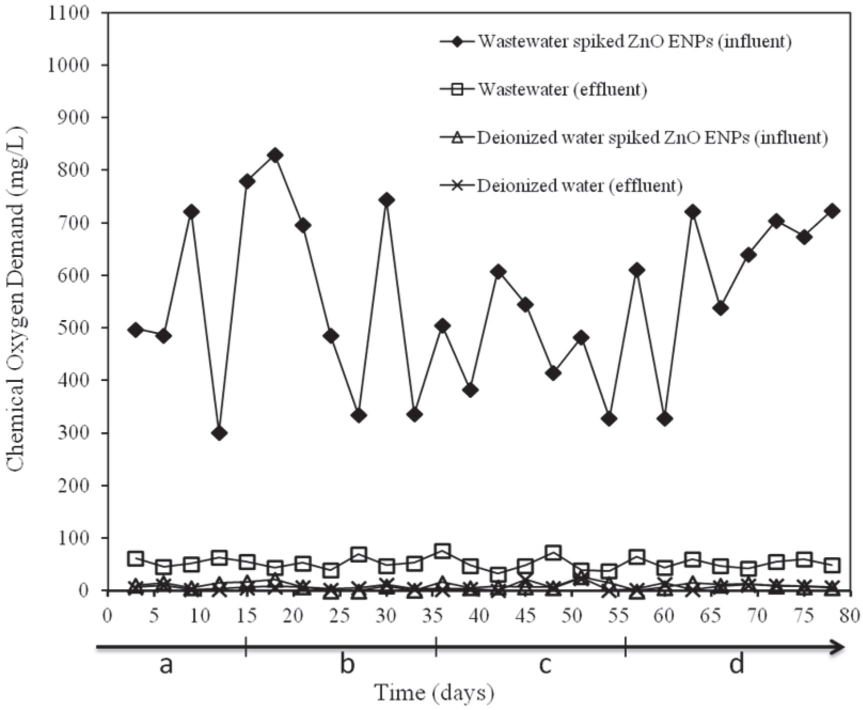

Figure 5.4: Chemical oxygen demand (COD) analysis for influent and effluent in the simulated wastewater treatment plant (test and control units) upon continuous exposure to (a) 0 mgL^{-1}, (b) 5 mgL^{-1}, (c) 10 mgL^{-1} and (d) 20 mgL^{-1} of ZnO ENPs.

5.1.2 ZnO ENPs removal during the simulated AS WWTP

Our findings as given in Fig. 5.5 show that 50-150 µgL^{-1} Zn is released in the effluent upon exposure of the 5 mgL^{-1} ZnO ENPs to wastewater in the simulated WWTP. However, deionized water spiked with a similar ZnO ENPs concentration, used as the control unit, exhibited higher levels of about 1 mgL^{-1} Zn in the effluent as given in Fig. 5.6. The absence of the biomass in the control aeration chamber could be responsible for such high effluent zinc release. Therefore, zinc removal in the test unit would be attributed to other pathways rather than abiotic factors that solely govern the control unit. In addition, the continuous stirring process of the aeration chamber provided great surface area for the biomass to interact with ZnO ENPs spiked to the influent wastewater. As a result, significant removal of ZnO from influent domestic wastewater was observed.

Figs. 5.5 and 5.6 show the levels of zinc entering and leaving the simulated AS WWTP in a daily basis. These findings are in line with the published data on the behaviour of metal oxide ENPs in simulated WWTPs. Kiser and co-workers (2009) reported the sorption of titanium from TiO_2 ENPs to biomass during wastewater treatment. However, 10-100 μgL^{-1} Ti still remained in the effluents. Limbach and co-workers (2008) observed the presence of 2-5 ppm of cerium oxide in the effluent following exposure of 100 ppm cerium oxide ENPs into a model wastewater treatment process. They considered nanoparticle adsorption to the biomass the main removal mechanisms.

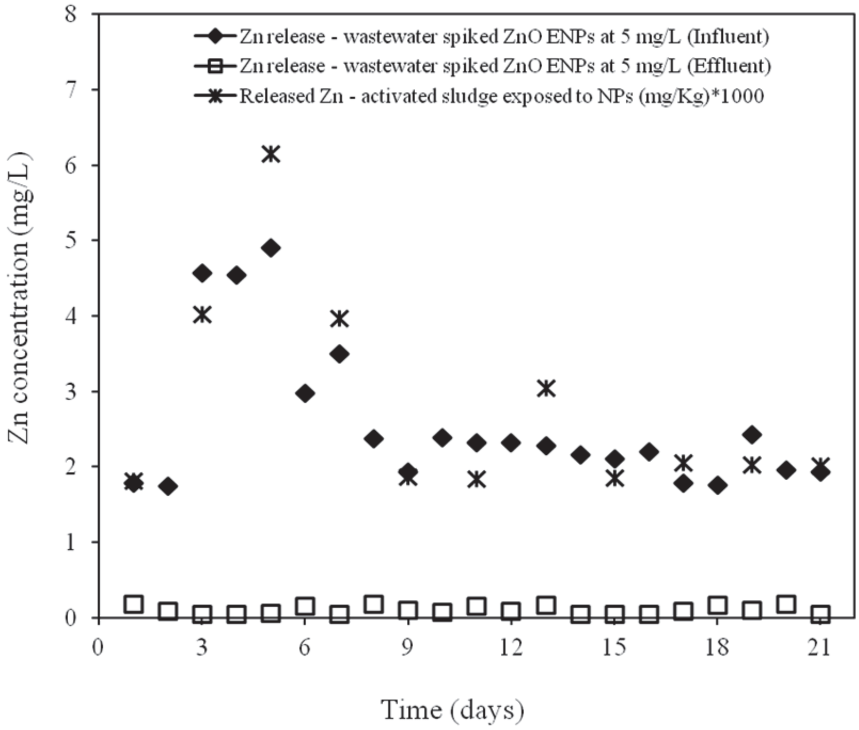

Figure 5.5: Zinc release from wastewater spiked using ZnO ENPs 5 mgL^{-1} in a daily basis (test unit).

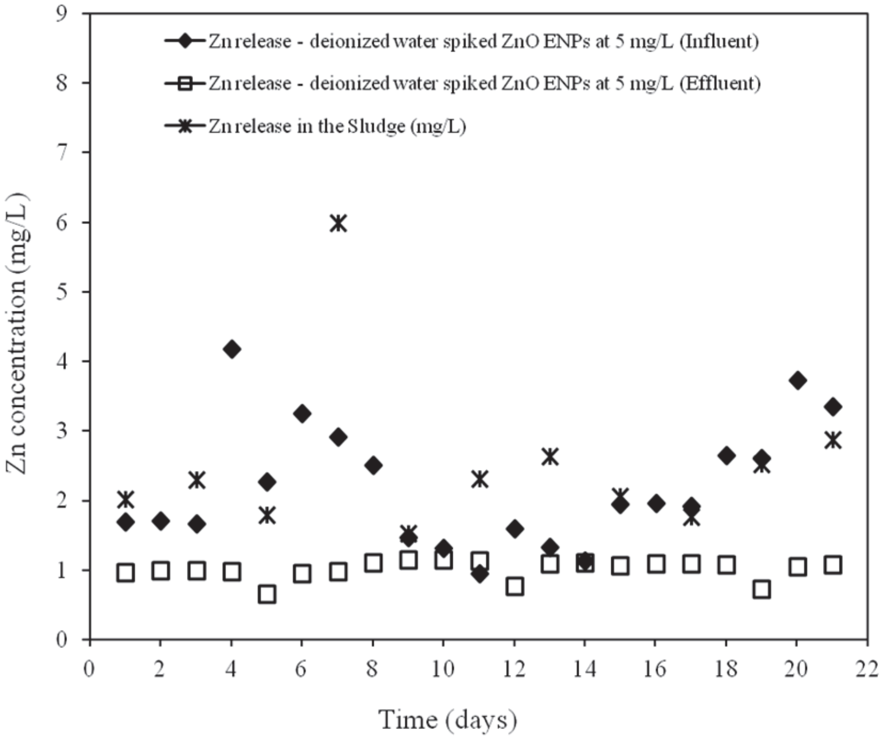

Figure 5.6: Zinc release from deionized water spiked using ZnO ENPs 5 mgL^{-1} in a daily basis (control unit).

The significant difference on the released zinc levels from the effluent wastewater and deionized water spiked using ZnO ENPs, respectively, constitutes strong evidence of the different removal pathways taking place in the test and control units. The change in speciation of ZnO ENPs to Zn species normally occurring in wastewater including ZnS has been reported by Lombi and collaborators (2012) during anaerobic digestion and post-treatment processing of sewage sludge. This finding reinforces the role of water chemistry (i.e. organic matter, electrolytes, pH, and ionic strength) on the fate and behaviour of ENPs in the environment. However, our findings indicated efficiency removal of ZnO ENPs from influent wastewater during wastewater treatment in a simulated WWTP. Furthermore, increasing the spiked levels of ZnO ENPs in the influent wastewater up to 20 mgL^{-1} showed a linear increase in the released zinc in the effluent though not significant comparing to the corresponding amount discharged in the effluent control unit as given in Fig. 5.7.

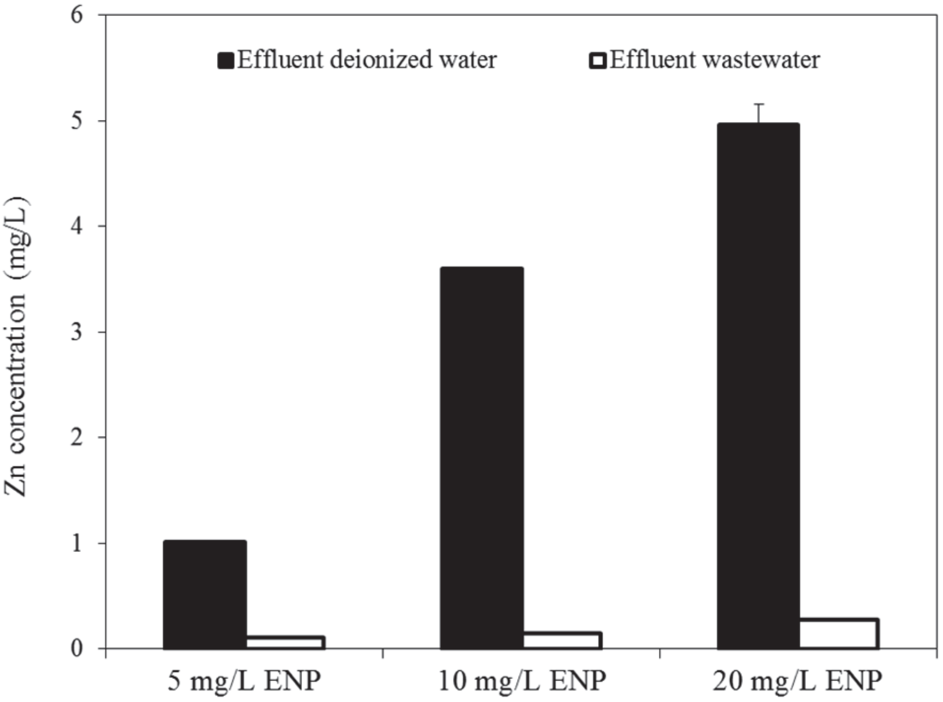

Figure 5.7: Comparison of zinc release in the effluent for the control (deionized water) and test (wastewater) units upon exposure to 5, 10, 20 mgL^{-1} ZnO ENPs during wastewater treatment.

Sorption of ENPs to biomass during the aerobic wastewater treatment process has been reported elsewhere (Kiser et al., 2009; Limbach et al., 2008). Based on the high Zn levels detected in the sludge as given in Fig. 5.5, suggesting strong affinity of ZnO ENPs for the sludge, the nature of the ENPs on the sludge surface was further characterized by XRD. However, XRD patterns could not confirm the presence of ZnO ENPs in the sludge exposed to wastewater spiked using 5 mgL^{-1} ZnO ENPs. Nevertheless, increasing ZnO ENPs concentration in the influent wastewater to 10 mgL^{-1}, the presence of ZnO in the sludge was detected despite the relatively low signal peak intensities. Further increase of the spiked ZnO ENPs concentration to wastewater to 20 mgL^{-1} resulted in slightly increased peak intensities of ZnO as given in Fig. 5.8. In addition, using UV-Vis spectrophotometer coupled with UV-Probe for solid state analysis of the sludge, we observed the absence of the excitonic absorption peak at 368 nm, revealing the absence of ZnO nanoparticles as reported by Sornalatha and Murugakoothan (2013). On the other hand, both pure ZnO ENPs and the sludge exposed to influent wastewater spiked with 10 mgL^{-1} ZnO ENPs presented the excitonic absorption pick at 368 nm (Fig. 5.9). Overall, the findings suggest that ZnO ENPs are removed during the simulated activated sludge wastewater treatment.

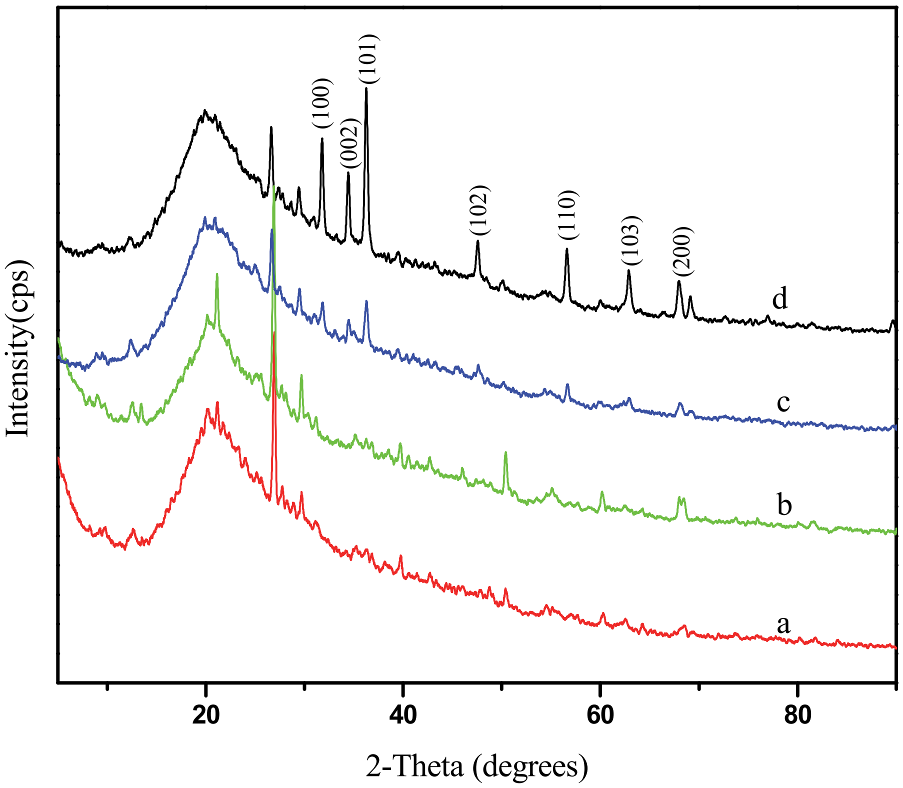

Figure 5.8: X-Ray diffraction (XRD) analysis of the sludge following wastewater influent exposure to a) 0 mgL^{-1}, b) 5 mgL^{-1}, c) 10 mgL^{-1} and d) 20 mgL^{-1} of ZnO ENPs.

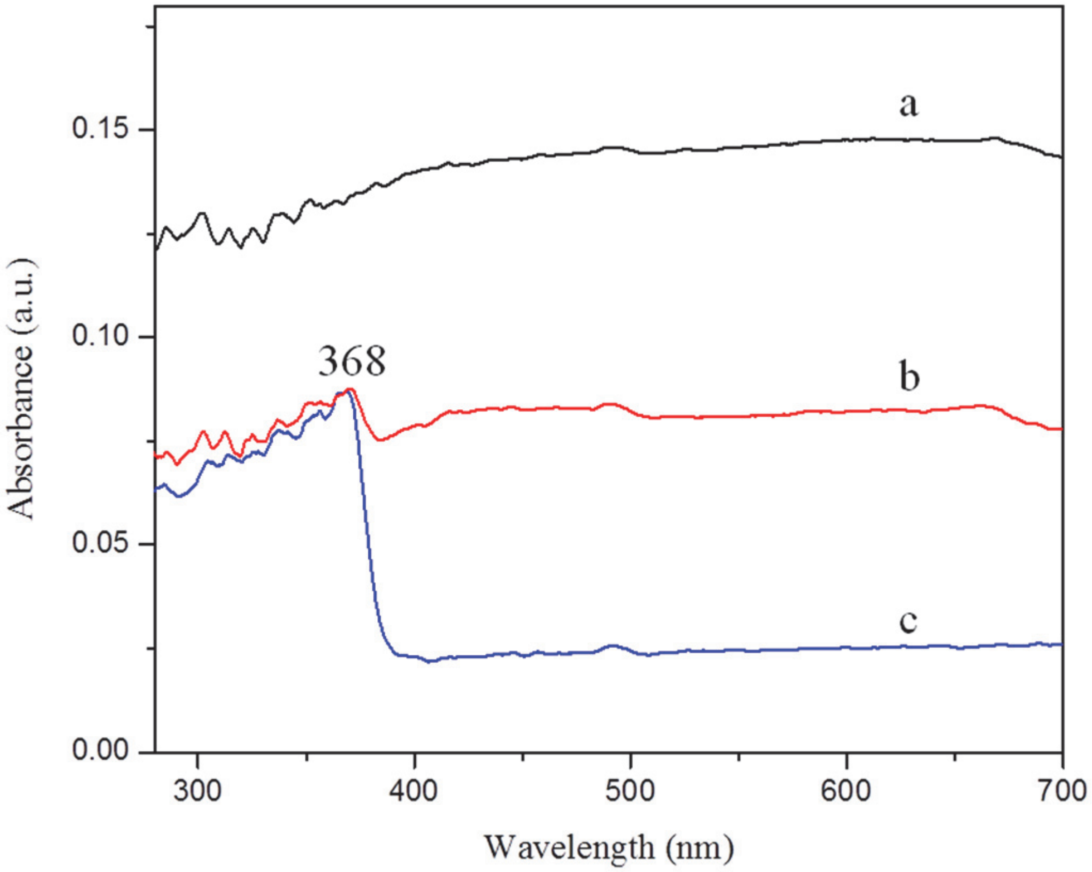

Figure 5.9: UV-Vis absorbance spectra of the sludge exposed to (a) 5 mgL^{-1} ZnO ENPs and (b) 10 mgL^{-1} ZnO ENPs; compared to the spectrum of (c) ZnO ENPs.

5.1.3 Possible mechanisms of ZnO ENPs removal during simulated wastewater treatment process

The difference on the released zinc levels in the influent and effluent for both control and test units (Figs. 5.3 and 5.4) revealed the removal of ZnO ENPs during wastewater treatment. However, the extent of the zinc released from the two units suggested different removal mechanisms. The control unit, devoid of activated sludge, the nanoparticles removal mechanism was governed solely by abiotic (e.g. pH) factors. On the other hand, the high nanoparticle removal in the test unit could not be assigned merely to abiotic factors provided the presence of the activated sludge. The activated sludge provides great surface area for contaminants adsorption while the organic matter may enhance their stability. Keller and co-workers, (2010) have reported enhanced stability of metal-oxides such as ZnO, TiO_2 and CeO_2 ENPs with organic matter adsorption to particle surface providing a barrier to aggregation. In addition, the presence of organic matter in freshwater was also found to enhance ENPs stability by allowing their coating and diffusion (Peralta-videa et al., 2011). Furthermore, the stability of ZnO ENPs was found to directly depend on the pH and ionic strength of wastewater (Chauque et al., 2013). The environmental concentration of humic acid was also reported to stabilize ZnO ENPs even at high concentrations (Omar et al., 2014). Therefore, considering the pH range of the activated sludge observed (7.00 ± 0.50) for the current work, stabilization of ZnO ENPs enhanced by organic matter would be expected. Since WWTPs operate with biomass ranging from 1000-5000 mgL^{-1} of TSS (Metcalf and Eddy, 2002), in our study, the biomass was kept within 2000-3000 mgL^{-1} range with the sludge retention time (SRT) of 6 days in average. The average crystallite size, L, of ZnO in the sludge was determined using the Scherer´s equation given as follows (Monshi et al., 2012):

$$L = \frac{k\lambda}{\beta \cos\theta} \tag{5.1}$$

where D is the diameter of the particle, K is the geometric factor taken to be 0.9, λ is the X-ray wavelength (0.15406 nm), θ is the diffraction angle and β is the full width at half maximum of the diffraction main peak at 2θ. The average ZnO particle size in the sludge exposed to wastewater influent contaminated with ZnO ENPs at 10 and 20 mgL^{-1} during the wastewater treatment was 29.22 ± 2.47 nm. The ZnO size distribution in the sludge showed that the adsorption of nanoparticles to the activated sludge was preponderant removal mechanisms compared to aggregation. Kiser and co-workers, (2010), have reported ENPs removal to be dependent on the amount of heterotrophic wastewater biomass to which the ENPs are exposed. Considering that the amount of the biomass reported elsewhere quite compares to the biomass levels in our study, we would expect significant biosorption and biosolid settling of the ZnO ENPs during wastewater treatment, and this is significantly affected by ENPs concentration. This is supported by high levels of zinc released from sludge (3 000 mg/Kg) also confirmed by the presence of ZnO in the sludge (Figs. 5.8 and 5.9). Therefore, the ZnO ENPs removal during simulated AS WWTP process can be considered to be of a complex nature though involving physi-sorption, chemisorption and/or intracellular microorganism metabolism and these are subject to future investigations.

5.2 Conclusions

Under the conditions of the study, which are closely related to the real WWTPs, the consortium of bacteria collected from a well operated WWTP and employed in the aeration chamber were able to remove the organic matter in the wastewater added ZnO ENPs. We observed that both COD and DOC were not significantly affected by changes in ENPs concentration, a phenomenon suggesting adaptation ability of microorganisms responsible for organic matter degradation during wastewater treatment upon long term exposure to ENPs. However, our findings on the potential release of zinc in the wastewater effluent as ENPs concentration changes indicate that, although the Zn levels were low, the potential release increased with ENP concentration, with a larger fraction of the ENPs associated with the sludge. This implies that the sludge treatment process would require additional steps to remove the elevated concentrations of metals, particularly in the South Africa context where more than 90% of the sludge from WWTPs is utilized for agriculture. In addition, the removal mechanisms of ZnO ENPs during wastewater treatment remain complex in nature, although abiotic, bio-sorption, and bio-solid settling mechanisms have been proposed. Furthermore, using wastewater and de-ionized water as test and control media, has allowed the understanding of ENPs removal induced by abiotic factors compared to the removal induced by the presence of the biomass.

CHAPTER 6

EXPOSURE EXPERIMENTS OF ENMs TO MICROBIAL ORGANISMS UNDER CONTROLLED WWTPs CONDITIONS

6.0 Preamble

The assessment of factors that govern bacterial growth in the wastewater sample was initially carried out. This was followed by the measurement of the minimum inhibition concentration (MIC) of the nanomaterials (NMs) on selected microbes (such a protozoa and bacteria) commonly found in typical wastewaters. Bacterial susceptibility to NMs of Ag and Zn was also investigated by the extraction and analysis of the bacterial extracellular polymer substrate (EPS). The survival limit of the microorganisms after exposure to different pH conditions was also determined.

6.1 Introduction

The extensive production, manufacturing and application of metal and metal oxides commercial nanomaterials (NMs) has remarkably increased over the past years. This is due to their unique surface -to- volume ratio, size/quantum effect and increased atoms at the grains boundaries, making them different from the bulk material counterparts (Heinlaan et al., 2008; Akbari et al., 2011; Premanathan et al., 2011). Of all the commercial NMs, zinc oxide (*n*ZnO) and silver (*n*Ag) have been among the most produced NMs, due to their physicochemical properties indicating different spectrums activities and morphologies. It has been reported that *n*ZnO have unique ceramic texture, photocatalytic capacity, piezoelectric properties used as additives (to functionalize as semiconductor), and photo-oxidizing ability against chemical and biological species (Adams et al,. 2006; Ju-Nam and Lead 2008; Padmavathy and Vijayaghavan, 2008; Aruoja et al., 2009; Premanathan et al,. 2011). On the other hand, silver nanomaterials have found usage in medical devices for over 2 000 years, leading to a widespread attraction, exploitation and application in the medical field as a bactericidal and as a therapeutic agent and food preservation (Prabhu and Poulose 2012). This is owing to their high optical, thermal conductivity and electric properties, which lead to major applications use as catalysts, optical sensors of zeptomole (10−21) concentration in textile engineering, electronics and optics (Choi et al., 2008a; Ju-Nam and Lead 2008; Bystrzejewska-Piotrowska et al., 2009; Rai et al., 2009; Thwala et al., 2013).

Through their lifecycles, *n*ZnO and *n*Ag are likely to enter natural water bodies channelled via wastewater treatment plants (WWTPs) (Aruoja et al., 2009). Thereafter, leading to environmental risks associated to possible detrimental implication on microbial driven processes and public health concern (Neal 2008; Tso et al,. 2010; Baalousha et al,. 2013; Li et al., 2013; Beddow et al., 2014; Musee et al., 2014). It has been reported that municipal wastewater treatment plants (WWTPs) are the main sources of pollutants as they transport contaminated effluent into water surface, landfills and soils (Kiser et al., 2010). Biological treatment of wastewater involves confining naturally occurring bacteria at very much higher concentrations in tanks. These bacteria, together with some protozoa and other microbes, are collectively referred to as activated sludge. During the treatment, the bacteria remove small organic carbon molecules by degrading them and as a result the bacteria grow and the wastewater is cleansed. It has been reported that the control of the treatment process can be affected by the changes in the composition of the bacterial flora of the treatment tanks, and the changes in the sewage passing into the plant (Davies 2005). High concentrations of toxic chemicals can produce a toxic shock that kills the bacteria. This can result in inefficient performance of the wastewater treatment systems to produce effluents of the required standards.

Currently, majority of investigations have been focused on human health implications of NMs; very few efforts consider the environmental implications of NMs, including the fate, transport, and toxicity, to promote sustainable use of these novel materials (Ju-Nam and Lead, 2008). Furthermore, there is still a knowledge gap on the actual uptake mechanism, induce effect, transport in biological compartments and toxicity modes of action in particle specific (Ju-Nam and Lead 2008; Baker et al., 2013). Even if the exact antibacterial mode of action is yet to be discovered for *n*ZnO, the catalytic oxidation in silver promoted by metallic silver reacting with monovalent silver ions are likely to contribute to toxicity (Ju-Nam and Lead 2008). To date, antimicrobial research studies of *n*ZnO and *n*Ag have vastly increased towards microbial species and freshwater organism, including duckweed, nematodes (*Caenorhabditis elegans*), waterflea (*Daphnia magna*), zebra fish, and pond snails (*Lymnaea stagnalis*) (Adams et al., 2006; Heinlaan et al., 2008; Aruoja et al., 2009; Azam et al., 2012; Baker et al., 2013). It has been pointed out that it is the rate of exposure and effect of nanomaterials on bacterial strains that varies due to different cell physiological characteristics and metabolism (Adams et al., 2006). In addition, the bioavailability and toxicity of NMs towards bacteria may alter the normal ecological process, functions and productivities (Neal

2008). Thus, bacterial cells actively produce extracellular polymeric substances (EPS), which are polysaccharides rich in organic matter. These polymeric substances are known as a protective barrier for cell wall during exchange processes and in contact with environment (Kiser et al., 2010) and may stabilise NMs, due to their ability to produce soluble biomass associated products (Laspidou and Rittmann 2002).

A number of studies have depicted that NMs are able to (i) adhere to a cell, block essential pores and membrane functions; (ii) enter the cell by endocytosis via pores, degrades the lipopolysaccharide molecules and accumulate inside cells (Li et al., 2008; Liang et al., 2010; Musee et al., 2011; Baker et al., 2013), facilitate reactive oxygen species (ROS) production by redox reaction with oxygen, damage deoxyribonucleic acid (DNA), resulting in the loss of cell replication ability (Neal 2008; Padmavathy and Vijayaraghavan, 2008; Liang et al., 2010; Musee et al., 2011; Baker et al., 2013). Regardless of the belief that *n*ZnO are non-toxic, biosafe and biocompatible, toxicological activities reports have shown *n*ZnO to cause damages on the cell membrane due to oxidative stress (Huang et al., 2008). In addition, experimental studies showed near complete inhibition of *B. Subtilis* due to *n*ZnO and that in the presence of both light and in darkness, while *E. coli* has been found less susceptible to *n*ZnO in dark conditions (Adams et al., 2006; Dasiri et al., 2013). This is owing to novel physicochemical properties of NMs; among such is the size scale that is relative to that of bacteria and recalcitrant environmental pollutants (Choi and Hu 2008; Choi et al., 2008b).

This study focused on the assessment of factors that govern bacterial growth in the wastewater system. The measurements of the minimum inhibition concentration (MIC) of the nanomaterials (NMs) on selected microbes (such a protozoa and bacteria) commonly found in typical wastewaters have been conducted. Bacterial susceptibility to NMs of Ag and Zn was also investigated by the extraction and analysis of the bacterial extracellular polymer substrate (EPS). The survival limit of the microorganisms after exposure to different pH conditions was also determined.

6.2. Results

6.2.1. Characterization of the dry powdered phase of nanomaterials

The micrographs analysis of HRTEM and SEM images revealed the regular and irregular poly- dispersity shapes of *n*ZnO and spherical and diagonal shapes *n*Ag (Figure 6.1). These results were in agreement with the BET results that confirms the wide size distribution of *n*ZnO as shown in Figure. 6.1 A and B. Furthermore, *n*Ag images obtained from HRTEM and SEM micrographs showed narrow size distribution. Moreover, the images revealed the aggregation/agglomeration formation with both *n*ZnO and *n*Ag present in both HRTEM and SEM (Figure 1).

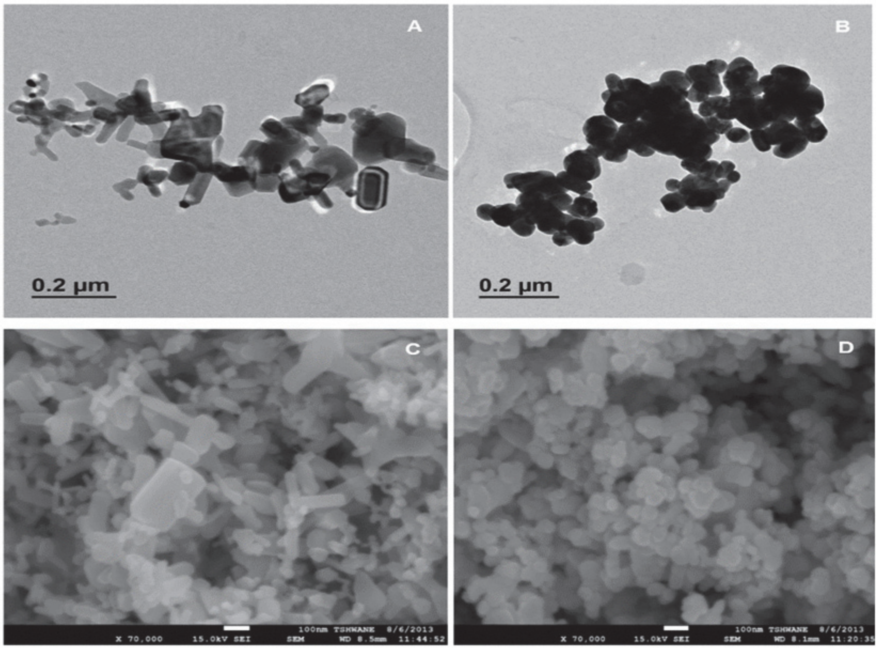

Figure 6.1: Images of the obtained from HRTEM and SEM for *n*ZnO (A & C) and *n*Ag (B & D).

The surface area analysis using Brauner-Emmett-Teller technique as shown in Table 6.1 indicated wide particle size distribution of *n*ZnO that were ranging from 10 -100 nm. The total particle surface area of *n*ZnO was found to be 15.88 m^3g^{-1}, with pore volume of 0.04 cm^3 g^{-1}. It was also revealed that *n*Ag demonstrated a narrow distribution of 30 to 50 nm in size with pore volume that is less compared to *n*ZnO of 0.03 cm^3 g^{-1} and particle surface of 4.98 m^2g^{-1}.

Table 6.1: BET results demonstrating the surface area of *n*ZnO and *n*Ag

Sample	BET$_{SA}$* (m^{2}g^{-1})	Point Surface (m^{2}g^{-1})	Particle size (nm)	Pore Volume (cm^{3}g^{-1})
*n*ZnO	15.88	15.42	10-100	0.04
nAg	5.37	4.98	30-50	0.03

The analysis of diffractions peaks patterns and inter-planar spacing obtained can be indexed as *n*ZnO confirming the wurtzite crystal structure (002) under the particular configuration, which matches with Bragg angle reflections (Figure. 2A). The XRD patterns of *n* ZnO are illustrated in Fig. 6.2 indicating the peaks indexed to be the zincite phase of ZnO. The micrographs further reveal that there were no impurity were observed, therefore, suggesting that high-purity ZnO were obtained. These micrographs analysis obtained at 2 Theta (Θ) values at 31, 34, 36, 49 and 49 correspond to [100], [002], [101], [102] and [110] planes of Zn, respectively indicated the crystallinity structure of the particles. It is further evident that the peaks identified belonged to high purity of hexagon crystal systems. The diffractograms of *n*Ag indicated the peaks that corresponded to the presence of crystalline reflecting face-centered cubic [111] (Figure. 6.2B). The exact nature of the *n*Ag can be constructed from the X-ray diffraction spectrum carried out to confirm the crystalline nature of the particles as shown in Fig. 6.3. The micrographs patterns obtained revealed intense peaks in the spectrum of 2Θ values ranging from 35 to 80. The XRD peaks were obtained at 2 Theta (Θ) values at 39, 44, 64 and 77 correspond to [111], [200], [220] and [311] planes of Ag, respectively.

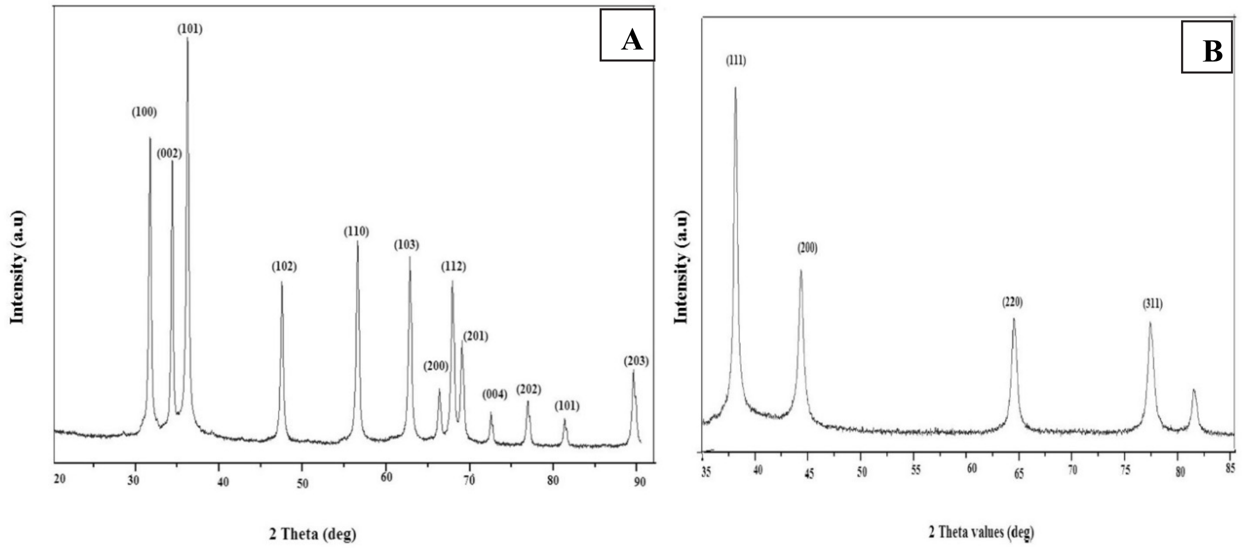

Figure 6.2: Diffraction peaks obtained from XRD (A) *n*ZnO and (B) *n*Ag

Fourier transforms infrared spectroscopy (FT-IR) absorption spectra of the *n*ZnO, in Figure. 6.3A revealed the presence of several vibration bands that were observed at 500, 600, 700, 850, 990, 1000, and 1050 cm^{-1} and could be attributed to C=O and C=N and C=C groups; and between 1490 -1600 cm^{-1} due to vibration bands of C-C stretch. Spectrometer graphs measurements were carried out to identify the functional groups present on the *n*Ag particles in Figure. 6.3B and this revealed bands s at 3000-2500 cm $^{-1}$ that are assigned to the stretching vibrations of amines, respectively corresponding to the bending vibrations of a weak double bond at the wavelength of 1600 cm^{-1}. There were also single bonds of -C=O H-C-H, -C-O, and -C-N stretching seen at 900 and 1500 cm $^{-1}$, respectively which confirms Amide I regions. Moreover, there was minor visible vibration peak at 2400 cm^{-1} which is the representative of O=C=O.

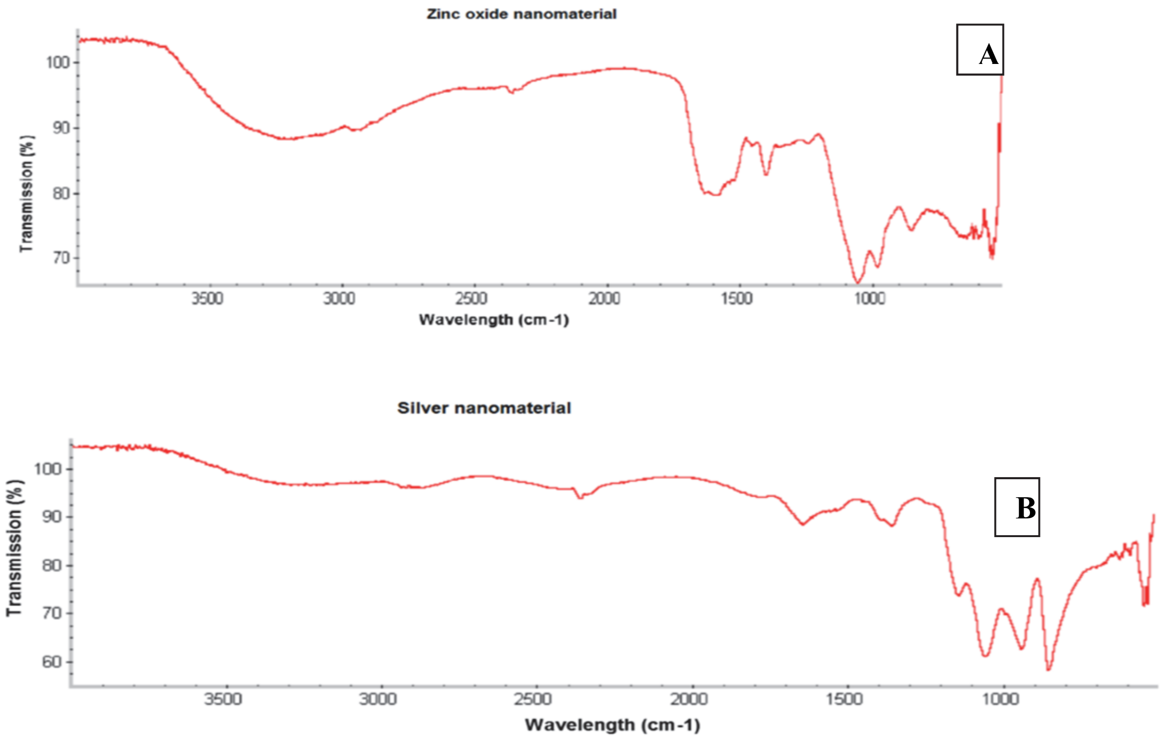

Figure 6.3: XRD micrographs and FT-IR spectra of ZnO nanopowders

6.2.2 Wastewater profile

The domestic wastewater samples collected from Daspoort WWTP were screened in terms of DO, COD, pH and other chemical contents (Table 6.2). The wastewater samples appeared to contain several chemical elements such as Ca, Mg and K which were found to be at a concentration of 23.07-23.52 mg/L, 11.59-11.60 mg/L and 6.96-7.02 mg/L, respectively. However, Zinc (0.48 mg/L) and silver (0.01 mg/L) as the targeted metals were present in the samples at a concentration below 0.5 mg/L. Other physicochemical parameters such as COD, DO and pH were also found at concentrations ranging between 110 and 143 mg/L, 7.29 mg/L and 7.79 mg/L, and 7.62 pH Units and 8.04 pH Units, respectively.

Table 6.2: Profile of the domestic wastewater sample

	First sampling period	Second sampling period
Hg (mg/L)	0.78	0.70
Mg (mg/L)	11.59	11.60
Pb (mg/L)	0.09	0.09
K (mg/L)	6.96	7.02
Ca (mg/L)	23.07	23.52
Zn (mg/L)	0.48	0.48
Fe(mg/L)	0.16	0.16
As (mg/L)	0.06	0.06
Ag (mg/L)	0.01	0.01
COD (mg/L)	0.110	0.143
DO (mg/L)	7.29	7.72
pH	8.04	7.62

6.2.3. Growth performance of pure bacterial isolates

This section discusses the bacterial growth curve in media without nanomaterials; bacterial performance in broth after 24 h of exposure to NMs; minimum inhibition concentration of bacterial isolates in the presence of NMs cultured on nutrient agar (NA); Kirby-Bauer disk diffusion study; bactericidal and bacteriostatic effects of NMs on cell membrane.

6.2.3.1. Bacterial growth curve in media without nanomaterials

Growth curves of *Bacillus , Brevibacillus and Pseudomonas* were evaluted in culturing nutrient media (NB) without NMs as shown in figure 6.4 A. In general, bacterial isolates showed a rapid growth in pH 7.1±0.2 (NB) reaching the exponential growth within the 24 h of incubation. This was evident that the selected bacterial isolates can survive in the media for 5 incubation days at 37ºC before they decline to lower biomass concentration.

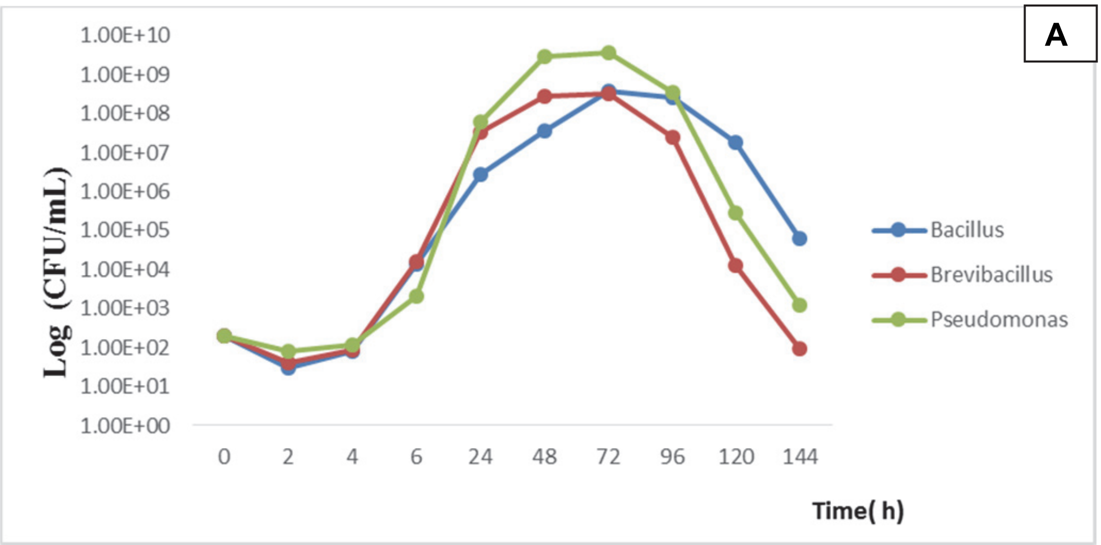

Figure 6.4: Growth curve of *Bacillus*, *Brevibacillus* and *Pseudomonas* obtained in NB (pH 7.1±0.2) over 5 days incubation at 37ºC

6.2.3.2. Bacterial performance in broth after 24 h of exposure to NMs

Figures 6.4B and C illustrate the growth responses of bacterial isolates in culture media (NB) containing various concentrations of *n*ZnO (0.015-20 g/L) and *n*Ag (0.015-1 g/L), separately. In general, the growth of *Bacillus*, *Brevibacillus* and *Pseudomonas* over 24 h incubation were observed to reduce in cell number in presence of *n*ZnO (Figure. 4B). Noticeably, the growth of *Bacillus*, *Brevibacillus* and *Pseudomonas* were reduced to approximately 70% at concentration of 0.105 g *n*ZnO /L. The increasing concentration of *n*ZnO to demonstrated a complete inhibition activity towards *Pseudomonas* at 0.65 g/L, and only 70% cell reduction of *Bacillus* and *Brevibacillus* at the same *n*ZnO concentration. A 100% growth inhibition was recorded for the all isolates when there were in the presence of 1 g/l nZnO. Therefore, these results indicated the MIC value in NB was obtained at 1 g/L for all bacterial isolates.

As shown in Figure 6.4C, *Bacillus*, *Brevibacillus* and *Pseudomonas* appeared to be more susceptible in the presence of *n*Ag. Bacterial growth were induced 100% recorded at 0.06 g/L, 0.06 g/L and 0.65 g/L for *Bacillus*, *Brevibacillus* and *Pseudomonas.*

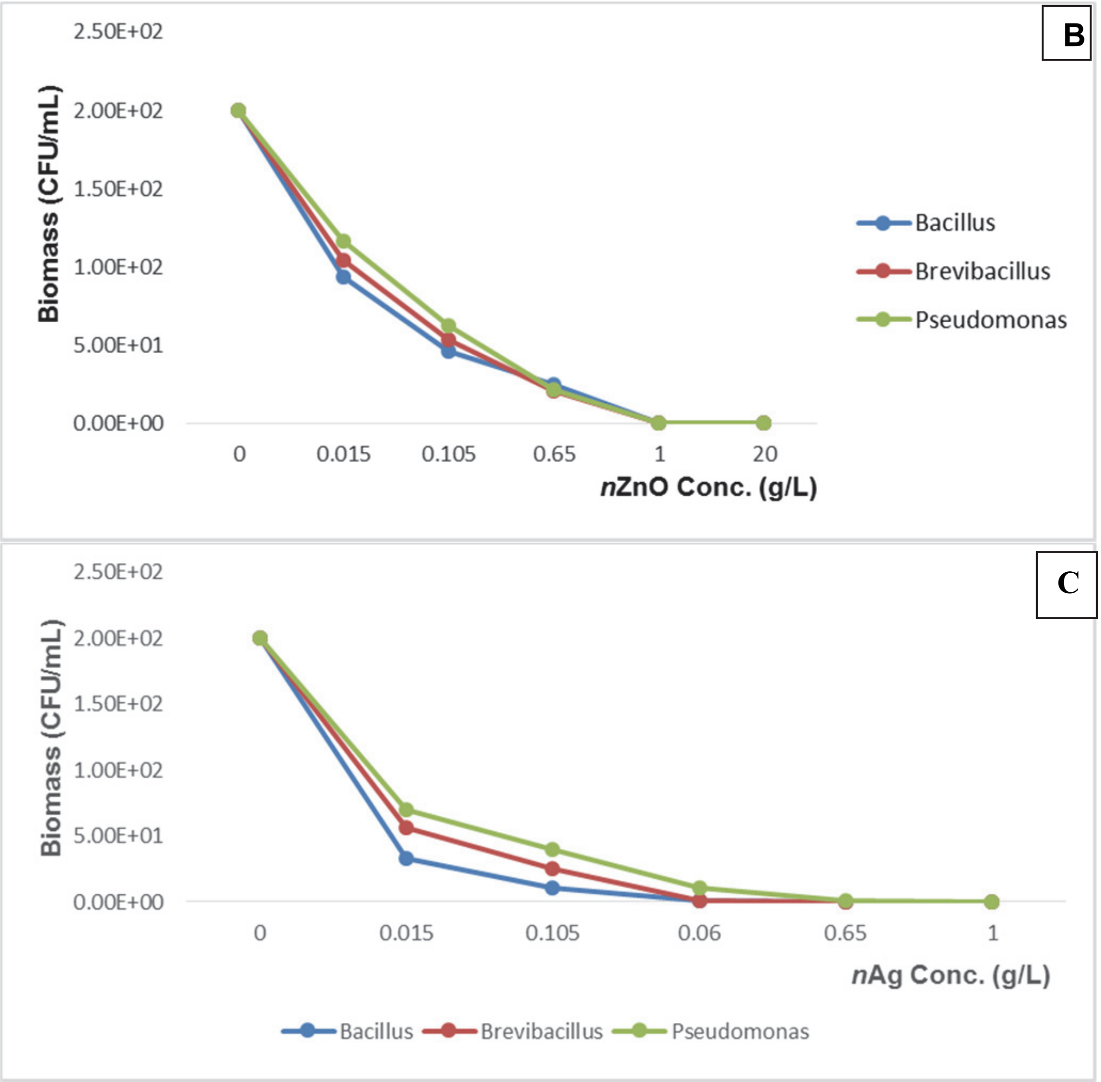

Figure 6.5: Minimum inhibition concentration of *Bacillus*, *Brevibacillus* and *Pseudomonas* obtained after 24 h incubation in NB (pH 7.1±0.2) (B) in the presence of increasing concentration of *n*ZnO and (C) in the presence of increasing concentration of *n*Ag

6.2.3.3. Minimum inhibition concentration of bacterial isolates in the presence of NMs cultured on nutrient agar (NA)

An exposure of *Bacillus*, *Brevibacillus* and *Pseudomonas* in the presence of *n*ZnO over 24 h resulted in a complete bacterial inhibition growth as shown in Figure 6.5(A, C & E). As *n*ZnO concentration increased, the growth of bacterial isolates was inhibited. These results demonstrated bacteriostatic effect of *n*ZnO obtained at MIC values of 1 g/L, 20 g/L and 20 g/L, for *Bacillus*, *Brevibacillus* and *Pseudomonas,* respectively. In comparison to *n*ZnO, the average MIC values of *n*Ag for *Pseudomonas* was obtained at 0.06 g/L, while *Bacillus* and *Brevibacillus* were both completely inhibited at 0.65 g/L *n*Ag (Figure 6.5 B, D & F) .

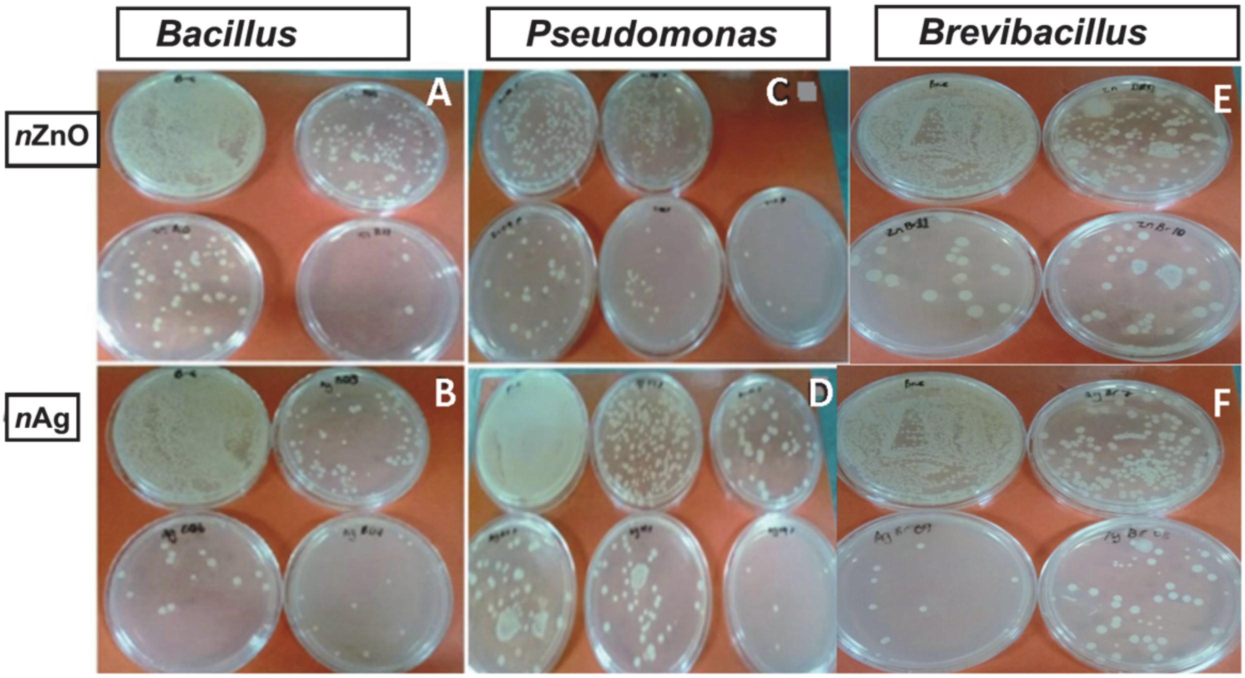

Figure 6.6: Minimum inhibition concentration of silver and zinc oxide NMs towards single bacterial isolates incubated over 24 h in agar plates

6.2.3.4. Kirby-Bauer disk diffusion study

The qualitative antibacterial toxic effects were assessed using disk diffusion assays to evaluate and determine susceptibility effects by measuring the zones of inhibition (Figure 6.6). The rupture of bacterial cells measured as inhibition zone indicated the bactericidal mechanism caused by *n*ZnO and *n*Ag. Cell growth inhibition were measured in terms of zone of inhibition (mm) and interpreted as sensitive, moderate and tolerant in the presence of *n*ZnO and *n*Ag (Table 6.3). Overall, bacterial isolates were susceptible to both *n*ZnO and *n*Ag. The results revealed that *Brevibacillus* cells were more sensitive, while *Bacillus* and *Pseudomonas* demonstrated a moderate inhibition effect to *n*ZnO. An exposure of bacterial isolates to *n*Ag showed that all target bacteria were susceptible with zones of inhibition indicating that the cells were sensitive to *n*Ag, distinctively. However, neither of the bacterial isolates could indicate whether they were tolerant when exposed to NMs. These results illustrated that *n*Ag had exhibited bactericidal effects and *n*ZnO exhibited bacteriostatic effects towards bacterial isolates.

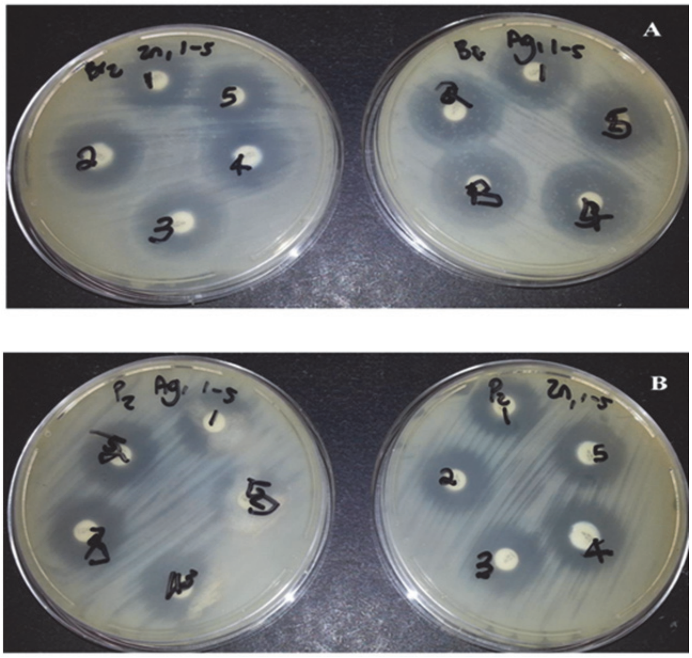

Figure 6.7: Susceptibility effect of silver and zinc oxide NMs using disk diffusion assays to by measuring zone of inhibition

Table 6.3: The susceptibility effect of *n*ZnO and *n*Ag on test isolates expressed in zone of inhibition (mm)

NMs conc. (g/L)	*n*ZnO			*n*Ag		
	Bacillus	***Pseudomonas***	***Brevibacillus***	***Bacillus***	***Pseudomonas***	***Brevibacillus***
0.015	1.5	1.7	2.7	0.9	0.9	0.9
0.030	1.3	1.7	3	1.3	1.5	1.5
0.045	1.2	1.4	3	1.1	1.3	0.8
0.060	1.3	0.8	2.6	1	1.1	1
0.075	1.3	1.5	2.4	1.2	1.2	0.9
0.090	1.1	1.4	3	1.2	1.1	1
0.105	1.2	1.6	6.3	1.3	1.3	1.1

6.2.3.5. Bactericidal and bacteriostatic effects of NMs on cell membrane

To assess the bactericidal and bacteriostatic effects of NMs on cell membrane, the exopolysaccharide substances were extracted and examined. The FTIR spectra of untreated (Figure 6.7) and treated bacterial isolates with *n*ZnO and *n*Ag are shown in Figures 6.8 and 6.9, separately. The results revealed the effects of NMs on the functional group of cell membrane elucidating their biosorption onto the membrane. Pronounced frequency at carbohydrates (C-O-C) bond regions indicated the stretching of polysaccharides and peptidoglycan at 1059, 1100 and 1060cm^{-1} for *Bacillus* and *Brevibacillus* and *Pseudomonas*, respectively as depicted in Figure 6.8. It was evident that exposure of *Bacillus*, *Brevibacillus* and *Pseudomonas* to *n*ZnO resulted in a significant broadening and shift of C-O-C bonds with dose increase (Figure. 6.8). The polysaccharides of *Brevibacillus* shifts were noted at frequency ranging between 900 -1200 cm^{-1}. The intensified shifts at the peaks area were observed, broadening to 1800 cm^{-1} for *Brevibacillus* and *Pseudomonas* shifted to 1581 cm^{-1} in the Amide I regions. Furthermore, *Brevibacillus* showed a single bond of C-H and –OH stretching vibration around 2900 cm^{-1} and broadened with an increase of *n*ZnO between 0.060 g/ L and 0.105 g/L. Similarly, *Bacillus* demonstrated the same patterns in the presence of *n*ZnO, except for *Pseudomonas.*

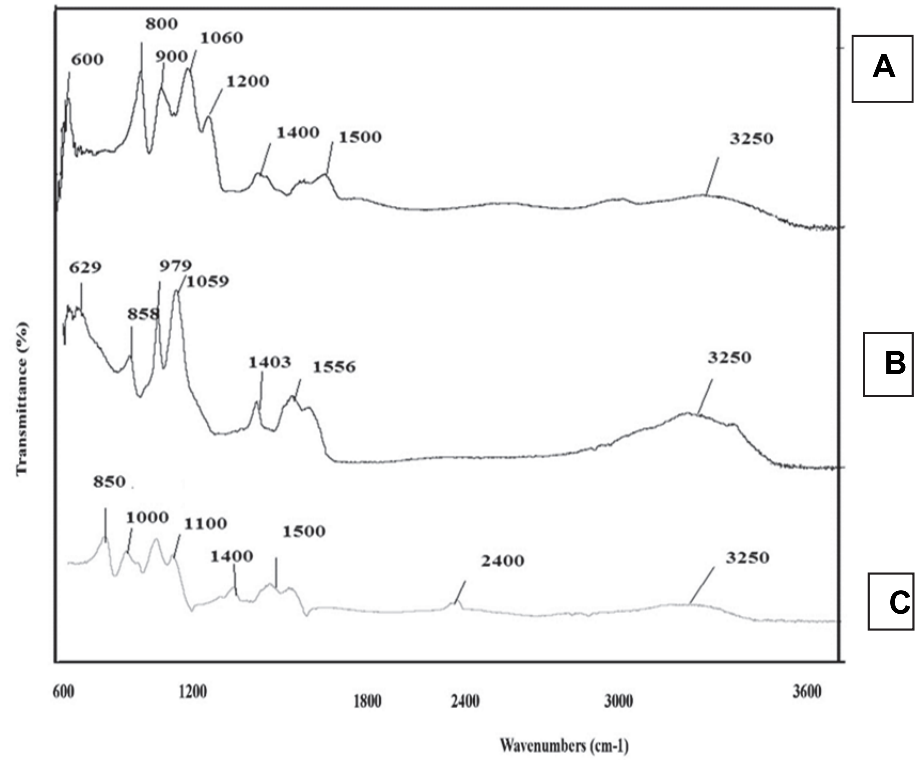

Figure 6.8: The FTIR spectra of untreated bacterial isolates showing functional groups present in the cell membrane of (A) *Pseudomonas* (B) *Bacillus* and (C) *Brevibacillus* bacterial isolates cultured in NB media for 24 h.

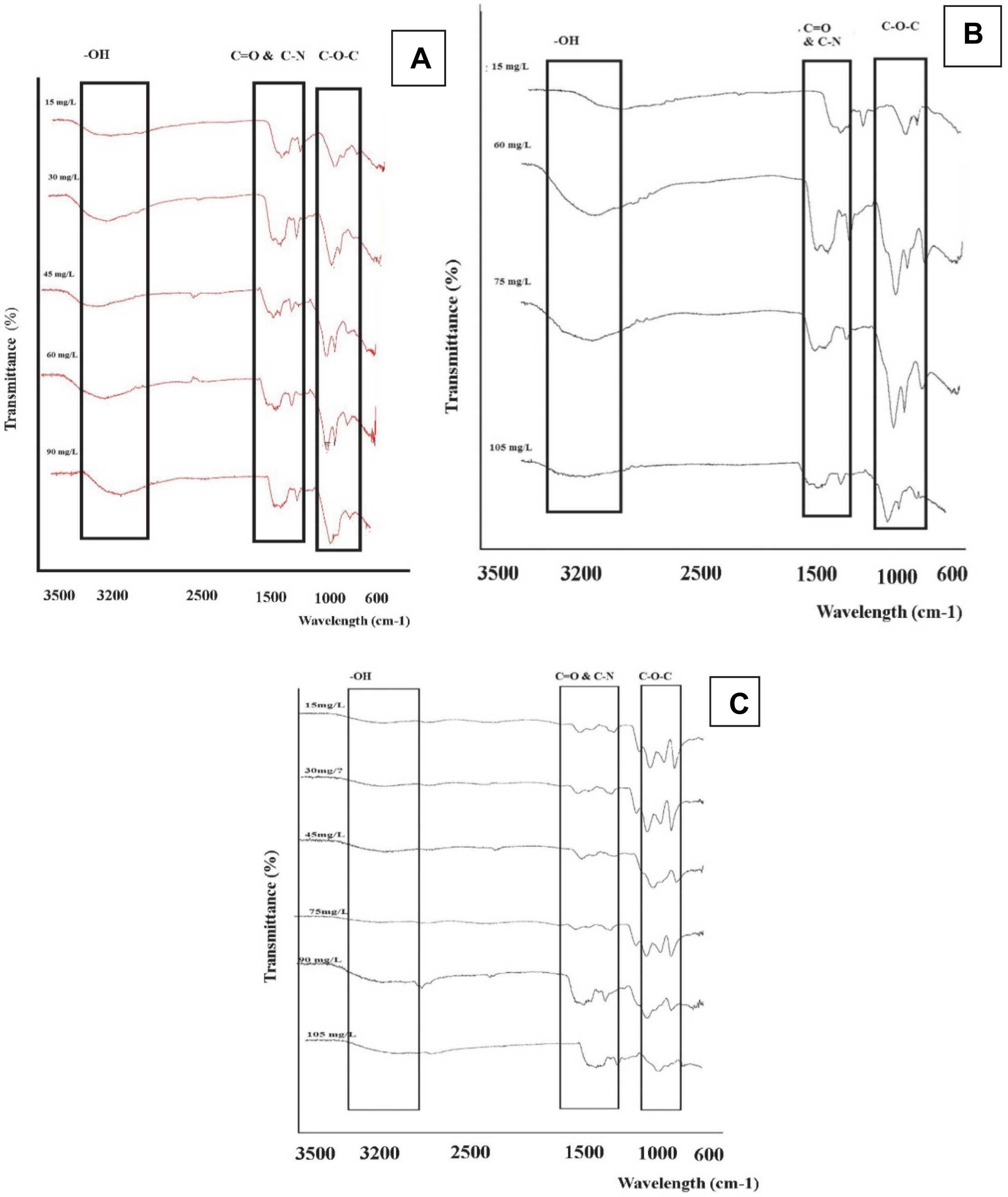

Figure 6.9: Micrographs of (A) P*seudomonas,* (B) *Bacillus* and (C) *Brevibacillus* in the presence of (0.015 g/L -20 g/L) *n*ZnO in the NB culturing media

When the bacterial strains were exposed to *n*Ag (Figure 6.9), *Pseudomonas* experienced a drastic change on the bands peaks at the skeleton vibration that shifted to 800 cm^{-1}. The C=O and C=N stretching also confirmed the changes in the Amide I regions with the shift to 1600 cm^{-1}. *Bacillus licheniformis* remarkably experienced an important shift on the functional groups at the highest concentration of *n*Ag, wherein, the C-O-C bands shifted to 1200 cm^{-1} and the Amide I and proteins peaks shifted to 1900 cm^{-1}. Even at the –OH, stretching vibration group showed a visible intense peak.

6.2.4. Evaluation of *n*ZnO and *n*Ag toxic effect towards single bacterial isolates in modified wastewater sample with change of pH values on a batch scale experiment

This section discusses the effect of pH on survival limit of bacterial biomass of single isolates exposed to nanomaterials; COD release/increase by single bacterial isolates exposed to nanomaterials in modified wastewater mixed liquor at pH 7; DO uptake/removal by single bacterial isolates exposed to nanomaterials in modified wastewater mixed liquor at pH 7.

6.2.4.1. Effect of pH on survival limit of bacterial biomass of single isolates exposed to nanomaterials

Figure 6.10 illustrates the inhibition effect of *n*ZnO and *n*Ag onto bacterial isolates (*Bacillus*, *Brevibacillus* and *Pseudomonas*) in modified wastewater adjusted to pH 2. Zinc oxide NMs prevented growth of *Bacillus* at concentrations 0.06 g/L, whereas concentrations 0.150 and 20 g/L prevented growth of *Pseudomonas* and *Brevibacillus,* respectively. These results demonstrate that exposure to *n*ZnO results in bactericidal effects at concentrations of 20 g/L for all bacterial isolates; cells were reduced with the presence of increasing *n*ZnO concentration in the media. The results contrary of bacterial isolates in the presence of *n*Ag revealed that bacterial cells was reduced and were completely absent after treatment respectively with 0.105, 0.65 and 0.65 g/L for *Bacillus*, *Pseudomonas* and *Brevibacillus*. Despite the toxicity of nZnO and nAg, it was also evident that pH also played an important role as bacterial isolates were shown to be unable to growth in wastewater sample adjusted to pH 2 when observing positive control (bacterial isolates inoculated in wastewater sample with known concentration, without NMs).

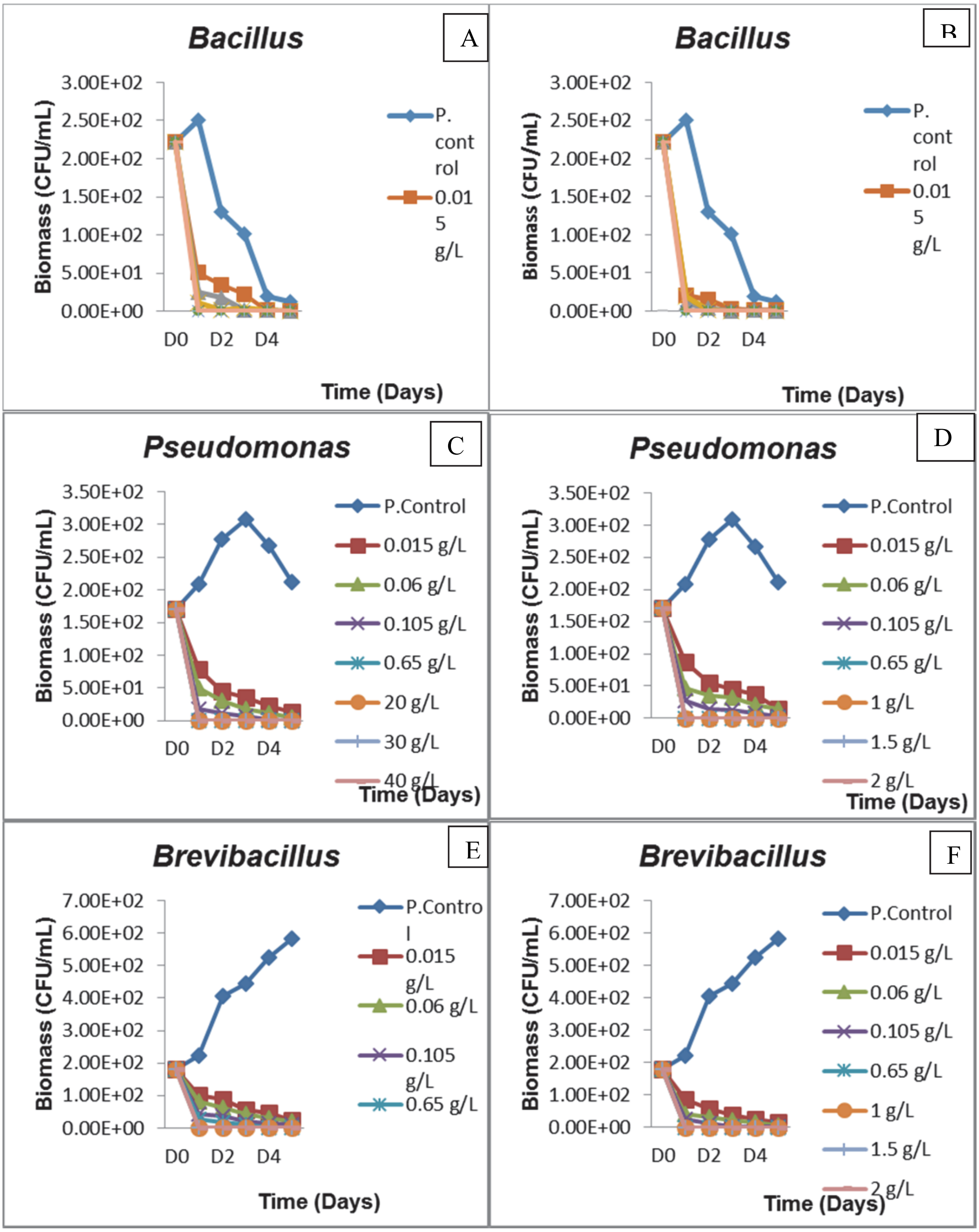

Figure 6.11: Behaviour of bacterial cells in a modified wastwater adjusted to pH 2 containing *n*ZnO (A) *Bacillus* (MIC:0.06 g/L) (C) *Pseudomonas* (MIC:0.150 g/L) and (E) *Brevibacillus* (MIC:20 g/L) and *n*Ag (B) *Bacillus* (MIC:0.105 g/L), (D) *Pseudomonas* (MIC:0.65 g/L) and (F) *Brevibacillus* (MIC:0.65 g/L).

When the modified wastewater sample was adjusted to pH 7, it was noted that the cells resulted to higher biomass concentration obtained from positive controls as shown in Figure 6.11. However, the survival of single bacterial isolates decreased dramatically over a wide concentration range of 0.015 to 40 g/L for *n*ZnO and 0.015 to 2 g/L for *n*Ag. It was noted that *Bacillus* and *Brevibacillus* cells were inhibited completely at 0.65 g/L with 0.105 g/L resulted to cell inhibition of *Pseudomonas* in the presence of *n*ZnO. The treatment with *n*Ag indicated antibacterial activity towards survivals of bacterial cells resulting to 100% induced at 0.65 g/L for all isolates.

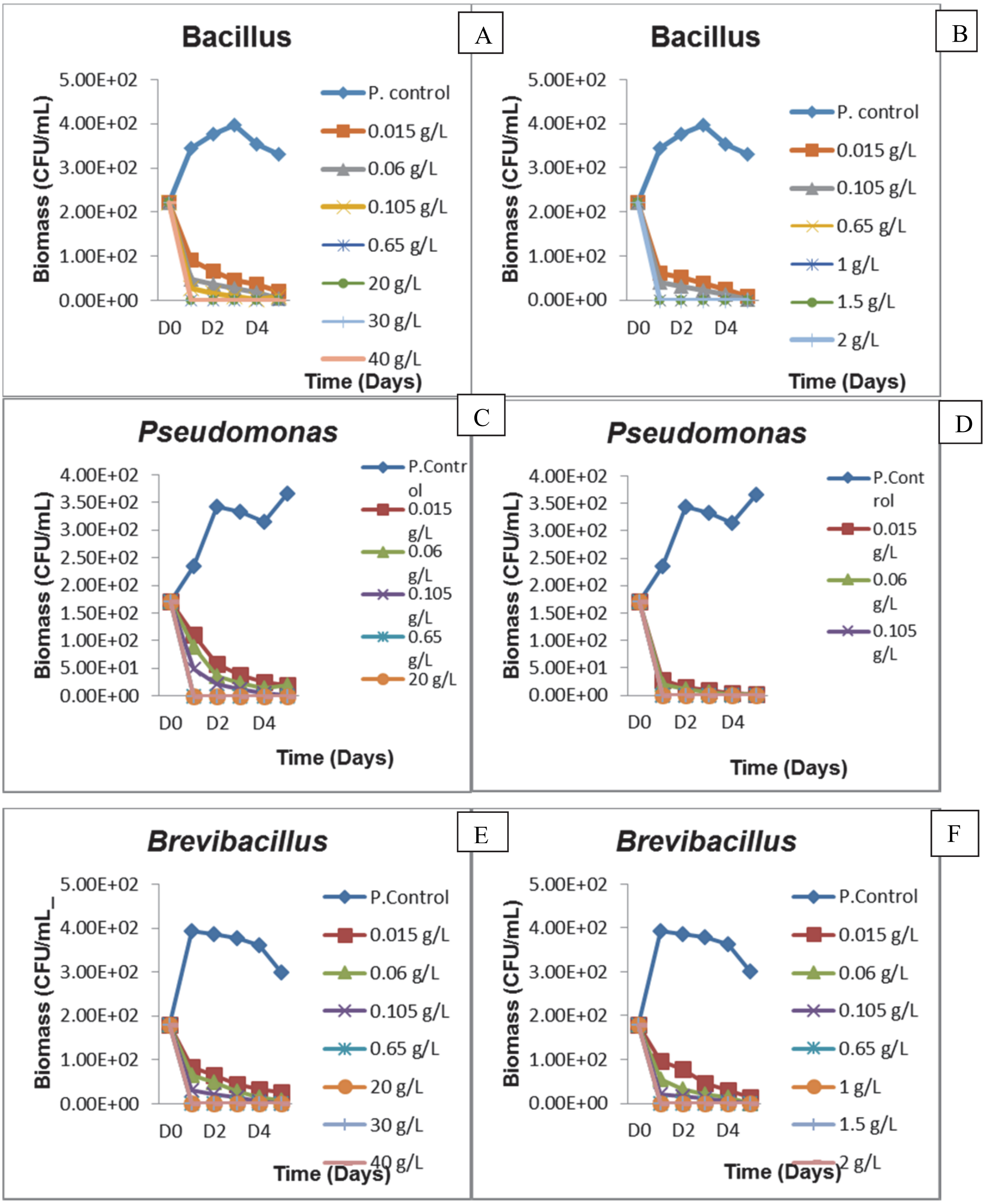

Figure 6.12: Behaviour of bacterial cells exposed to mixed liquor adjusted to pH 7 containing *n*ZnO (A) *Bacillus* (MIC:0.65 g/L) (C) *Pseudomonas* (MIC:0.105 g/L) and (E) *Brevibacillus* (MIC:0.65 g/L) and *n*Ag (B) *Bacillus* (MIC:0.65 g/L) , (D) *Pseudomonas* (MIC:0.65 g/L) and (F) *Brevibacillus* (MIC:0.65 g/L)

Further experiments were carried out by exposing the bacterial isolates to various concentrations of *n*ZnO and *n*Ag over 5 incubations days at pH 10 (Figure 6.12). There was cell reduction shown when bacterial isolates where in the presence of *n*ZnO and *n*Ag. In the presence of *n*ZnO, minimum concentrations that inhibited the cell growth were noted at 0.65 g/L, 0.65 g/L and 20 g/L of *n*ZnO for *Bacillus, Pseudomonas* and *Brevibacillus* isolates as depicted in Figure 6.12 (A, C and E). It was observed that the exposure of *n*Ag towards all bacterial isolates resulted to reduction of cell growth and eventually to bacteriocidal (Figure 6.12 B, D and F). Taking into consideration the total *n*Ag concentrations to complete growth inhibition was displayed when all bacterial isolates were exposed to 0.65 g/L *n*Ag.

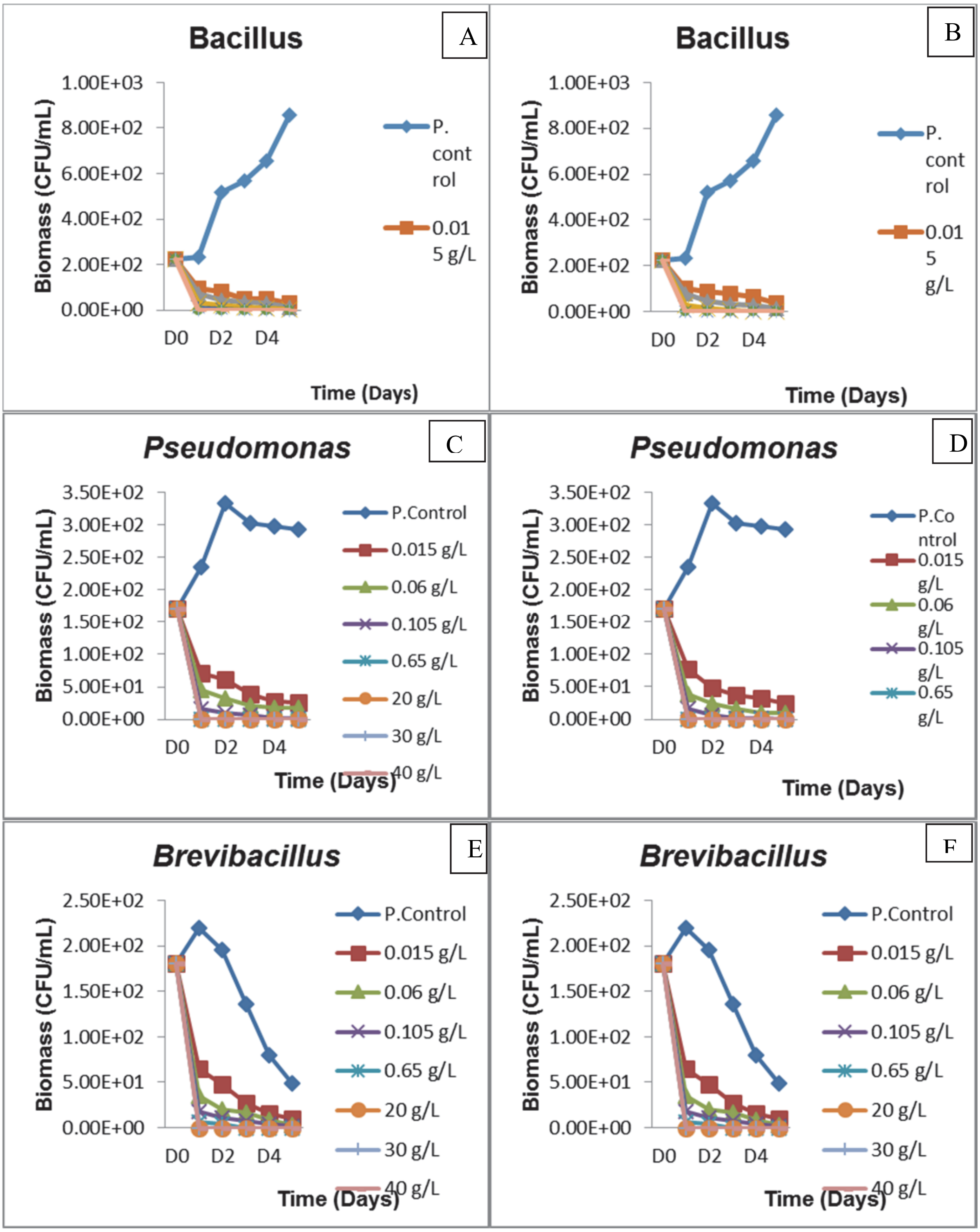

Figure 6.13: Behaviour of bacterial cells in modified pH 10 wastewater samples containing *n*ZnO (A) *Bacillus* (MIC:0.65 g/L) (C) *Pseudomonas* (MIC:0.65 g/L) and (E) *Brevibacillus* (MIC: 0.65 g/L) and *n*Ag (B) *Bacillus*(MIC:0.65 g/L), (D) *Pseudomonas* (MIC:0.65 g/L) and (F) *Brevibacillus* (MIC:0.65 g/L).

6.2.4.2. COD release/increase by single bacterial isolates exposed to nanomaterials in modified wastewater mixed liquor at pH 7

Table 6.4 illustrates the removal and removal of COD by *Bacillus, Brevibacillus* and *Pseudomonas* in modified wastewater samples treated with various concentrations of *n*ZnO at neutral pH 7. In general, the amount of COD removal was recorded to decrease with the increase of nZnO and nAg concentrations in the media. Such decrease of the COD uptake was resulted to release of COD to increase with the increase of nZnO, except at 40 g/L that showed the drastic decrease of COD release which could be due to high toxicity of nZnO towards *Brevibacillus*. The media with *n*ZnO and inoculated with *Bacillus* and *Brevibacillus*, separately revealed high COD release concentrations of -85% and -37% respectively at 30 g/L as compared to *Pseudomonas*(-28 g/L). Remarkably, Pseudomonas showed lower COD removal of 30.15% in the media without *n*ZnO, and only 7.27% and 1.85% was removed in the presence of 0.015 and 0.06 g/L respectively. There were strong evidence that when bacterial isolates where exposed to varying concentration of *n*Ag. The highest COD concentration was recorded in the modified mixed liquor containing and inoculated with *Bacillus* (41%). However, *Pseudomonas* exhibited the higher COD release in throughout the exposure period at concentration 0.06 g/L and these increased as the concentration increase, these isolates were only able to remove *n*Ag at the lower concentration of 0.015 g/L *n*Ag. It was observed that in the presence of *n*Ag *Bacillus* and *Brevibacillus* were removing COD, but released COD at 1 g/L.

Table 6.4: The removal/ release of COD in the presence of *n*ZnO and *n*Ag at neutral pH 7 mixed liqour

Conc. (g/L) nZnO	**Bacillus**	**Pseudomonas**	**Brevibacillus**	**Conc. (g/L) nAg**	**Bacillus**	**Pseudomonas**	**Brevibacillus**
	COD % removal/release				COD % removal/release		
P. control	42.59	30.15	51.89	**P. control**	41.00	39.71	39.16
0.015	32.66	7.27	19.64	**0.015**	32.00	6.43	30.37
0.06	10.15	1.85	10.15	**0.06**	22.98	-2.57	24.18
0.105	8.00	-6.56	7.05	**0.105**	19.39	-9.66	22.98
0.65	-28.00	-6.90	-27.85	**0.65**	2.65	-33.07	2.24
20	-35.00	-11.31	-36.19	**1**	-63.81	-49.36	-83.81
30	-85.00	-28.14	-37.35	**1.5**	-2.24	-53.85	-4.03
40	-25.00	-13.61	-31.10	**2**	-2.43	-69.44	-2.43
N Control	0	0	0	**N. Control**	0	0	0

6.2.4.3. DO uptake/removal by single bacterial isolates exposed to nanomaterials in modified wastewater mixed liquor at pH 7

The DO removal by single bacterial isolates in modified pH 7 wastewater media treated with various concentrations *n*ZnO or *n*Ag was evaluated. Average amount of DO removed by *Pseudomonas* was ±80%, in positive control as compared to *Bacillus* (±60%) and *Brevibacillus* (± 50%) positive control. The oxygen consumption by bacterial isolates was shown to decrease when the *n*ZnO increased in the wastewater sample, resulting to 20% DO removal as the concentration increased to 20 g/L, especially Pseudomonas that revealed uptake at 40%, while *Bacillus* and *Brevibacillus* yielded 50%. Nevertheless, decreasing behaviour was also recorded when bacterial isolates where exposed to *n*Ag which demonstrated lower DO uptake, compared in the presence of *n*ZnO. *Bacillus* uptake of the dissolved oxygen resulted to 10% removal in the presence of 0.105 g/Land 0.65 g/L *n*Ag. It was noted that the concentration between 1 g/L to 2 g/L of *n*Ag the removal was ±5% for all the isolates.

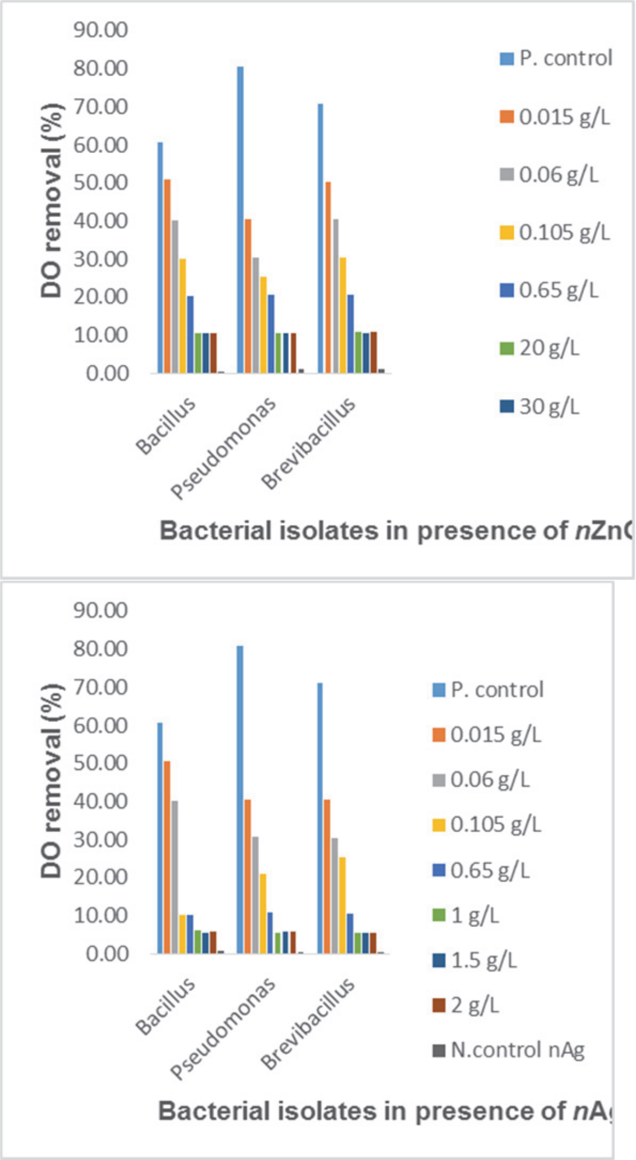

Figure 6.14: The average amount of DO removal by single bacterial isolates in pH 7 modified mixed liquor exposed to *n*ZnO and *n*Ag.

6.2.5. Evaluation of *n*ZnO and *n*Ag toxic effect towards consortium of protozoan and bacterial isolates in modified wastewater sample with change of pH values

This section discusses the effect of pH on survival limit of protozoan and bacterial consortium biomass exposed to nanomaterials; COD release/uptake by protozoan and bacterial consortium biomass exposed to nanomaterials in modified wastewater mixed liquor at pH 7; DO uptake/removal by protozoan and bacterial consortium biomass exposed to nanomaterials in modified wastewater mixed liquor at pH 7.

6.2.5.1. Effect of pH on survival limit of protozoan and bacterial consortium biomass exposed to nanomaterials

The main objective of this part of the study was to compare the level of antimicrobial ability of *n*ZnO and *n*Ag that could inhibit the growth or kill heterogeneous protozoan and bacterial isolates in modified wastewater samples at various pH (2, 7 and 10). Bacterial consortium consisted of *Bacillus licheniformis*, *Brevibacillus laterosporus* and *Pseudomonas putida* while the protozoan consortium included *Aspidisca* sp, *Trachelopyllum* sp and *Peranema* sp. Figure 6.14 represents the growth inhibition assays for both targeted microbial population in modified wastewater on a batch scale experiment at pH 2. The results revealed high bacterial biomass concentration growth compared to protozoan isolates in the positive controls. However, consortium isolates (protozoan and bacterial) were seen to be reduced once they were in the presence of increasing *n*ZnO and *n*Ag, reaching to similar MIC value at 20 g/L and 0.65 g/L for *n*ZnO and *n*Ag, respectively.

Similarly, pH 7 resulted in higher cell growth for both protozoa and bacterial when exposed to the positive controls (protozoan/bacterial isolates inoculated in wastewater sample with known concentration, without NMs). Such cell activities were noted to decrease when protozoan and bacterial isolates were exposed to increased concentration of *n*ZnO, but 20 g/L of *n*ZnO demonstrated a complete inhibition for both isolates. Furthermore, similar toxicity results were also observed when using *n*Ag suspension in the media. Drastic cell reduction was recorded and results suggest that MIC value were obtained at 0.65 and 0.105 g/L for protzoan isolates and bacterial isolates, respectively.

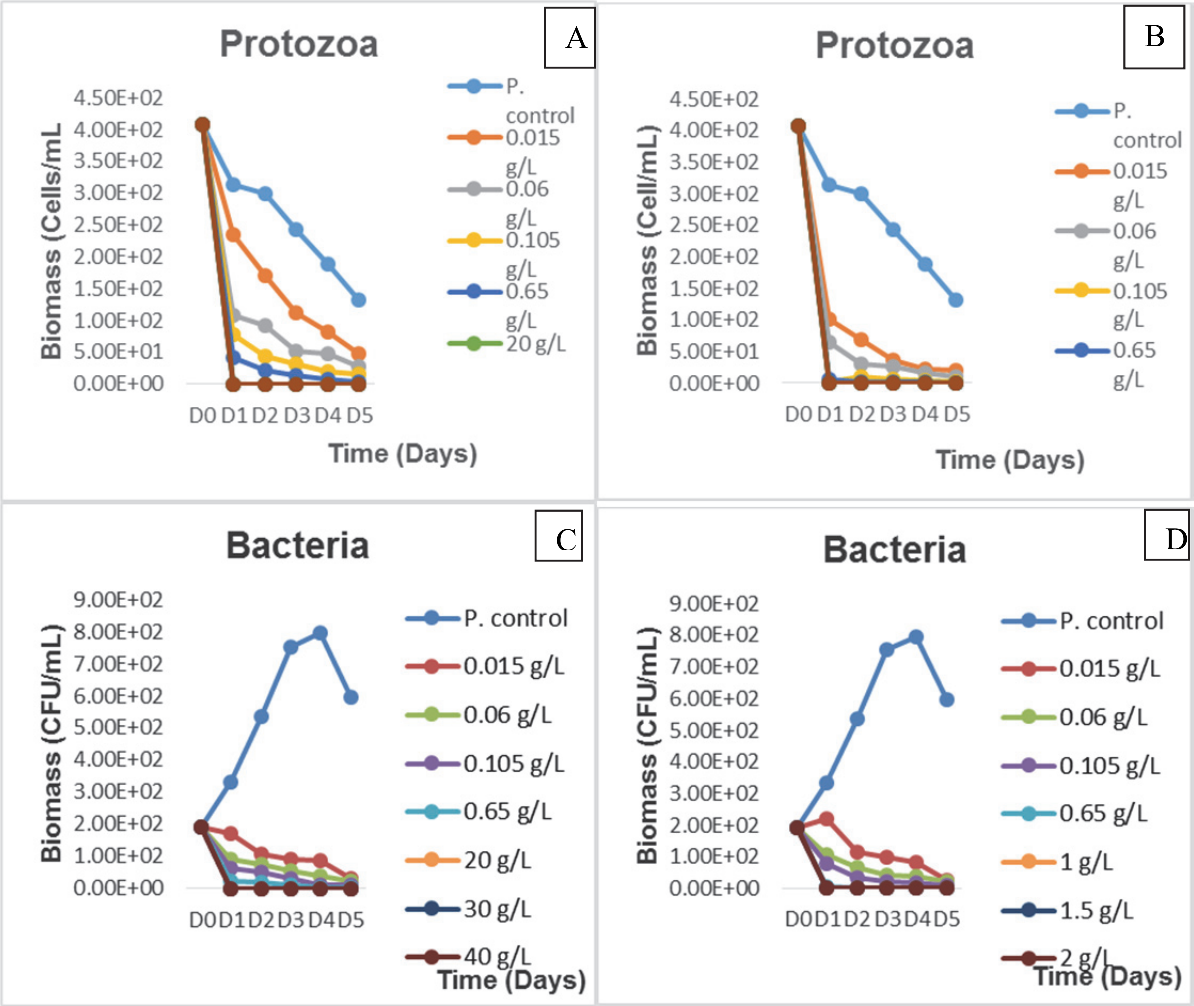

Figure 6.15: Comparison of toxicity effect towards protozoan isolates consortium in the presence of (A) *n*ZnO (MIC: 20 g/L) and (B) *n*Ag (MIC: 0.65 g/L); bacterial isolates consortium in the presence of (C) *n*ZnO (MIC: 20 g/L) and (D) *n*Ag (MIC: 0.65 g/L) in modified wastewater mixed liquor, pH 2

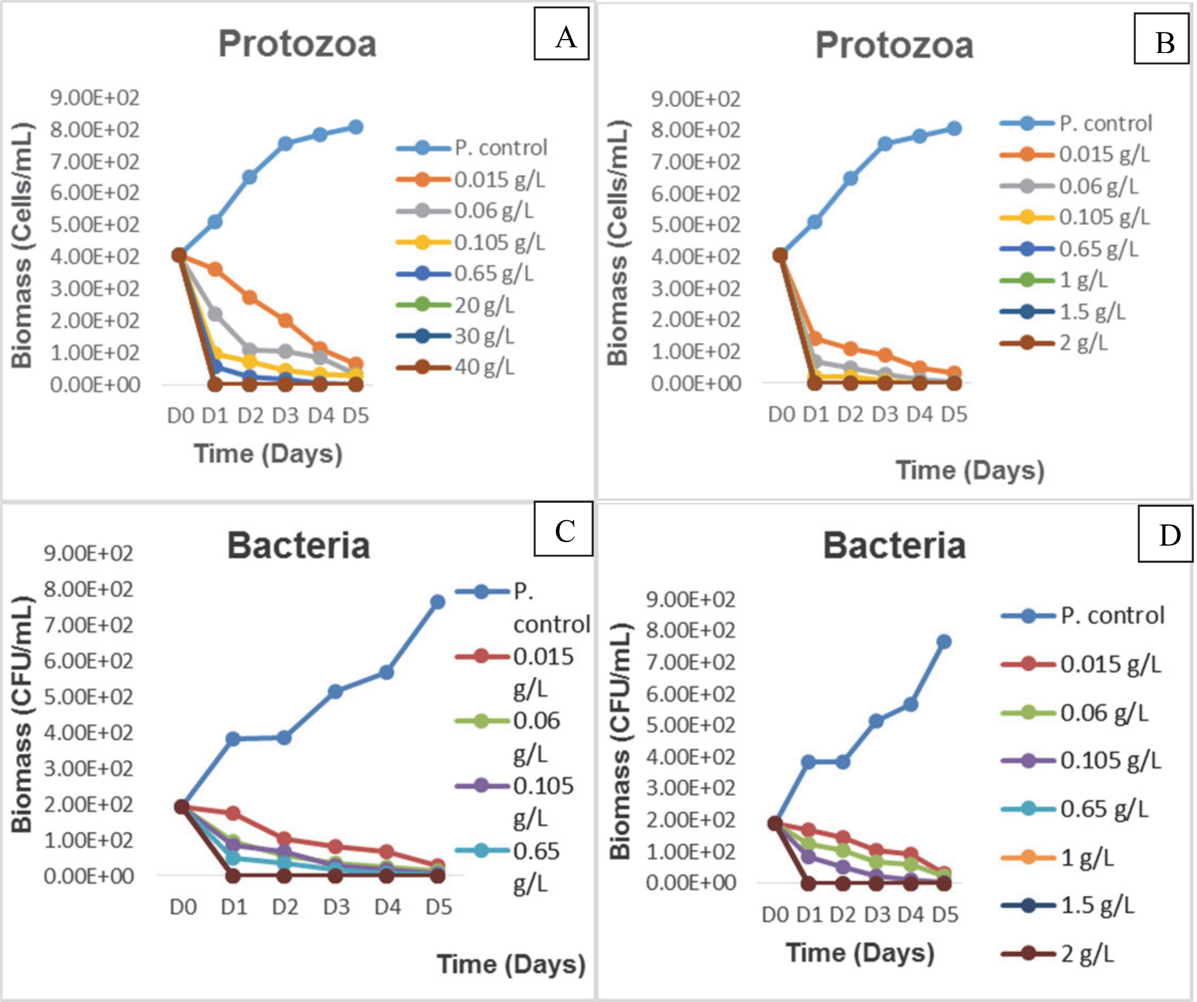

Figure 6.16: Comparison of toxicity effect towards protozoan isolates consortium in the presence of (A) *n*ZnO (MIC: 20 g/L) and (B) *n*Ag (MIC: 0.65 g/L); bacterial isolates consortium in the presence of (C) *n*ZnO (MIC: 20 g/L) and (D) *n*Ag (MIC: 0.105 g/L) in modified wastewater mixed liquor adjusted to pH 7

The inoculum of protozoan and bacterial consotium isolates in pH 10 modified wastewater samples reveal the toxic effect of *n*ZnO and *n*Ag towards protozoan and bacterial isolates. Zinc oxide NM suspension toxic effects was recorded to demonstrate MIC value at 20 and 0.65 g/L for protozoan isolates and bacterial isolates respectively. Also, protozoan and bacterial growth was impaired by incubation in 0.65 g/L of *n*Ag.

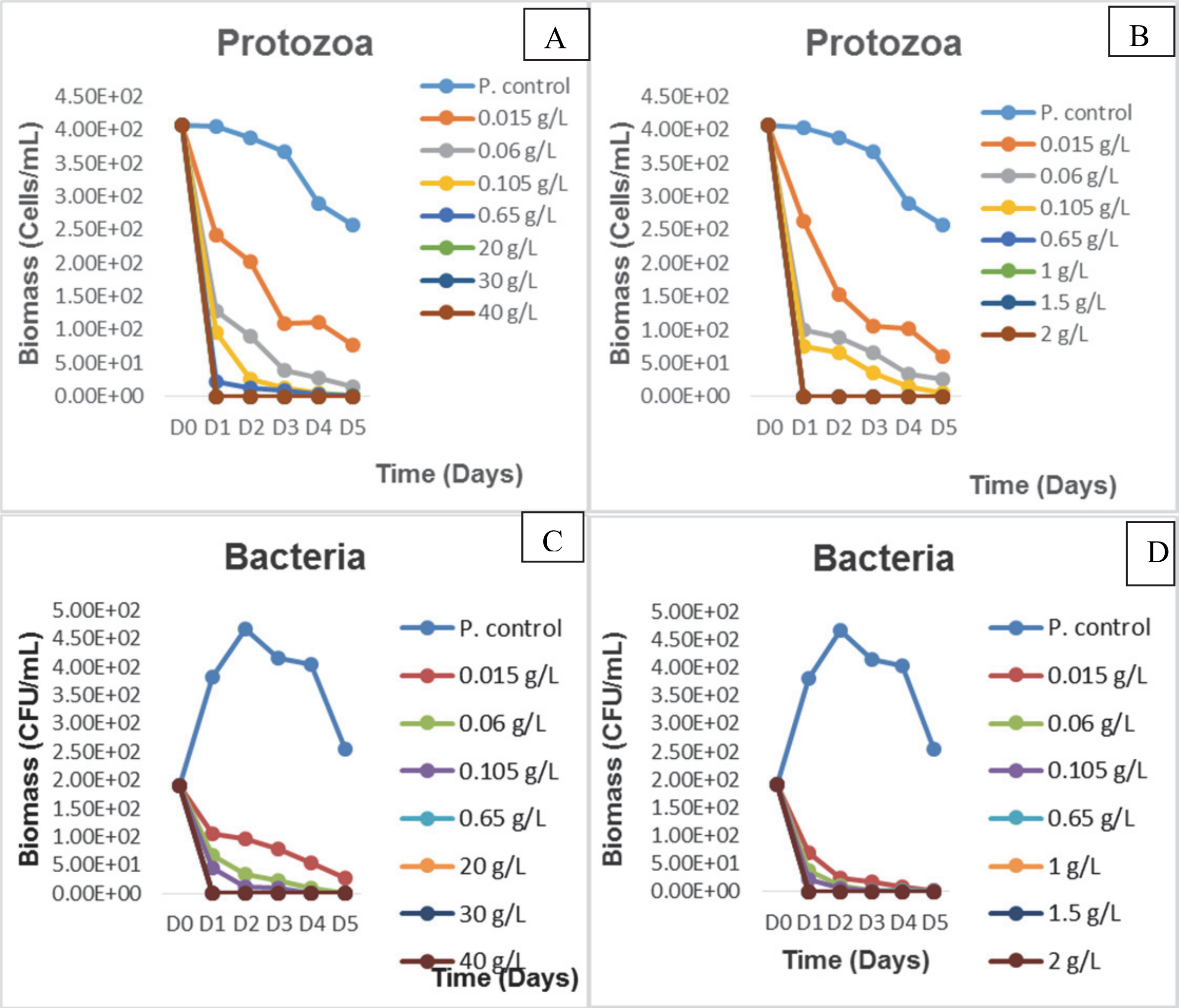

Figure 6.17: Comparison of toxicity effect towards protozoan isolates consortium in the presence of (A) *n*ZnO (MIC: 20 g/L) and (B) *n*Ag (MIC: 0.65 g/L); bacterial isolates consortium in the presence of (C) *n*ZnO (MIC: 0.65 g/L) and (D) *n*Ag (MIC: 0.65 g/L) in modified wastewater mixed liquor adjusted to pH 10

6.2.5.2. COD release/uptake by protozoan and bacterial consortium biomass exposed to nanomaterials in modified wastewater mixed liquor at pH 7

For protozoan isolates it was evident in Table 6.5 that the COD concentration uptake was higher in the modified wastewater samples at neutral pH 7 containing various concentrations of *n*ZnO and *n*Ag when compared to bacterial isolates. The presence of inoculated consortium of protozoan isolates in mixed liquor media containing *n*ZnO revealed the average difference was 56% decrease of COD uptake concentration with 77.25% COD removal in positive control to 20 g/L (21.23%). Whereas the media inoculated with consortium of bacterial isolates showed *n*Ag generating the lowest COD concentrations uptake with average difference of 66%. As the *n*ZnO and *n*Ag concentration increased there was COD released in the media, for bacterial and protozoan isolates.

Table 6.5: The COD removal and increase of *n*ZnO and *n*Ag at pH 7

Conc. (g/L)	Protozoan	Bacterial	Conc. (g/L)	Protozoan	Bacterial
		*n*ZnO		*n*Ag	
P. control	77.25	80.32	**P. control**	33.20	69.67
0.015 g/L	45.69	28.13	**0.015 g/L**	20.88	21.34
0.06 g/L	42.07	22.71	**0.06 g/L**	21.23	13.04
0.105 g/L	39.53	14.34	**0.105 g/L**	10.96	10.64
0.65 g/L	24.11	-12.78	**0.65 g/L**	-1.59	8.67
20 g/L	21.23	-8.67	**1 g/L**	-3.99	-8.38
30 g/L	-12.21	-5.32	**1.5 g/L**	-6.88	-6.52
40 g/L	-13.73	-2.72	**2 g/L**	-6.19	-3.35
N. control	0	-0.28	**N. control**	0	0

6.2.5.3. DO uptake/removal by protozoan and bacterial consortium biomass exposed to nanomaterials in modified wastewater mixed liquor at pH 7

The biomass concentration of protozoan isolates demonstrated the higher consumption of oxygen as illustrated in the positive control that showed 80% of DO removal in the modified mixed liquor when compared to bacterial isolates. The highest DO uptake of the consortium was observed for protozoan isolates to uptake 80% even at the presence of 0.65 g/L *n*ZnO. Bacterial isolates uptake of the available oxygen were shown do decrease considerably with increase of *n*ZnO concentration. These resulted to 30% DO removal in the presence of 0.65 g/L of *n*ZnO. Thus, in the presence of nAg the average amount f DO removal was shown to decrease considerable with increase of nAg, with 10% and 5% observed at concentration of 1, 1.5 and 2 g/L for protozoan and bacterial isolates, respectively. It was noted that the increase of *n*ZnO and *n*Ag in the wastewater mixed liquor media resulted in the decrease of DO removal.

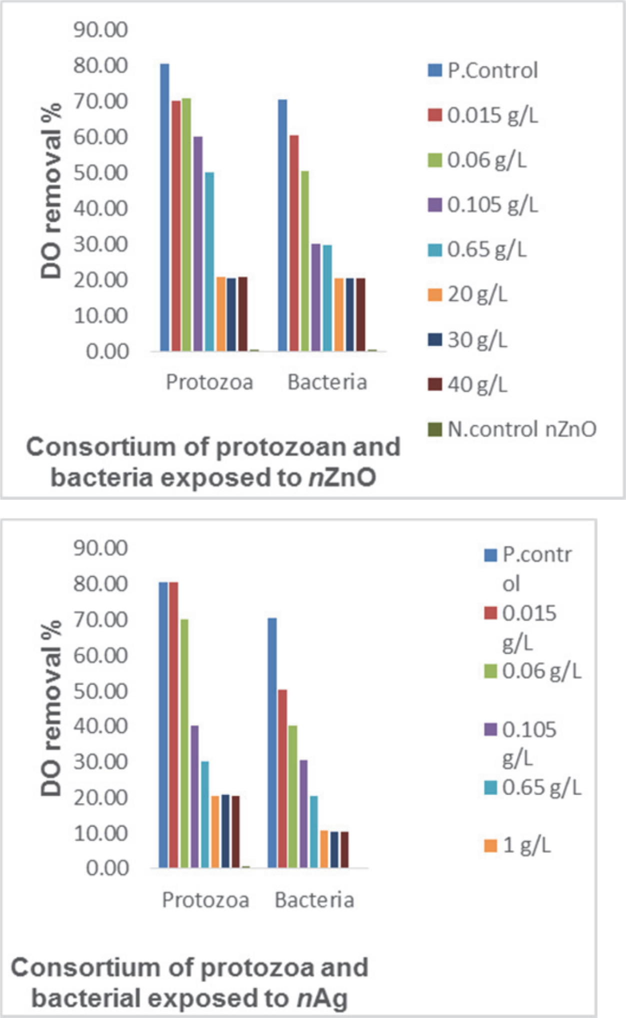

Figure 6.18: The average amount of DO removal by consortium of protozoan and bacterial isolates in pH 7 modified mixed liquor containing *n*ZnO and *n*Ag.

6.2.6. Morphological response of bacterial and protozoan isolates in the presence of *n*ZnO and *n*Ag

High resolution transmission electron microscopy (HRTEM) analysis of heterogeneous bacterial samples was used to visualize the morphological changes in bacterial cells upon their contact with varying concentration of *n*ZnO (0.015-40 g/L) and *n*Ag (0.015-2 g/L) in a mixed liquor medium adjust to pH 7 (Fig. 6.18). The HRTEM images shows that there was NMs-bacterial interaction on the surface of the bacterial cells (Fig. 6.18 A and B). Moreover, this contact resulted in cell wall damage and disorganization. In parts C and D of Fig. 6.18, EDS detector with NSS software was used to detect the chemical composition around the bacterial isolates. Elementary mapping did confirm the presence of *n*ZnO (Fig. 6.18C) and *n*Ag (Fig. 6.18D) attached to the surface of the bacterial cells. Considerably morphology changes occurred with cellular internalization which resulted from leakage of intercellular contents due to cell pits and these was not due to apoptosis. The detection spectrum results demonstrated high concentrations of *n*ZnO (Fig. 6.18E) and *n*Ag (Fig. 6.18F) present inside and outside the bacterial isolate including the lipopolysaccharides released by the bacterial in the surrounding.

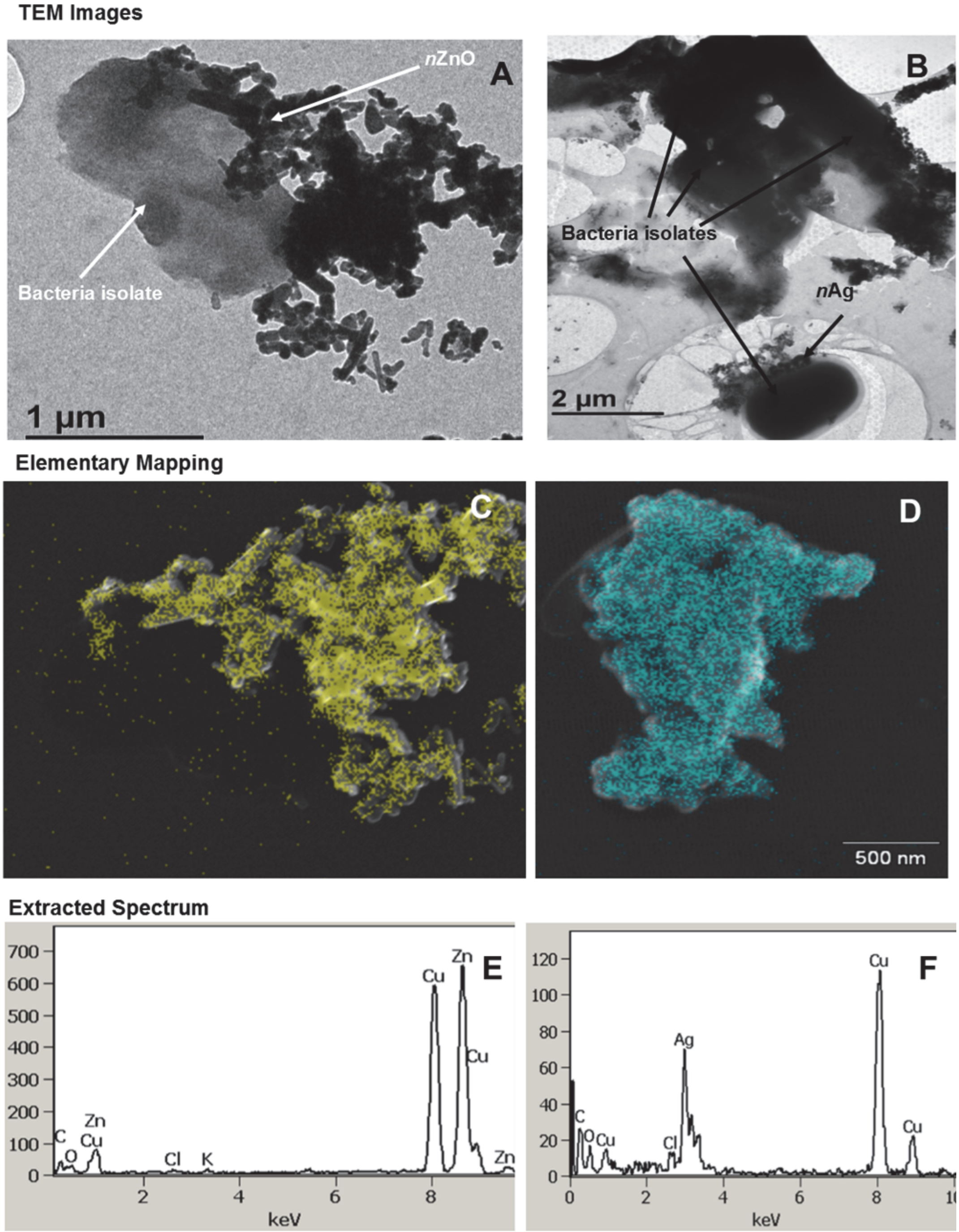

Figure 6.19: HRTEM images of bacterial isolates exposed to *n*ZnO and *n*Ag in pH 7 modified mixed liquor revealing cell membrane adsorbed by *n*ZnO (A) and *n*Ag (B) on the bacterial isolate; the magnification image of A &B showing the elementary mapping in (C) *n*ZnO and (D) *n*Ag ; the detection of extracted spectrum demonstrating presence of (E) *n*ZnO and (F) *n*Ag on the cell surface of bacterial isolates

For protozoan isolates exposed to various concentrations of *n*ZnO (0.015-40 g/L) and *n*Ag (0.015-2 g/L) as shown in Figure 6.19, HRTEM micrographs revealed excess inhibition activity of *n*ZnO and *n*Ag towards protozoan isolates by adhering and adsorbed on the cell surface. There was cell membrane that changed and damaged by *n*ZnO (Fig. 6.19 A) and *n*Ag (Fig. 6.19 B) even in the presence of aggregation state of both *n*ZnO and *n*Ag. The internalization of *n*ZnO and *n*Ag resulted in the intercellular to be compromised and morphology changed to an irregular and distorted form. Considerable morphology changes and the detachment from the cell membrane were observed from protozoan isolates after exposure to *n*ZnO (Fig. 6.19A and C). The magnified confirmation images for the same isolate shown in Fig. 6.19 A and B mapping elementary components (Fig. 6.19C and D) together with extracted spectrum bends (Fig. 6.19 E and F) illustrated high concentrations of *n*ZnO and *n*Ag on the protozoan surface and their surroundings.

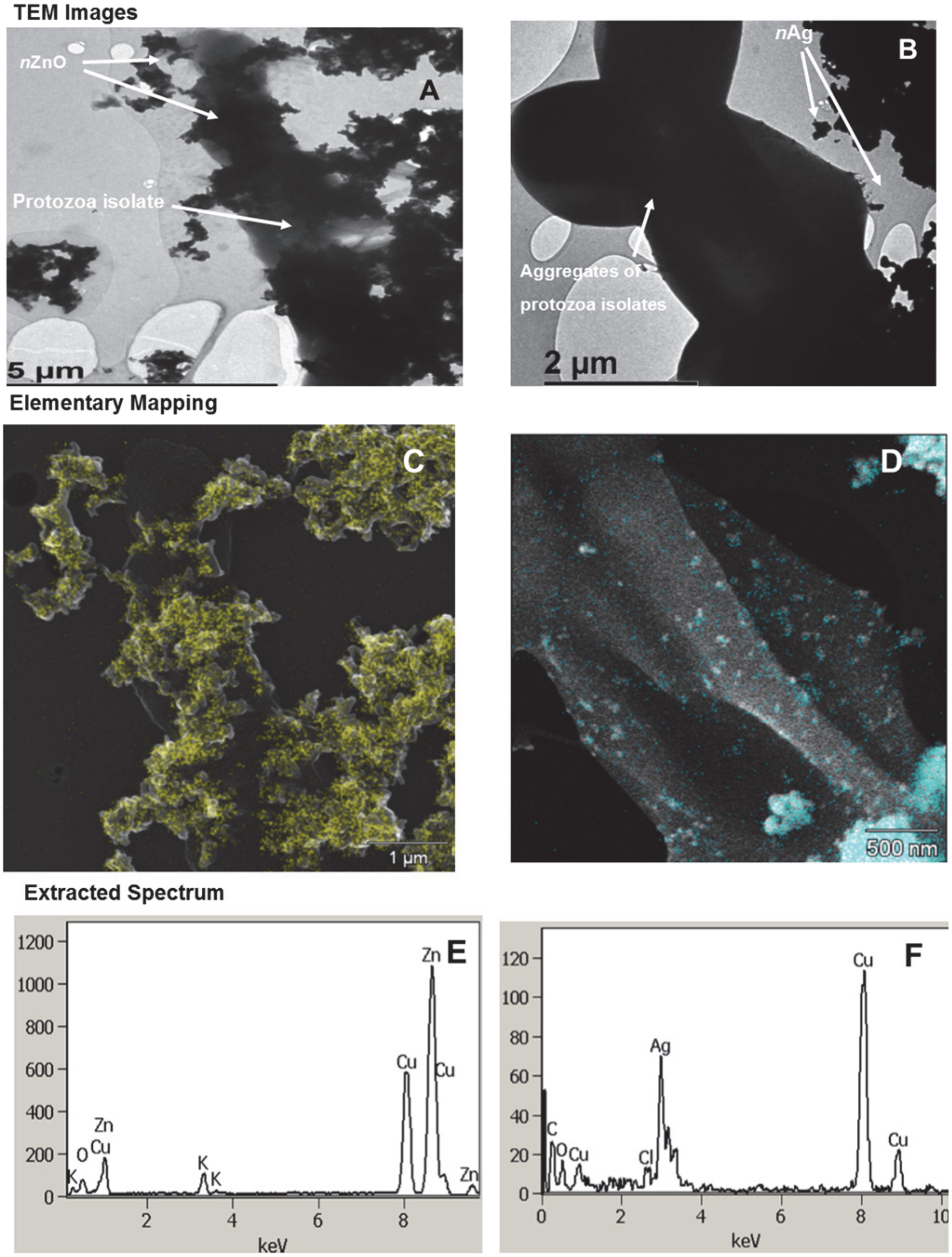

Figure 6.20: HRTEM images of protozoan isolates exposed to *n*ZnO and *n*Ag in pH 7 modified mixed liquor revealing cell membrane adsorbed by *n*ZnO (A) and *n*Ag (B) on the protozoan isolate; the magnification image of A &B showing the elementary mapping in (C) *n*ZnO and (D) *n*Ag ; the detection of extracted spectrum demonstrating presence of (E) *n*ZnO and (F) *n*Ag on the cell surface of protozoan isolates

6.3 Discussion

The rapid production of commercial NMs has stimulated the greater likelihood of their release into the environment. According to Huang et al. (2008), exposure to NMs poses serious problems to the liver, lungs and other organs, which further cause more inflammation compared to their larger counterparts when delivered in the same mass dose. It is important to note that bacteria are essential receptor tools in environmental nanotoxicology due to their ability to assist in rapid hazard identification, effective toxicological screening, and efficient environmental risk assessment. These give an insight to toxicity impact at subcellular, population, community, and ecosystem scales. Furthermore, bacteria are reportedly able to affect NMs behaviours, their fate, their bioavailability and their transport in the environment by binding to or breaking down NMs (Huang et al., 2008; Thwala et al., 2013; Musee et al., 2014).

During the study period, prior to their exposure towards selected microbial isolates, the target NMs were characterized using HRTEM, XRD and BET to validate their particle size, shape and surface area. HRTEM images showed a typical formation of secondary particles and polydispersity. The formation of secondary particles are held together by forces such as van der Waals, capillary forces or chemical bonds (Labille and Brant 2010; Akbari et al., 2011; Thwala et al., 2013). Results of this study indicated that the selected NMs were within the range of 1-100 nm particles size and had no impurities components. Diffraction peaks obtained for *n*ZnO were found to be attributed by the inhomogeneous lattice strains and faults in crystalline structure. Poly-crystallite peak sizes inferred were confirmed with images obtained from HRTEM (Figure. 1). Nanopowder of *n*Ag also demonstrated peaks that indicated pure crystalline components reflected at (111) face-centered cubic. Both *n*ZnO and *n*Ag peaks observed during the experimental study were similarly reported to those obtained by Thwala et al. (2013) and Musee et al. (2014), in their experimental studies. According to Akbari et al. (2011), the atomic planes within crystalline obtained from XRD could be linked to the images of HRTEM in Figure 1. Total surface areas of a primary particle were 15.88 and 5.37 m^2g^{-1} for *n*ZnO and *n*Ag, respectively (Table 1). This is a confirmation that even though there was presence of agglomaration, the particles were not bond too close and tigthly together as the nitrogen gas can access most of the surface area of each particle (Akbari et al., 2011). FT-IR absorption spectra of the *n*ZnO revealed Amide I vibrations of C=O and C=N and C=C groups that resembles 500 to 1600 cm^{-1} which are assigned to the symmetric and asymmetric stretching modes; vibrations which were also observed by Esparza et al. (2011)

and Viswanatha et al. (2012). According to Becheri et al. (2008) the peaks intensity at 3450 and 2350 cm^{-1} could be interpreted as the presence of –OH and C=O residues. On the other hand, for *n*Ag the Amide 1 were also visible represented by single bonds of C=O H-C-H, -C-O, and -C-N functional groups at wavelength between 900 and 1500 cm^{-1} with a minor shift at wavelength of 2400 cm^{-1} representing of O=C=O functional group. The outcomes of this study were similar to those reported by Khan et al. (2014), however, there were minor shift on the vibrations as compared to those obtained by Theivasanthi and Alagar (2011).

In the present study, screened wastewater samples revealed that COD (0.110 and 0.143 mg/L), Ag and Zn trace metals were within the South African permissible limits as reported by previous investigators (Kamika and Momba, 2011b). However, the higher concentration of DO (Table 2) obtained during the study period might be due to the presence of floc structures found in activated sludge (Schroeder, 1997; Holder-Snyman et al., 2005). The three bacterial species *Bacillus licheniformis*-ATCC12759, *Brevibacillus laterosporus* -ATCC64 and *Pseudomonas putida*-ATCC31483 were firstly assessed for their growth in a NB media without the presence of NMs. The biomass of bacterial isolates revealed growth for two incubation days prior cells decline. Such growth were observed by Kamika and Momba (2011; 2013) in the nickel and vanadium free medium. Moreover, *Pseudomonas* isolate was found to displace similar growth trends than *Bacillus* and *Brevibacillus* as also reported by Kamika and Momba (2011). Furthermore, the presence of *n*ZnO and *n*Ag showed growth reduction compared to those not treated with NMs in nutrient broth. Zinc oxide NMs was less toxic, and high concentrations were required to inhibit bacterial cells in the media. Increasing *n*ZnO concentrations resulted in a gradual increase in toxicity with 70% growth reduction in cells exposed to 0.650 g-*n*ZnO/L (Figure 4C). There is sufficent evidence that *n*ZnO demonstrated concentration-dependent toxicity efficacies towards the bacterial isolates. The present findings are in agreement with those reported by Jiang et al., 2009; Yamamoto 2001; Brayner et al., 2006; Zhang et al., 2007; Padmavathy and Vijayaghavan 2008). Findings of this study also corroborates the toxicological experimental findings reported by both Brayner et al. (2006) and Padmavathy and Vijayaghavan (2008) who demonstrated that at lower concentration, *n*ZnO shows no bactericidal efficacy to *E. coli* after 24h incubation. Yet, Bondarenko et al. (2013) reported the toxicity trends of *n*ZnO towards microorganisms were concentration dependent, especially, bacteria with MIC value of 622 mg/L. Our results, contrary revealed complete inhibition of cells growth indicating bacteriocidal effect in the presence of *n*Ag at 0.06 g/L for *Bacillus* and *Brevibacillus* and 0.65 g/L for *Pseudomonas,* respectively. Matzeke et al. (2014) found that *Pseudomonas putida* reacted sensitively towards Ag, EC_{50} value of 0.043 μg L^{-1} for $AgNO_3$ and between 0.13 and 3.41 μg L^{-1} for the different Ag NP. Findings by Okafor et al. (2013) revealed that Ag NPs at concentrations between 2 and 15 ppm resulted in a bacterial growth reduction towards *S. aureus*, *Kocuria rhizophila*, *Bacillus thuringiensis*, *E. coli*, *Pseudomonas aeruginosa*, and *Salmonella typhimurius*. Additianally, the outcomes of the present study were also in agreement with results by Pal et al. (2007) and Dasari and Hwang (2010) who also found that bacterial inhibition by *n*Ag was dependent on the concentration of this nanomaterial. Even though the influent concetration of silver NMs into the WWTPs according to Matzeke et al. (2014) are predicted to range between 100 ng/L *n*Ag. It is however, recorded that effluent from wastewater discharge higher concentration of *n*Ag into the receiving water bodies with concentration ranging of 38-127 ng but toxicity values range are found to range from ng Ag/L to mg Ag/L. Hence, the use of higher concentrations of *n*Ag used in this study as compared to other published work (Pal et al., 2007; Dasari and Hwang 2010; Espinosa-Cristóbal et al., 2012; Okafor et al., 2013; Beddow et al., 2014).

The results obtained when bacterial isolates were exposed to varying concentrations of *n*ZnO and *n*Ag in broth and agar plates were considerably different. Agar plates demonstrated more toxic effect as compared to broth media. Such phenomenon is a postulation that the mechanism used by NMs to inhibit the bacterial growth in solid media is by releasing ions from the surfaces of the NMs (Martines-Castanon et al., 2008). Furthermore, these results are in agreement with the MIC results; when bacterial suspensions were exposed to *n*ZnO and *n*Ag in a broth medium, coagulation formation were observed and these decreased *n*Ag and *n*ZnO effectiveness compared to agar plates, which is related to charge neutralization mechanism (Pal et al., 2007; Choi et al., 2008). However, *Brevibacillus* were seen to be more susceptible towards *n*ZnO as compared to *Pseudomonas* and *Bacillus*. Similarly, Khan et al. (2014) also found that silver NMs where present on the surface of the nutrient agar plates, therefore, could completely inhibit the bacterial growth compared to liquid broth. Furthermore, it has been illustrated that the toxicty can be attibuted by the media type, as Li and co-workers (2011) have demonstrated the adherence ability of five commonly used media (ultrapure water, 0.95% NaCl, phosphate-buffered saline, minimal davis, and Luria-Bertani) attributing toxicity of *n*ZnO towards *E. coli.* They observed a drastic toxicity decrease of Zn^{2+} ions concentration in minimal Davis and Luria-Bertani media, concluding that *n*ZnO relied on the free ions and labile Zinc complexes as the main components of toxicty. Additionally, they showed that complex components presence in the medium as a form of PO_4^3, citrate, etc. can play a crucial role in influencing the dissolution and the change on their species and affect their toxicities.

A parallel study was conducted to assess the toxic effect of of *n*ZnO and *n*Ag in varying concentrations towards single bacterial isolates and corsortium (protozoan and bacterial isolates) in the modified wastewater mixed liquor at varying pH (2,7 and 10). It was noted that cell death was encaraged as NMs concentrations increased which was concetration dependent for both *n*ZnO and *n*Ag, and in all environmetal control condition (pH 2, 7 and 10) at constant 37ºC. Pronounced inhibition was observed when *Bacillus* and *Pseudomonas* were in the presence of 0.06 and 0.150 g/L of *n*ZnO, except for *Brevibacillus* (20 g *n*ZnO/L). These results are supported by Kasemets et al. (2009) who also pointed out that *n*ZnO had concentration dependent toxicity effects on yeast growth , yielding about 80% inhibition of the growth that was observed at 250 mg ZnO/L level for both types of ZnO formulations. Similar patterns were observed in bacteria where *n*ZnO below 1 mg/L were much less toxic for *vibrio fischeri* but MIC value was achieved at 200 mg/L (Heilaan et al., 2008). The exposure of *n*Ag also exhited antibacterial activity towards bacterial isolate which was concentration dependent with inhibition achieved at 0.65 g/L for all bacterial isolates at pH 2, 7 and 10 except for *Bacillus* that was susceptible at 0.105 g/L at pH 2 (Figure 10). The results obtained by Jin et al. (2010) indicated that *Pseudomonas* was more adaptable in the presence of oligotrophic inorganic electrolytes compared to *B. subtilis*, making *Pseudomonas* more resistant to the antibacterial activity of silver nanomaterials. It was therefore concluded that the antimicrobial effects of silver nanomaterials are associated with the characteristics of certain bacterial species. Such results are in agreement with the results obtained in the present study as *Pseudomonas* was found to be susceptible to 0.65 g/ L of *n*Ag in pH 2, 7 and 10. When Daphnia magna (*D. magna*) was exposured to *n*Ag in a 96-h acute exposure study concentration-dependent mortality was observed in *D. magna* neonates, with 100% mortality achievd at 10 and 1 mg/L. furthermore, chronic 21 days exposure, revealed that lower concentrations of *n*Ag did not cause significant mortality (Gaiser et al., 2011).

We conducted further toxicity study to assess the heterogeneous of protozoan isolates and bacterial isolates exposed to various concentration of *n*ZnO and *n*Ag with change of pH (2,7 and 10) at constant temprature of 37ºC over 5 incubation days, rotated at 100 rpm. Our results showed that selected isolated exhibited antimicrobial effects in varying degrees after tretment with *n*ZnO and *n*Ag when compared to the positive control. It was also noted that the toxicity effects were concentration-dependent, especially for *n*ZnO. Overall these results revelaved that both isolates were less susceptible to the presence of *n*ZnO with MIC values achieved at 20 g/L across all pH values, except of bacterial isolates which were inhibited at 0.65 g/L at pH 10. There were also similar observations in a previous study, where *n*ZnO manifested concentration-dependent toxicity effect on mouse macrophage Ana-1 cells (Song et al., 2010). On the other hand, the antimicrobial activity of *n*Ag towards consortium of protozoan and bacterial isolates were shown to inhibit cell growth at concentration of 0.65 g/L, except of bacterial isolate that exhibited MIC value at 0.105 g/L at pH 7. These results are supported by (Dimkpa et al., 2011) who showed that antimicrobial effects of commercial Ag NP was attributed by concentration-dependent activity towards *E.coli* and *Staphylococcus aureus*. Fabrega et al. (2009a) also investigated the interaction of *Pseudomona* biofilm with commercial Ag NPs in the presence and absence of Suwannee River fulvic acid (SRFA) at pH 6 and 7.5 found that biofilms cell growth were impacted in the absences of SRFA by Ag NPs in a dose-dependent manner.

Noteworthy was the influence of pH towards toxicity of *n*ZnO and *n*Ag which was evaluated using bacterial growth, determininig rates of degradation and the bioavailability of compounds. According to Burgess et al. (1999), the majority of wastewater treatment plants operate activated sludge at pH 7.0, but alkaline conditions are reported to be inhibitory to most species than acidic ones. The present study showed that the selected single bacterial isolates, consortium of protozoan isolates and consortium of bacterial isolates biomass increased exceptionally at pH 7, however, it was noted that *Bacillus*, *Pseudomonas* and *Brevibacillus* had higher biomass concentration at pH 10, 7 and 2, respectively. While the mixture of protozoan isolates were found to be more alive at pH 10, and bacterial isolates were seen to be active at pH 2. Similarly, all isolates were reported by Kamika and co-worker (2011a) to grow at and tolerate pH 8; more especially *Brevibacillus laterosporus* and *Trachelophyllum* sp were observed to persist at pH 10, 4 and 6, respectively. Experimental study on the phosphate and nitrate removal using protozoa showed that the protozoan isolates were found to successfully in removing phosphate and nitrate at optimum pH ranges of 7 to 9 and 5 to7 (Akpor, 2009). The present study's results revealed that the pH has an effect on the toxicity of NMs towards all selected isolates especially at pH 2 *Bacillus*, *Pseudomonas* and protozoan isolates biomass conctration was considerably lowere and at pH 10 *Brevibacillus* and consortium bacterial isolates biomass concentration were quite low. The influence of pH on toxicity was found to increase when pH was adjusted to pH 8 toxicity towards *Pseudokirchneriella subcapitata* (Aruoja et al., 2009). Sorption toxicity study illustrated increased toxicity of *n*ZnO towards Folsomia Candida with the increase of pH (Waalewijn-Kool et al., 2013). When *Pseudomonas putida* were exposed to *n*Ag with change of pH 6 and 7.5, the results revealed higher uptake at pH 6 compared to pH 7.5 (Fabrega et al., 2009b). There was also growth reduction of *Pseudomonas fluorescens* over 24 h exposure towards *n*Ag at pH values of 6-9 at all pH values, irrespective of the presence of Suwannee River humic acids (SRHA). Remarkably, the cell reduction were observed at pH 9, resulting to approximately 50% reduced growth. It was after 24 h of exposure at high concentration of nAg (2000 ppb) that yield 90% decreased of population density by reducing growth, for all pH values (Fabrega et al., 2009b).

According to (Akpor, 2009) the existence of microorganisms in water is an indication for nutrient enrichment and water quality, which is monitored using parameters such as turbidity, conductivity, chemical oxygen demand (COD), and biological oxygen demand (BOD). For the purpose of this study removal and release of COD was monitored when the microbial isolates where exposed to the increasing concetration of nZnO and nAg. Our results obtained demostarted that there was minimal removal of COD in lower concentration but as concentration increase these inversely decreased the removal and as the media became toxic for the microbes there was release of COD. This contributed to the bacterial biomass/biofilm as pointed out by Kiser et al. (2010), COD being itself a source of organic matter, surrounded by EPS which mediates exchange processes with the cells' environments, absorb water to hydrate cell and preserve biofilm lifestyle. Therefore, bacterial and protozoan isolates secreted EPS in the media when it became more toxic for their survival, however, such release of EPS results in COD becoming negative value. A similar behaviour of removal decreased as the concentration of both nickel and vanadium increased in the wastewater samples and evetually COD released increased was noted when bacterial isolated were exposed to both nickel and vanadium heavy metal in varying concentration and found that *Pseudomonas* revealed the highest uptake of 256.6% and 237.11% at 10 ppm of nickel and vanadium, respectively but decrased with increased concetration of nickel and vanadium (Kamika and Momba, 2011 a,b). On the contrary another study investigated the short-term exposure of ZnO and Ag ENPs in simulated wastewater treatment process and the presence of Zn and Ag in high concentration did not display significantly impact on COD removal efficiency (Musee et al., 2014).

The ability of bacterial isolates to remove the DO was also evaluated at a constant temperature of 37ºC. The important role of DO is for microbial growth, and an indication of the aerobic quality condition,which aerobic bacteria grow adequately in the presence of 1-2 mg/L dissolved oxygen concentration (Kamika & Momba, 2011a; Holder-Snyman et al., 2005). Results obtained in the study revealed a decrease in microbial isolates (single bacterial isolates; consortium bacterial and protozoan isolates) as the concentrations of *n*ZnO and *n*Ag increased in the modified wastewater mixed liquor samples which also resulted in the decrease in DO uptake, further corroborated with COD removal and release results discussed above. On the other hand, a comparable trend was also observed when bacterial isolates were in the presence of increasing concentration of nickel and vanadium; wherein a gradual decrease of DO uptake occurred when the Ni^{2+} and V^{5+} increase (Kamika & Momba, 2011a).

Biofilms are a complex microbial community that forms by adhesion to a solid surface by secretion of a matrix (proteins, DNA, and extra-polysaccharide), which assist in communicating and enhancing interaction through the process known as quantum sensing over the bacterial cell community against emerging toxics and antibiotics (Hajipour et al., 2012). Therefore, secretion of extracellular polymeric substances (EPS) in activated sludge also function to reduce nutrients for bacterial growth and restrict contaminants in the WWTP (Wingender et al., 1999; Kiser et al., 2010). Additionally, high concentration of microbial organism tends to excrete polysaccharide substances that promote formation of biofilm in the aqueous system and resist to the antibacterial effect. Furthermore, layers within the cell membrane also play a crucial role to predict the resilient or resistance of the bacterial cell in toxic environment. Consequently, the functional of polysaccharides and proteins represented as adsorption bonds were determined for single bacterial isolates (Figure 7, 8 and 9) using FTIR. These adsorption bonds further indicate the morphological difference in cell shapes and variation in absorbance indicate present cell composition and components. Changes in cell polysaccharide structures were observed and these vibrations indicate the binding of NMs on the cell surface (Bandyopadhyay et al., 2012). Micrographs revealed that *n*ZnO and *n*Ag were likely to bind to the sulfur-containing proteins on the membrane or inside the cells and phosphorus-containing element like DNA, hence, stimulating the toxicity of NMs to be able to destroy the permeability of bacterial membrane. It is suggested that the interaction of metallic silver and metal zinc oxide and bacteria cells can be attributed to Zn^{+} and Ag^{2+} ions that interrupt bacterial respiration and adenosine triphosphate (ATP) production. Subsequently reacting with thiol groups by inactivating the cellular proteins by combining the

–SH groups of enzymes (Pal et al., 2007; Ju-Nam and Lead 2008; Thwala et al., 2013; Matzeke et al., 2014).

Intriguingly, the secretions at high cell density can results in suffocation of one strains when there is high competition in long-lived chronic situations (Nadell et al., 2008). Therefore, the current experimental study evaluated interaction varying concentrations of *n*ZnO and *n*Ag towards consortium of protozoan isolates and bacterial isolates separately in a modified wastewater mixed liquor medium adjusted to pH 7 (Fig. 18 and 19). The HRTEM images showed that there was NMs-bacterial interaction on the surface of the bacterial and protozoan isolates resulting in cell wall damage and disorganization (Figure 18 and 19). Furthermore, cellular internalization was assumed to be the cause of intercellular contents leakage due to cell pits existed by both *n*ZnO and *n*Ag. It was noted on the images that there was slight morphological changes observed when NMs where in contact with an aggregate of isolates, both protozoan and bacterial isolates (Fig. 18B and 19B). Comparable results were observed when microorganisms were exposed to *n*Ag, suggesting that individual isolates are prone to the toxicity as compared to the mixture culture of isolates that indicate symbiotic effects among bacterial biofilms which increase survival and significantly contribute to their tolerance under *n*Ag treatment (Hong et al., 2008; Becheri et al., 2008, Raghupathi et al., 2011). Nonetheless, treatment of 200 mg Ag/L on biofilms from biological wastewater treatment processes were found to be highly tolerant resulting to insignificant heterotrophic plate counts after 24 h (Sheng and Liu, 2011). Marambio-Jones and Hoek (2010) indicated a recent accumulation and uptake of Ag NPs on the cell membrane within *V. cholera, P. aeruginosa* and *S. typhus*. Results for the current study are in agreement with the images obtained from SEM microscopy used to evaluate the surface morphology of treated *E. coli* in Luria-Bertani (LB) medium. The images showed damages, with formation of “pits” in their cell walls. There was accumulation of NMs on the cell membrane, while some of them successfully penetrated into the cells, resulting to leaking of intracellular substances and coagulation of NMs at the bacterial (Sondi and Salopek-Sondi 2004). The elementary *n*ZnO and *n*Ag existing on the treated bacterial and protozoan isolates confirmed the incorporation of *n*ZnO and *n*Ag onto the cell membrane structure detected (Figure 18 C&D, and Figure 19 C& D). This suggests the antimicrobial mechanisms of Zn+ ions and Ag+ ions (Feng et al., 2000; Sondi and Salopek-Sondi 2004). Similar phenomenon have been observed after treating *E.coli* and *S. aureus* with $AgNO_3$, where the morphology changed and the cytoplasm membrane were detected to be detached from the cell wall and there were small dense electron granules surrounding the cell wall and deposited inside the cells (Feng et al., 2000). The exact inhibitory mechanisms action of Zn^+ ions is still not well understood, whereas , Ag^+ ions is partially known (Feng et al., 2000). However, the HRTEM images shows the NMs bind with the microorganism membrane and interact with its building element, causing degradation and structural changes resulting to cell death (Feng et al., 2000). Therefore, the presence of nanoparticles that are converted to ions, could bind to functional groups of proteins and result in protein denature, dismantle deoxyribonucleic acid (DNA) replication ability and other cellular structures (Feng et al., 2000). However, regardless of the mechanism of interaction involved, it is evident that *n*ZnO and *n*Ag attached to microbial cell membranes increase permeability and disturb respiration (Marambio-Jones and Hoek 2010).

CHAPTER 7

GENERAL CONCLUSIONS AND RECOMMENDATIONS

7.1 General conclusions

The objectives of this WRC REPORT were achieved based on the findings presented throughout the work. The fate and behaviour of ZnO nanoparticles in wastewater were found to be impacted upon by the presence of electrolytes, ionic strength, organic matter and pH during the activated sludge wastewater treatment.

The release of zinc from ZnO ENPs suspension in wastewater was found to be more significant under acidic conditions and low ionic strength. However, the release of zinc from ZnO ENPs in wastewater is lower compared to de-ionized water indicating the pivotal role of the wastewater biomass adsorptive ability for the removal of contaminants. In addition, under alkaline conditions, a large fraction of the metal-oxide ENPs showed strong affinity for the sewage sludge rather than dissolved or dispersed in the filtrate. The depositions of ENPs on sludge suggest their removal by abiotic, bio-sorption and bio-solid settling mechanisms. Furthermore, the size of ZnO ENPs was found to significantly increase upon exposure to wastewater, an observation that suggests the sorption and stabilization ability of NOM such as humic acid present in wastewater.

Under the conditions of the study, which are closely related to the real WWTPs, the consortium of bacteria collected from a well operated WWTP and employed in the aeration chamber were able to remove the organic matter in the wastewater added ZnO ENPs. We observed both COD and DOC were not significantly affected by changes in ENPs concentration, a phenomenon suggesting adaptation ability of microorganisms responsible for organic matter degradation during activated sludge wastewater treatment upon long term exposure to ENPs. However, our findings on the potential release of zinc in the wastewater effluent as ENPs concentration changes indicate that, although the Zn levels were low, the potential release increased with ENPs concentration, with a larger fraction of the ENPs associated with the sludge. This implies that the sludge treatment process would require additional steps to remove the elevated concentrations of metals, particularly in the South

Africa context where more than 90% of the sludge from WWTPs is utilized for agriculture. In addition, the removal mechanisms of ZnO ENPs during wastewater treatment remain complex in nature, although abiotic, bio-sorption, and bio-solid settling mechanisms have been proposed. Furthermore, using wastewater and de-ionized water as test and control media, respectively, have allowed understanding ENPs removal induced by abiotic factors compared to removal induced by the presence of the biomass.

Selected bacteria and protozoan species commonly found in wastewater systems were used to underline and understand the impact of ZnO and Ag NMs on the microbial population of the wastewater treatment plants. The characterization of the commercial ZnO and Ag NMs used during this investigation are found to be within the recommended nanoparticle sizes ranging between 1 and 100 nm. Evidently the presence of these commercial NMs in the modified wastewater revealed that they were toxic towards bacterial and protozoan isolates. However, their toxicity effects are found to be concentration-dependent. The antimicrobial toxicity was noted to be further influenced by the pH of the media, with the pH 2 and pH 10 being attributed to be more toxic towards microbial activity compared to pH 7. The interaction of the target NMs and microbial cell membrane of the selected bacteria and protozoa could alter the polysacharrides present on the cell wall by adsorption and eventually causing cell death. Overall, the antimicrobial activities of *n*ZnO and *n*Ag are revealed to be reduced slowly and hindered by the production of the EPS in the media, hence, increasing the concentrations of NMs in the media which results in the inhibition of the microorganims. Therefore, the present study indicates that the bacterial isolates and protozoan isolates are useful in NM ecotoxicological assessment and there is a tremendous need for an intergrated environmental toxicology assessment. Still, the toxicity of commercial NMs may be different from the manufactured ones as they demonstrate that they are not size and surface dependent.

In conclusion, in a typical wastewater treatment systems, engineered nanomaterials are therefore likely to be introduced into the environment through the use of sludge for agricultural purposes as well as possible release as fly ash. The release of zinc from ZnO ENPs suspension in wastewater was found to be more significant under acidic conditions and low ionic strength. Results using HRTEM show that the NMs bind with the microorganism membrane and interact with its building element, causing degradation and structural changes resulting to cell death of the organism. Therefore, the presence of nanoparticles that may be converted to ions, could bind to functional groups of proteins and result in protein denature, dismantle deoxyribonucleic acid (DNA) replication ability and other cellular structures.

Regardless of the mechanism of interaction involved, it was evident from this study that *n*ZnO and *n*Ag attached to microbial cell membranes resulted in an increase in permeability therefore disturbing respiration of the microorganisms.

7.2 Recommendations and future works

The objectives of this WRC Project were achieved based on the results obtained from our study. However, as the study is a pioneer of its kind in South Africa, relevant gaps have been identified for future work, as follows:

i. The present work addressed the fate and behaviour of ZnO nanoparticles during activated sludge WWTPs. However, the organic matter content of wastewater is rich with complexing and precipitating agents such as humic acid, tannic acid, sulphides, and among others, just to mention a few, that are pH dependent. Therefore, investigating the speciation of ZnO nanoparticles in WWTPs may contribute to the development of appropriate methodologies for the removal of nanoparticles before the disposal or reuse of bio-solids;

ii. The investigation of the bacterial species highly sensitive to the presence of ZnO nanoparticles, will help understand which stages of the activated sludge wastewater treatment processes are more affected by the presence of nanoparticles in order to develop methodologies to overcome the adverse effect;

iii. The high levels of zinc in the wastewater biomass (sludge) as a result of the ZnO nanoparticles removal with waste activated sludge (WAS), suggests further investigations of their adverse impacts to the wastewater treatment processes, such as anaerobic digestion.

iv. Research on the simulated wastewater treatment plant would be further helpful to give a better understanding of the impacts on the microbial (protozoan and bacterial isolates) susceptibility towards NMs. It should be noted that in the actual environment, microoganisms are higher in concentration (hence, release of EPS) and other organic and inorganic constituents are present in WWTPs, and such have been shown that NMs adsorb on the biofilm therefore, suggesting NMs will be removed from the treatment.

v. Finally, further work is required to elucidate the long-term effect accumulation of NMs on biofilms and landfills as the concentration will be increasing.

REFERENCES

Adams L, Lyon D, Alvarez P (2006) Comparative eco-toxicity of nanoscale TiO2, SiO_2 and ZnO water suspensions. Water Res 40:3527-3532.

Adams LK, Lyon DY, Alvarez PJJ (2006) Comparative eco-toxicity of nanoscale TiO_2, SiO_2, and ZnO water suspensions. Water Res., 40, 3527-3532.

Akan JC, Abdulrahman FI, Dimari GA, Ogugbuaja VO (2008) Physicochemical determination of pollutants in wastewater and vegetable samples along the Jakara Wastewater Channelin. European Journal of Scientific Research, Vol. 23 No. 1, pp.122-133.

Akbari B, Tavandashti M, Zandrahimbi M (2011) Partilce size characterization of nanoparticles-A practical approach. Iran J Mater Sci Eng 8:48-56.

Akpor OB (2009) The role of protozoa in the removal of phosphorus and nitrogen activated sludge systems. Doctor Technologiae, Department of Environmental, Water and Earth Sciences, Tshwane University of Technology, Pretoria: Tshwane University of Technology

APHA (2001) Standard methods for the examination of water and wastewater. American Public Health Association (APHA), Washington D.C.

Applerot G, Lipovsky A, Dror R, Perkas N, Nitzan Y, Lubart R, Gedanken A (2009) Enhanced Antibacterial Activity of Nanocrystalline ZnO Due to Increased ROS-Mediated Cell Injury. Adv. Funct. Mater. 19, 842-852.

Aruoja V, Dubourguier H, Kasemets K, Kahru A (2009) Toxicity of nanoparticles of CuO, ZnO and TiO_2 to microalgae *Pseudokirchneriella subcapitata*. Sci Total Environ 407:1461-1468.

Auffan M, Rose J, Bottero JY, Lowry GV, Jolivet JP, Wiesner MR (2009) Towards a definition of inorganic nanoparticles from an environmental, health and safety perspective. Nat. Nanotechnol. 4:634-641.

Auffan M, Rose J, Wiesner MR, Boterro JY (2009) Chemical stability of metallic nanoparticles: a parameter controlling their potential cellular toxicity in vitro. Environ. Pollut. (157), 1127-1133.

Azam A, Ahmed A, Oves M, Khan M, Habib S, Memic A (2012) Antimicrobial activity of metal oxide nanoparticles against Gram-positive and Gram-negative bacteria: A comparative study. Intern J Nanomed 7: 6003-6009.

Baalousha M, Nur Y, Römer I, Tejamaya M, Lead JR (2013). Effects of monovalent and dilevnt cations, anions and fulvic acid on aggregations of citrate-coated silver nanoparticles. Sci Total Environ 454:119-131.

Baker R (2012) Membrane Technology and Applications. Wiley.

Baker T, Tyler C, Gallowway T (2013) Impacts of metal and metal oxide nanoparticles on marine organisms. Environ Pollut 186:257-271.

Bandyopadhyay S, Peralta-Videa J, Plascencia-Villa G, José-Yacamán M, Gardea-Torresdey J (2012) Comparative toxicity assessment of CeO2 and ZnO nanoparticles towards *Sinorhizobium meliloti*, a symbiotic alfalfa associated bacterium: Use of advanced microscopic and spectroscopic techniques. J Hazard Mater 241-242:379-386.

Baun A, Hartmann NB, Grieger K, Kusk KO (2008) Ecotoxicity of engineered nanoparticles to aquatic invertebrates: A brief review and recommendations for future toxicity testing. *Ecotoxicology* 17:387-395.

Becheri A, Durr M, Nostro P, Baglioni P (2008) Synthesis and characterization of zinc oxide nanoparticles: application to textiles as UV-absorbers. Journal of Nanoparticles Research 10: 679-689. doi:DOI 10.1007/s11051-007-9318-3.

Beddow J, Stolpe B, Cole P, Lead J, Sapp M, Lyon B, Colbeck I, Whitby C (2014) Effects of enginered silver nanoparticles on the growth and activity of ecologically importants microbes. Environ Microbiol Rep 6: 448-458.

Bian SW, Mudunkotuwa IA, Rupasinghe T, Grassian VH (2011) Aggregation and dissolution of 4 nm ZnO nanoparticles in aqueous environments: Influence of pH, ionic strength, size, and adsorption of humic acid. Langmuir, 27, 6059-6068.

Biswas P, Wu CY (2005) Critical review: Nanoparticles and the environment. J. Air & Waste Manage. Assoc. 55:708-746.

Blinova I, Ivask A, Heinlaan M, Mortimer, Kahru A (2010) Ecotoxicity of nanoparticles of CuO and ZnO in natural water. Environ. Pollut. 158, 41-47.

Boeije, G, Corstanje R, Rottiers A, Schowanek D (1999) Adaptation of the CAS test system and synthetic sewage for biological nutrient removals Part I: Development of a new synthetic sewage. Chemosphere 38: 699-709.

Bolyard SC, Reinhart DR, Santra S (2013) Behavior of engineered nanoparticles in landfill leachate. Environmental Science and Technology. 47, 8114−8122.

Bondarenko O, Ivask A, Kahru A, Juganson K, Kasemets K, Mortimer M (2013) Toxicity of Ag, CuO and ZnO nanoparticles to selected environmentally relevant test organisms and mammalian cells in vitro: a critical review. Arch Toxicol 87:1181-1200.

Boxall ABA, Tiede K, Chaudhry Q (2007) Engineered nanomaterial in soils and water: How do they behave and could they pose a risk to human health? Nanomedicine 2:919-927.

Brar SK, Verma M, Tyagi RD, Surampalli RY (2010) Engineered nanoparticles in wastewater and wastewater sludge – Evidence and impacts. Waste Management 30, 504-520.

Brayner R, Ferrari-Illiou R, Brivois N, Djediat S, Benedetti M, Fievet F (2006) Toxicological impact studies based on *Escherichia coli* bacteria in ultrafine ZnO nanopartilces colloidal medium. Nano Lett 6:866-870.

Brydson R (2008) Nanocharacterization. (Kirkland, A.; and Hutchison, J., ed.). Chap 4. RSC, USA.

Bystrzejewska-Piotrowska G, Golimowski J, Urban P (2009) Nanoparticles: Their potential toxicitity, waste and environmental management. Waste Manage 29:2587-2595.

Bystrzejewska-piotrowska G, Golimowski J, Urban PL (2009) Nanoparticles: Their potential toxicity, waste, and environmental management. Waste Management. 29:2587-2595.

Chaúque EFC, Zvimba JN, Ngila JC, Musee N (2014) Stability studies of commercial ZnO engineered nanoparticles in domestic wastewater. J. Phys. Chem. Earth, 67-69 (2014) 140-144.

Choi O, Deng K, Kim N, Ross jr. L, Surampalli R, Hu Z (2008) The inhibitory effects of silver nanoprtilces, silver ions, and silver chloride colloid on microbial growth. Water Res 42:3066-3074.

Choi O, Hu Z (2008) Size dependent and reactive oxygen species related nanosilver toxity to nitrifying bacteria. Eviron Sci Technol 42:4583-4588.

Choi OK, Hu ZQ (2009) Nitrification inhibition by silver nanoparticles, Water Sci. Technol., 59(9), 1699-1702.

Clark NA, Lunacek JH, Benedek GB (1970) A study of Brownian motion using light scattering. Am. J. Phys. Volume 38, number 5.

Crewe AV (2009) Handbook of Charged Particle Optics. (J. Orloff, ed), Chap 10. Second Edition, CRC Press. USA.

Dasari T, Hwang H (2010) The effect of humic acids on the cytotoxicity of silver nanoparticles to a natural aquatic bacterial assemblage. Sci Total Environ 408:5817-5823.

Davies P (2005) The biological basis of wastewater treatment. Strathkelvin Instrument Ltd, Glasgow, UK.

Degen A, Kosec M (2000) Effect of pH and impurities on the surface charge of zinc oxide in aqueous solution. J. Eur. Cera. Soc., 20, 667-673.

Dimkpa CO, Calder A, Gajjar P, Merugu S, Huang W, Britt DW, McLean JE, Johnson WP, Anderson AJ (2011) Interation of silver nanoparticles with an environmentally beneficial bactrium, Pseudomonas chlorophis. J. Hazar. Mat. 428-435.

Dobbs RA, Wang L, Govind R (1989) Sorption of Toxic Organic Compounds on Wastewater Solids: Correlation with Fundamental Properties. Environ. Sci. Technol. 23, 1092-1097.

Du W, Sun Y, Ji R, Zhu J, Wub J, Guo H (2011) TiO_2 and ZnO nanoparticles negatively affect wheat growth and soil enzyme activities in agricultural soil. J. Environ. Monit, 13, 822-828.

Eaton AD, Clesceri LS, Greenberg AE, Franson MAH (2005) Standard Methods for the Examination of Water and Wastewater; American Public Health Association: Washington, DC.

Esparza I, Paredes M, Martinez R, Gaona-Couto A, Sanchez-Loredo G, Flores-Velez LM, Dominguezo O (2011) Solid state reactions in Cr2O3-ZnO nanoparticles synthesized by Triethanolamine chemical precipitation. Materials Sciences and Applications 2: 1584-1592.

Fabrega J, Fawcett SR, Renshaw JC, Lead JR (2009b) Silver nanoparticle impact on bacterial growth: Effect of pH, concentration, and organic matter. Environ. Scie & Technol. 43: 7285-7290.

Fabrega J, Renshaw JC, Lead JR (2009a) Interactions of Silver nanoparticles with Pseudomonas putida biofilms.Environ. Sci. Technol. 43: 9004-9009.

Farré M, Sanchís J, Barcelo D (2011) Analysis and assessment of the occurrence, the fate and the behaviour of nanomaterials in the environment. Trends Anal. Chem. 30: 517-527.

Feng QL, Wu J, Chen GQ, Cui FZ, Kim TN, Kim JO (2000). A mechanistic study of the antibacterial effect of silver ions on *Escherichia coli* and *Staphylococcus aureus*. Journal Biomed Materials 52: 662-668.

Formica J (1997) Handbook of instrumental techniques for analytical chemistry (F. Settle, ed.) Chap 18. Prentice Hall, New Jersey.

Franklin N, Rogers NJ, Apte S, Batley G, Gadd G, Casey P (2007) Comparative Toxicity of Nanoparticulate ZnO, Bulk ZnO, and $ZnCl_2$ to a Freshwater Microalga (*Pseudokirchneriella subcapitata*): The Importance of Particle Solubility. Environ. Sci. Technol. 41, 8484-8490.

Gaiser BK, Biswas A, Rosenkranz P, Jepson MA, Lead JR, Stone V, Tyler CR, Fernandes TF (2011) Effects of silver and cerium dioxide micro- and nano-sized particles *Daphnia magna*. J.Environ. Monit. 13:1227

Gartiser S, Flach F, Nickel C, Stintz M, Damme S, Schaeffer A, Erdinger L, Kuhlbusch TAJ (2013) Behavior of nanoscale titanium dioxide in laboratory wastewater treatment plants according to OECD 303 A. Chemosphere, *In Press*; http://dx.doi.org/10.1016/j.chemosphere.2013.11.015

Ge Y, Schimel JP, Holden PA (2011) Evidence for Negative Effects of TiO_2 and ZnO Nanoparticles on Soil Bacterial Communities. Environ. Sci. Technol. 45, 1659-1664.

Gottschalk F, Sonderer T, Scholz R, Nowack B (2009) Modeled environmental concentrations of engineered nanomaterials (TiO_2, ZnO, Ag, CNT, Fullerenes) for different regions. Environ. Sci. Technol. 43, 9216-9222.

Gottschalk F, Sonderer T, Scholz RW, Nowack B (2010) Possibilities and limitations of modeling environmental exposure to engineered nanomaterials by probabilistic material flow analysis, Environ. Toxicol. Chem., 29(5), 1036-1048.

Grassian VH, Bian S-W, Mundunkotuwa IA, Rupasinghe T (2011) Aggregation and Dissolution of 4 nm ZnO Nanoparticles in aqueous environments: influence of pH, ionic strength, size, and adsorption of humic acid. Langmuir (27), 6059-6068.

Hajipour MJ, Fromm KM, Ashkarran AA, de Aberasturi DJ, de Larramendi IR, Rojo T, Serpooshan V, Parak WJ, Mahmoudi M (2012) Antibacterial properties of nanoparticles. Trends in Biotechnology 30: 499-511. http://dx.doi.org/10.1016/j.tibtech.2012.06.004.

Hammond KD, Conner JR, Wm C (2013) Chapter one: Analysis of catalyst surface structure by physical sorption. Adv. Catal. 56, 1-101.

Han J, Qiu W, Gao W (2010) Potential dissolution and photo-dissolution of ZnO thin films. J. Hazard. Mater. 178, 115-122.

Heinlaan M, Ivask A, Blinova I, Dubourguier H, Kahru A (2008) Toxicity of nanosized and bulk ZnO, CuO and TiO_2 to bacteria *Vibro fischeri* and crustaceans *Daphnia magna* and *Thanocephalus platyurus*. Chemosphere 71:1308-1316.

Heinlaan M, Ivask A, Blinova I, Dubourguier HC, Kahru, A (2008) Toxicity of nanosized and bulk ZnO, CuO and TiO_2 to bacteria Vibrio fischeri and crustaceans Daphnia magna and Thamnocephalus platyurus. Chemosphere, 71, 1308-1316.

Hong R., Pan T, Qian J, Li H (2006) Synthesis and surface modification of ZnO nanoparticles. Chemical Engineering Journal 119: 71-81

Hou X, Jones BT (2000) Inductively coupled plasma/Optical emission spectrometry. In Meyers, R. A. (ed.) Encyclopedia of Analytical Chemistry. Chichester: John Wiley & Sons Ltd.

Hu CW, Lia M, Cui YB, Li DS, Chen J, Yang LY (2010) Toxicological effects of TiO2 and ZnO nanoparticles in soil on earthworm Eisenia fétida. Soil Biol. Biochem. 42, 586-591.

Huang M.H, Li Y.M, Gu G.W (2010) Chemical composition of organic matters in domestic wastewater. Desalination, 262, 36-42.

Huang Z, Zheng X, Yan D, Yin G, Liao X, Kang Y, Yao Y, Huang D, Hao B (2008) Toxicological effects of ZnO nanoparticles based on bacteria. Langmuir 24:4140-4144.

Huang Z, Zheng X, Yan D, Yin G, Liao X, Kang Y, Yao Y, Huang D, Hao B (2008) Toxicological Effect of ZnO Nanoparticles Based on Bacteria. Langmuir, 24, 4140-4144.

Jiang W, Mashayekhi H, Xing B (2009) Bacterial toxicity comparison between nano- and micro-scaled oxide particles. Environ Pollut 157: 1619-1625.

Jiang W, Mashayekhi H, Xing B (2009) Bacterial toxicity comparison between nano- and micro-scaled oxide particles. Environmental Pollution, 157, 1619-1625.

Jin-Ho J, Sedky HAH, Sang-Eun O (2010) Comparative study of biosorption of $Zn^{2+}$by *Pseudomonas aeruginosa* and *Bacillus cereus*. International Biodeterioration & Biodegradation 64:734-741.

Jones N, Ray B, Ranjit KT, Manna AC (2007) Antibacterial activity of ZnO nanoparticle suspensions on a broad spectrum of microorganisms. Research Letter, Federation of European Microbiological Societies, Blackwell Publishing.

Ju-Nam Y, Lead J (2008) Manufactured nanoparticles: An overview of their chemistry, interactions and potential environmental implications. Sci Total Environ 400:396-414.

Kaegi R, Voegelin A, Sinnet B, Zuleeg S, Hagendorfer H, Burkhardt M, Siegrist H (2010) Behavior of Metallic Silver Nanoparticles in a Pilot Wastewater Treatment Plant, Environmental Science and Technology, 45 (9), 3902-3908.

Kamika I, Momba MNB (2011a) Comparative the tolerance limit of selected bacterial and protozoan species to nickel in wastewater systems. Scie Total Environ 410-411: 172-181.

Kamika I, Momba MNB (2011b) Comparison of the tolerance limits of selcted bacterial and protozoan species to vanadium in wastewater systems. Water Air and Soil Pollution 223: 2525-2539.

Kamika I, Momba MNB (2013) Assessing the resistance and bioremediation ability of selected bacterial and protozoan species of heavy metals in metal rich industrial wastewater. BMC Microbiol 13:1-14.

Kasemets K, Ivask A, Dubourguier HC, Kahru A, (2009) Toxicity of nanoparticles of ZnO, CuO and TiO2 to yeast *Saccharomyces cerevisiae*. Toxicol. In Vitro 23: 1116-1122.

Keller AA, Wang H, Zhou D, Lenihan HS, Cherr G, Cardinale BJ, Miller R, Ji Z (2009) Stability and aggregation of metal oxide nanoparticles in natural aqueous matrices. Environ. Sci. Technol. 44, 1962-1967.

Khan SD, Ahmed B, Raghuvanshi SK, Wahab MA (2014) Structual, morphological and optical properties of silver doped polyvinylpyrrolidone composites. Indian Journal of Pure & Applied Physics 52: 192-197.

Kiser M, Ryu H, Jang H, Hristovski K, Westerhoff P (2010) Biosorption of nanoparticles to heterotrophic wastewater biomass. Water Res 44:4105-4114.

Kiser MA, Ryu H, Jang H, Hristovski K, Westerhoff P (2010) Biosorption of nanoparticles to heterotrophic wastewater biomass. Water Research, 44, 4105-4114.

Kiser MA, Westerhoff P, Benn T, Wang Y, Perez-rivera J, Hristovski K (2009) Titanium nanomaterial removal and release from wastewater treatment plants. Environ. Sci. Technol., 43, 6757-6763.

Labille J, Brant J (2010) Stability of nanopaticles in water. Nanomed 5:985-998.

Larner F, Dogra Y, Dybowska A, Fabrega J, Stolpe B, Bridgestock LJ, Goodhead R, Weiss DJ, Moger J, Lead JR, Valsami-Jones E, Tyler CR, Galloway TS, Rehkämper M (2012) Tracing Bioavailability of ZnO Nanoparticles Using Stable Isotope Labeling. Environ. Sci. Technol. 46, 12137−12145.

Laspidou CS, Rittmann BE (2002) A unified theory for extracellular polymeric substances, soluble microbial products, and active and inert biomass. Water Res 11:2711-2720.

Li M, Lin D, Zhu L (2013) Effects of water chemistry on the dissolution of ZnO nanoprtilces and their toxicity of *Escherichia coli*. Environ Pollut 173:97-102.

Li M, Pokhrel S, Jin X, Madler L, Damoiseaux R, Hoek EMV (2011) Stability, Bioavailability, and Bacterial Toxicity of ZnO and Iron-Doped ZnO Nanoparticles in Aquatic Media. Environ. Sci. Technol., 45, 755-761.

Li M, Zhu L, Lin D (2011) Toxicity of ZnO nanoparticles of *Escherichia coli*: Mechanism and the influence of medium componets. Environ Sci Technol 45:1977-1983.

Li M, Zhu L, Lin D (2011) Toxicity of ZnO Nanoparticles to Escherichia coli: Mechanism and the Influence of Medium Components. Environ. Sci. Technol. Vol. 45, No. 5, 1977-1983.

Li Q, Mahendra S, Lyon DY, Brunet L, Liga MV, Li D, Alvarez PJJ (2008) Antimicrobial nanomaterials for water disinfection and microbial control: Potential applications and implications. Water Research, 42: 4591-4602.

Liang Z, Das A, Hu Z (2010) Bacterial response to a shock load of nanaosilver in an activated sludge treatment sytems. Water Res 44:5432-5438.

Limbach LK, Bereiter R, Muller E, Krebs R, Galli R, Stark WJ (2008) Removal of oxide nanoparticles in a model wastewater treatment plant: Influence of agglomeration and surfactants on clearing efficiency. Environ. Sci. Technol. 42, 5828-5833.

Liu G, Wang D, Wang J, Mendoza C (2011) Effect of ZnO particles on activated sludge: Role of particle dissolution. Sci. Total Environ. 409, 2852-2857.

Lombi E, Donner E, Tavakkoli E, Turney TW, Naidu R, Miller BW, Scheckel KG (2012) Fate of zinc oxide nanoparticles during anaerobic digestion of wastewater and post-treatment processing of sewage sludge. Environmental Science and Technology. 46, 9089−9096.

López-Moreno M, De Larosa G, Hernandez-Viezcas J, Castillo-Michel H, Botez CE, Peralta-Videa J, Gardea-Terresdey JL (2010) Evidence of the Differential Biotransformation and Genotoxicity of ZnO and CeO_2 Nanoparticles on Soybean (*Glycine max*) Plants. Environ. Sci. Technol. 44, 7315-7320.

Ma H, Williams PL, Diamond SA (2013) Ecotoxicity of manufactured ZnO nanoparticles – A review. Environ. Pollut. 172, 76-85.

Marambio-Jones C, Hoek EMV (2010). A review of the antibacterial effects of silver nanomaterials and potential implications for human health and the environment. Journal of Nanoparticles and Research 12: 1531-1551.

Martin TD, Creed JT, Brockhoff CA (1994) Sample preparation procedure for spectrochemical determination of total recoverable elements. U. S. Environmental Protection Agency. Environmental Monitoring Systems Laboratory – Office of research and development. Cincinnati INCINNATI, OHIO 45268, Revision 2.8, Method 200.2

Martin TD, Creed JT, Brockhoff CA (1994). Sample preparation procedure for spectrochemical determination of total recoverable elements. U. S. Environmental Protection Agency. Environmental Monitoring Systems Laboratory – Office of research and development. Cincinnati INCINNATI, OHIO 45268, Revision 2.8, Method 200.2

Martines-Castanon G, Nino-Martinez N, Martinez-Gutierrez F, Martinez-Mendoza J, Ruiz F (2008) Synthesis and antibacterial activity of silver nanoprtilces with different sizes. J Nanopart Res 10:1343-1348.

Matzeke M, Jurkschat K, Backahaus T (2014) Toxicity of differently sized and coated silver nanopartilces to the bacterium Pseudomonas putida: rsiks for the aquatic environment? Ecotoxicology 23:818-829.

Mayinger F, Feldman O (2002) Optical measurements: Techniques and Applications. 2nd Edition, Springer, New York.

Maynard AD, Aitken RJ, Butz T, Colvin V, Donaldson K, Oberdorster G, Philbert MA, Ryan J, Seaton A, Stone V, Tinkle SS, Tran L, Walker NJ, Warheit DB (2006) Safe handling of nanotechnology. Nature, 444:267-269.

Maynard AD, Warheit D and Philbert MA (2011) The New Toxicology of Sophisticated Materials: Nanotoxicology and Beyond. Toxicological Sciences. 120(S1), S109-S129.

Metcalf, Eddy (2002) Wastewater engineering: treatment and reuse. 4th ed. Mcgraw Hill, New York.

Metcalf, Eddy (2004) Wastewater engineering, treatment and reuse. 4th Edition, McGraw-Hill, New York, United States of America.

Molina R, Al-Salama Y, Jurkschat K, Dobson PJ, Thompson IP (2011) Potential environmental influence of amino acids on the behaviour of ZnO nanoparticles. Chemosphere 83, 545-551.

Monshi A, Foroughi MR, Monshi MR (2012) Modified Scherrer equation to estimate more accurately nano-crystallite size using XRD. World J. Nano Sci. Engine. 2, 154-160.

Moore MN (2006) Do nanoparticles present ecotoxicological risks for the health of the aquatic environment? Environ. Int. 32:967-976.

Mu H, Chen Y (2011) Long-term effect of ZnO nanoparticles on waste activated sludge anaerobic digestion. Water Res., 45, 5612-5620.

Mudunkotuwa IA, Rupansinghe T, Wu C.M, Grassian VH, (2012) Dissolution of ZnO nanoparticles at circumneutral pH: a study of size effects in the presence and absence of citric acid. Langmuir, 28, 396-403.

Musee N (2010) Nanotechnology risk assessment from a waste management perspective: are the current tools adequate? Hum. Exp. Toxicol. 30(8) 820-835.

Musee N (2011) Nanowastes and the environment: potential new waste management paradigm. Environ. Int., 37 (1), pp. 112.

Musee N, Thwala M, Nota N (2011) The antibacterial effects of engineered nanomaterials: Implications for wastewater treatment plants. Journal of Environmental Monitoring, 13: 1164-1183.

Musee N, Thwala M, Nota N (2011) The antibacterial effects of engineered nanomaterials: implications for wastewater treatment plants. J. Environ. Monitoring 13: 1164-1183.

Musee N, Zvimba J, Schaefer L, Nota N, Sikhwivhilu L, Thwala M (2014) Fate and behaviour of ZnO and Ag engineered nanopartilces and a bacterial viabilty assessment in a simulated wastewater treatment plant. J Eviron Sci Health Part A 49:59-66.

Musee N, Zvimba JN, Schaefer LM, Nota N, Sikhwivhilu LM, Thwala M (2014) Fate and behaviour of ZnO- and Ag-engineered nanoparticles and a bacterial viability assessment in a simulated wastewater treatment plant. J. Environ. Sci. Health, Part A, 49, 59-66.

Nadell CD, Xavier JB, Levin SA, Foster KR (2008) The evolution of quorum sensing in bacterial biofilms. Plos Biology 6: 0171-0179.

Nair S, Sasidharan A, Rani VVD, Menon D, Nair S, Manzoor K, Raina S (2009) Role of size scale of ZnO nanoparticles and microparticles on toxicity toward bacteria and osteoblast cancer cells. J Mater Sci: Mater Med. 20, S235-S241.

Nanoscience and Nanotechnologies: Opportunities and Uncertainties (The Royal Society and The Royal Academy of Engineering, London, 2004).

Navarro E, Baun A, Behra R, Hartmann NB, Filser J, Miao AJ, Quigg A, Santschi PH, Sigg l (2008) Environmental behaviour and ecotoxicity of engineered nanoparticles to algae, plants, and fungi. Ecotoxicology, 17:372-386.

Neal A (2008) What can be inferred from bacterium-nanoparticles interactions about the pontetial consequences of environmental exposure to nanoparticles? Ecotoxicology 17:362-371.

Nowack B, Bucheli TD (2007) Occurrence, behaviour and effects of nanoparticles in the environment. Environ. Pollution.150, 5-22.

Nowack B, Ranville JF, Diamond S, Gallego-Urrea JA, Metcalfe C, Rose J, Horne N, Koelmans AA, Klaine SJ (2012) Potential scenarios for nanomaterial release and subsequent alteration in the environment. Environ. Toxic. Chem. 31, 50-59.

OECD 303A (2001) Aerobic Sewage Treatment – activated sludge units. Guidelines for the testing of chemicals.

OECD 303A. (2001). Aerobic Sewage Treatment – activated sludge units. Guidelines for the testing of chemicals.

Okafor F, Janen A, Kuthtareva T, Edwards V, Curley M (2013) Green synthesis of silver nanopartilces, their characterization, application and antibacterial activity. Int J Environ Res Public Health 10:5221-5238.

Omar FM, Aziz HA, Stoll S (2014) Aggregation and disaggregation of ZnO nanoparticles: Influence of pH and adsorption of Suwannee River humic acid. Sci. Total Environ. 468-469, 195-201.

Padmavathy N, Vijayaghavan R (2008) Enhanced bioactivity of ZnO nanoprtilces-an antimicrobial study. Sci. Technol. Adv. Mater 9: 1-7.

Pal S, Tak Y, Song J (2007) Does the antibacterial activity of silver nanoparticles depends on the shape of the nanopartilcles? A study of Gram-negative bacterium Escherichia coli. Appl Environ Microb, 73:1712-1720.

Peralta-Videa JR, Zhao L, Lopez-Moreno ML, De La Rosa G, Hong J, Gardea-Torresdey JL (2011) Nanomaterials and the environment: A review for the biennium 2008-2010. J. Hazard. Mater. 186, 1-15.

Prabhu S, Poulose E (2012) Silver nanoparticles: mechanism of antimicrobial action, synthesis medical applications, and toxicity effects. Int Nano Lett 2:32

Premanathan M, Karthikeyan K, Jeyasubramanian K, Manivannan G (2011) Selective toxicity of ZnO nanoparticles toward Gram-positive bacteria and cancer cells by apoptosis through lipid peroxidation. Nanomed-Nanotechnol 7:184-192.

Premanathan M, Karthikeyan K, Jeyasubramanian K, Manivannan G (2011) Selective toxicity of ZnO nanoparticles toward Gram-positive bacteria and cancer cells by apoptosis through lipid peroxidation. Nanomedicine, 7, 184-192.

Raghupathi KR, Koodali RT, Manna AC (2011) Size-Dependent bacterial growth inhibition and mechanism of antibacterial activity of zinc oxide nanoparticles. American Chemical Society 27: 4020-4028

Rai M, Yadav A, Gade A (2009) Silver nanoparticles as a new generation of antimicrobials. Biotechnol Adv 27:76-83.

Reimer L, Kohl H (2008) Transmission electron microscope: Physics of image formation. Springer series in optical sciences 36. Fifth edition. Springer, New York.

Rupasinghe RA Thilini perera (2011) "Dissolution and aggregation of zinc oxide nanoparticles at circumneutral pH; a study of size effects in the presence and absence of citric acid." Master's thesis, University of Iowa.

Scott MJ, Jones MN (2000) The biodegradation of surfactants in the environment – Review. Biochim. Biophys. Acta, 1508, 235-251.

Sheng GP, Zhang ML, Yu HQ (2008) Characterization of adsorption properties of extracellular polymeric substances (EPS) extracted from sludge. Colloids and Surfaces B: Biointerfaces 62, 83-90.

Sheng Z, Liu Y (2011) Effects of silver nanoparticles on wasterwater biofilm. Water Res 45:6038-6050.

Sondi I, Salopek-Sondi B (2004) Silver nanoparticles as antimicrobial agent: a case study on E.coli as a model for Gram-negative bacteria. Journal of Colloid and Interface Science 275: 177-182

Song, W, Zhang J, Guo J, Zhang J, Ding F, Li L, Sun Z (2010) "Role of the dissolved zinc ion and reactive oxygen species in cytotoxicity of ZnO nanoparticles." Toxicology Letters 199: 389-397.

Sonune A, Ghate R (2004) Developments in wastewater treatment methods. Desalination 167, 55-63.

Sornalatha DJ, Murugakoothan P (2013) Room temperature synthesis of ZnO nanostructures using CTAB assisted sol-gel method for application in solar cells. Int. J. Emerging Technol. and Adv. Engine.. Vol. 3 (9).

Spellman FR (2003) Handbook of water and wastewater treatment plant operations. CRC Press, Boca Raton.

Spence J (1999) The future of atomic resolution electron microscopy for materials science. Mat. Sci. Engine. 26, 1-49.

Stone V, Nowack B, Baun A, Van Den Brink N, Von Der Kammer F, DusINSKA M, Handy R, Hankin S, Hassellov M, Joner E, Fernandes TF (2010) Nanomaterials for environmental studies: classification, reference material issues, and strategies for physico-chemical characterisation, Sci. Total Environ., 408(7), 1745-1754.

Strom PF, Jenkins D (1984) Identification and significance of filamentous organisms in activated sludge. Water Pollut. Contr. Fed. 49 (5) 584-589.

Sykes RM (2003) The Civil Engineering Handbook (W.F. Chen and J.Y.R. Liew ed) Chap 11. 2nd Edition, CRC Press, Boca Raton.

Theivasanthi T, Alagar M (2011) Electrolytic synthesis and characteizations of silver nanopowder. arXiv preprint arXiv:1111.0260.

Thwala M, Musee N, Sikhwivhilu L, Wepener V (2013) The oxidative toxicity of Ag and ZnO nanopartilces towards the aquatic plant Spirodela puntucta and the role of testing media parameter. Environ Sci Process Impacts 15:1830-1843.

Tomlinson AAG (2011) Nanoporous Materials. Advanced Techniques for Characterization, Modeling, and Processing. (N. Kanellopoulos, ed.). Chap 3. CRC Press. USA.

Tso C, Zhung C, Shih Y, Tseng Y, Wu S, Doong R (2010) Stability of metal oxide nanoprticles in aqueous solutions. Water Sci Technol 61:127-133.

Viswanatha R, Venkatesh TG, Vidyasagar CC, Arthoba Nayaka Y (2012) Preparation and Characterization of ZnO and Mg-ZnO nanoparticles. *Archives of Applied Science Research* 4: 480-486. Accessed January 2, 2015. http://scholarresearchlibrary.com/archive.html.

Wang Y, Westerhoff P, Hristovski KD (2012) Fate and biological effects of silver, titanium dioxide, and C60 (Fullerene) nanomaterials during simulated wastewater treatment processes. J. Hazard. Mat. 201-202 16-22.

Weckhuysen BM (2004) In-situ spectroscopy of catalysts. American Scientific Publishers. USA, California.

Wegner G (1992) “The benefits of biosolids from a farmer´s perspective.” Proceedings, the future direction of municipal sludge (biosolids) management, WEF Specialty conference, 39-44, Portland, OR.

Westerhoff P, Song G, Hristovski K, Mehlika AK (2011) Occurrence and removal of titanium at full scale wastewater treatment plants: implications for TiO_2 nanomaterials. J. Environ. Monitor. 13, 1195-1203.

Westerhoff P, Song G, Hristovski K, Mehlika AK (2011) Occurrence and removal of titanium at full scale wastewater treatment plants: implications for TiO_2 nanomaterials. J. Environ. Monit. 13, 1195-1203.

Wiench K, Wohlleben W, Hisgen V, Radke K, Salinas E, Zok S, Landsiedel R (2009) Acute and chronic effects of nano- and non-nano-scale TiO_2 and ZnO particles on mobility and reproduction of the freshwater invertebrate Daphnia magna. Chemosphere 76, 1356-1365.

Wingender J, Neu T, Flemming H (1999) Microbial Extracellular Polymeric substance: Characteristics Structures and Function. Springer-Verlag Berlin Heidelberg. doi:10.1007/978-3-642-60147-7

Wong SWY, Leung PTY, Djurišić AB and Leung KMY (2010) Toxicities of nano zinc oxide to five marine organisms: influences of aggregate size and ion solubility. Anal. Bioanal. Chem. 396, 609-618.

Wu X, Hou L, Li K, Ding Y, Li Y, Chen J, Li X (2012) Removal of silver nanoparticles in simulated wastewater treatment processes and its impact on COD and NH_4 reduction. Chemosphere (87), 248-252.

Xia T, Kovochich M, Liong M, Madler L, Gilbert B, Shi H, Yeh JI, Zink JI, Nel AE (2008) Comparison of the Mechanism of Toxicity of Zinc Oxide and Cerium Oxide nanoparticles Based on Dissolution and Oxidative Stress Properties. J. Am. Chem. Soc., VOL. 2, NO. 10, 2121-2134.

Yamamoto O (2001) Influence of partilces size on the antibacterial activity of zinc oxide. Int J Inorg Mater 3:643-646.

Yin H, Casey PS, McCall MJ and Fenech M (2010) Effects of Surface Chemistry on Cytotoxicity, Genotoxicity, and the Generation of Reactive Oxygen Species Induced by ZnO Nanoparticles. Langmuir, 26(19), 15399-15408.

Zanjanchi MA, Noei H and Moghimi M (2006) Rapid determination of aluminum by UV-vis diffuse reflectance spectroscopy with application of suitable adsorbents. Talanta, 70, 933-939.

Zhang L, Jiang Y, Ding Y, Povey M, York D (2007). Investigation into the antibacterials behaviour of suspensions of ZnO nanopartilces (ZnO nanofluids). J Nanopart Res 9:479-489.

Zhang XQ, Yin LH, Tang M, Pu YP (2011) ZnO, TiO_2, SiO_2, and Al_2O_3 Nanoparticles induced Toxic Effects on Human Fetal Lung Fibroblasts. Biomed. Environ. Sci., 24(6): 661-669.

Zhang Y, Chen Y, Westerhoff P, Crittenden J (2009) Impact of natural organic matter and divalent cations on the stability of aqueous nanoparticles. Water Res. 43, 4249-4257.

Zhang Y, Chen Y, Westerhoff P, Hristovski K, Crittenden JC (2008) Study of commercial metal oxide nanoparticles in water. Water Res. 42, 2204-2212.

Zhou D and Keller AA (2010) Role of morphology in the aggregation kinetics of ZnO nanoparticles. Water Res. 44, 2948-2956.

APPENDIX

Simulated AS WWTP components dimensions

Aeration chamber – dimensions

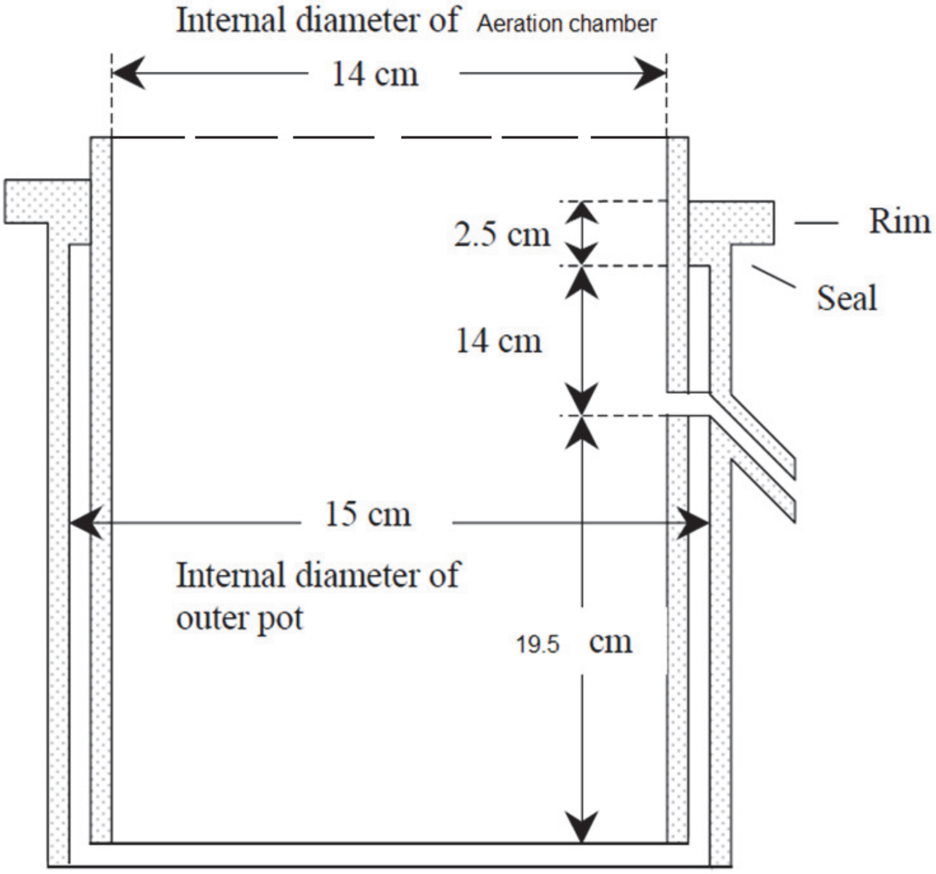

Settling vessel – dimensions

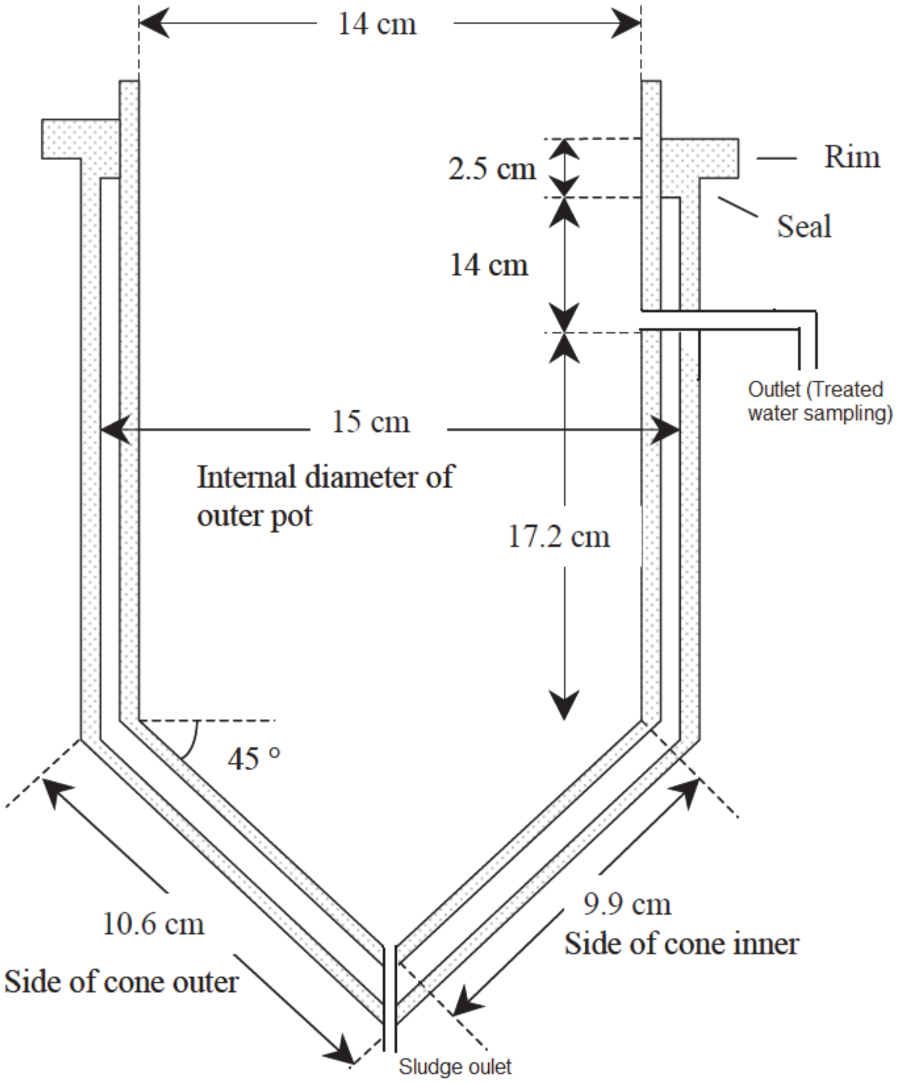

RESEARCH ACHIEVEMENTS

Conference Presentations

1. Eutilério F. C. Chaúque, J. Catherine Ngila*, Ndeke Musee and John N. Zvimba (2012**)**. Studies on chemical stability of commercial ZnO nanoparticles in domestic wastewater. 13th Waternet WARFSA, Birchwood Hotel, Johannesburg , South Africa. 30 October -1 Nov 2012.
2. Eutilério F. C. Chaúque, John N. Zvimba, J. Catherine Ngila, Ndeke Musee (2013). Fate and behaviour of commercial ZnO engineered nanoparticles in a simulated domestic wastewater treatment plant. **O**14WaterNet/WARFSA/GWP-SA, Whitesands Hotel Dar-es-Salaam Tanzania, 30 October-1 November 2013
3. A.Mboyi , I. Kamika, N. Musee, J.N. Zvimba and M.N.B. Momba (2015). Nanotoxicity effects of Zinc oxide and Silver nanomaterials on selected bacterial population. *Oral Presentation*, 9thAnnual Africa Young Graduate Scholars Conference, University of Cape Town, South Africa.
4. A.Mboyi , N. Musee, J.N. Zvimba and M.N.B. Momba (2014). Toxicity effects of Ag and ZnO engineered nanoparticles on wastewater bacteria: Environmental risks, *Poster Presentation,* NanoAfrica 2014 international conference (30 March-2 April 2014).
5. A.Mboyi , N. Musee, J.N. Zvimba and M.N.B. Momba (2014). Potential effects of Ag and ZnO engineered nanoparticles on selected wastewater bacteria. *Oral Presentation*, WISA Biennial Conference & Exhibition 2014 (25-29 May 2014).
6. A.Mboyi, I. Kamika, N. Musee, J.N. Zvimba and M.N.B. Momba (2014). pH effect on nanomaterials toxicity towards bacterial species. *Poster Presentation*. Tshwane University of Technology Research Day (29 August 2014).

Publications

1. E. F. C. Chaúque, J. N. Zvimba, J. C. Ngila, N. Musee (2014). Stability studies of commercial ZnO engineered nanoparticles in domestic wastewater. *Journal of Physics and Chemistry of the Earth*, **67-69** (2014), 140-144.
2. E. F. C. Chaúque, J. N. Zvimba, J. C. Ngila, N. Musee (2016). Fate, behaviour, and implications of ZnO nanoparticles in a simulated wastewater treatment plant. *Water SA* 42(1) (2016) 72

3. Anza-vhudziki Mboyi, Sudharshan Sekar, Ilunga Kamika, Maggy NB Momba (2014). How nanoscale applications and development change African Perceptions. *(In preparation)*
4. A.Mboyi, I. Kamika, N. Musee, J.N. Zvimba and M.N.B. Momba (2014). Nanotoxicity effects of Zinc oxide and Silver nanomaterials on selected bacterial population. *(In preparation)*
5. A.Mboyi, I. Kamika, N. Musee, J.N. Zvimba and M.N.B. Momba (2014). Assessing the antibacterial effects of zinc oxide and silver nanomaterials towards selected bacterial species in wastewater system. *(In preparation)*
6. A.Mboyi, I. Kamika, N. Musee, J.N. Zvimba and M.N.B. Momba (2014). Comparative survival limit of selected wastewater bacterial and protozoan isolates in the presence of engineered nanomaterials. *(In preparation)*